Geological Society of America
Memoir 179
1992

Chapter 12

An overview of basaltic volcanism of the eastern Snake River Plain, Idaho

Mel A. Kuntz
U.S. Geological Survey, MS 913, Box 25046, Federal Center, Denver, Colorado 80225
Harry R. Covington
U.S. Geological Survey, Box 327, Mercury, Nevada 89023
Linda J. Schorr
Department of Earth Resources, Colorado State University, Fort Collins, Colorado 80523

ABSTRACT

More than 95% of the eastern Snake River Plain (ESRP) is covered by basaltic lava flows erupted in the Brunhes Normal-Polarity Chron; thus they are younger than 730 ka. About 13% of the area of the ESRP is covered by lava fields of latest Pleistocene and Holocene age <15 ka. More than 90% of the basalt volume of the ESRP is included in coalesced shield and lava-cone volcanoes made up dominantly of tube- and surface-fed pahoehoe flows. Deposits of fissure-type, tephra-cone, and hydrovolcanic eruptions constitute a minor part of the basalt volume of the ESRP.

Eight latest Pleistocene and Holocene lava fields serve as models of volcanic processes that characterize the basaltic volcanism of the ESRP. The North Robbers, South Robbers, and Kings Bowl lava fields formed in short-duration (a few days), low-volume (each <0.1 km^3), fissure-controlled eruptions. The Hells Half Acre, Cerro Grande, Wapi, and Shoshone lava fields formed in long-duration (several months), high-volume (1 to 6 km^3), lava cone- and shield-forming eruptions. Each of these seven lava fields represents monogenetic eruptions that were neither preceded nor followed by eruptions at the same or nearby vents. The Craters of the Moon lava field is polygenetic; about 60 flows were erupted from closely spaced vents over a period of 15,000 years.

Most of the basaltic volcanism of the ESRP is localized in volcanic rift zones, which are long, narrow belts of volcanic landforms and structures. Most volcanic rift zones are collinear continuations of basin-and-range-type, range-front faults bordering mountains that adjoin the ESRP. It is not clear whether the faults extend into the ESRP in bedrock beneath the basaltic lava flows.

The great bulk of basaltic flows in the ESRP are olivine basalts of tholeiitic and alkaline affinities. The olivine basalts are remarkably similar in chemical, mineralogical, and textural characteristics. They were derived by partial melting of the lithospheric mantle at 45 to 60 km, and they have been little affected by fractionation or contamination. Evolved magmas having SiO_2 contents as high as 65% occur locally in and near the ESRP. The chemical and mineralogical variability of the evolved rocks is due to crystal fractionation in the crust and to contamination by crustal minerals and partial melts of crustal rocks. The trace-element compositions of the olivine basalts and the most primitive evolved basalts do not overlap, suggesting that the evolved rocks were derived from parent magmas that are fundamentally different from the parent magmas of the olivine basalts.

Kuntz, M. A., Covington, H. R., and Schorr, L. J., 1992, An overview of basaltic volcanism of the eastern Snake River Plain, Idaho, *in* Link, P. K., Kuntz, M. A., and Platt, L. B., eds., Regional Geology of Eastern Idaho and Western Wyoming: Geological Society of America Memoir 179.

The distribution and character of volcanic rift zones in the ESRP are partly controlled by underlying Neogene rhyolite calderas. Areas that lack basalt vents and have only poorly developed volcanic rift zones overlie calderas or parts of calderas filled by thick, low-density sediments and rocks, which served as density barriers to the buoyant rise of basaltic magma. Volcanic rift zones are locations of concentrated extensional strain; they define regional stress patterns in the ESRP.

INTRODUCTION

We studied the Quaternary basaltic lava fields of the eastern Snake River Plain (ESRP), Idaho, in the period 1975 through 1981 and at various times since then. The study area covers 20,000 km^2 within nearly 250 7½-minute quadrangles and extends from Twin Falls to Ashton (Fig. 1). Our studies included interpretation of volcanic features on aerial photos; field mapping of vents, flow features, and contacts; and sampling of flows and inclusions for petrographic, petrochemical, and dating investigations.

This chapter characterizes the basaltic volcanism of the ESRP based on our field and laboratory studies and the studies of coworkers. We emphasize the latest Pleistocene and Holocene

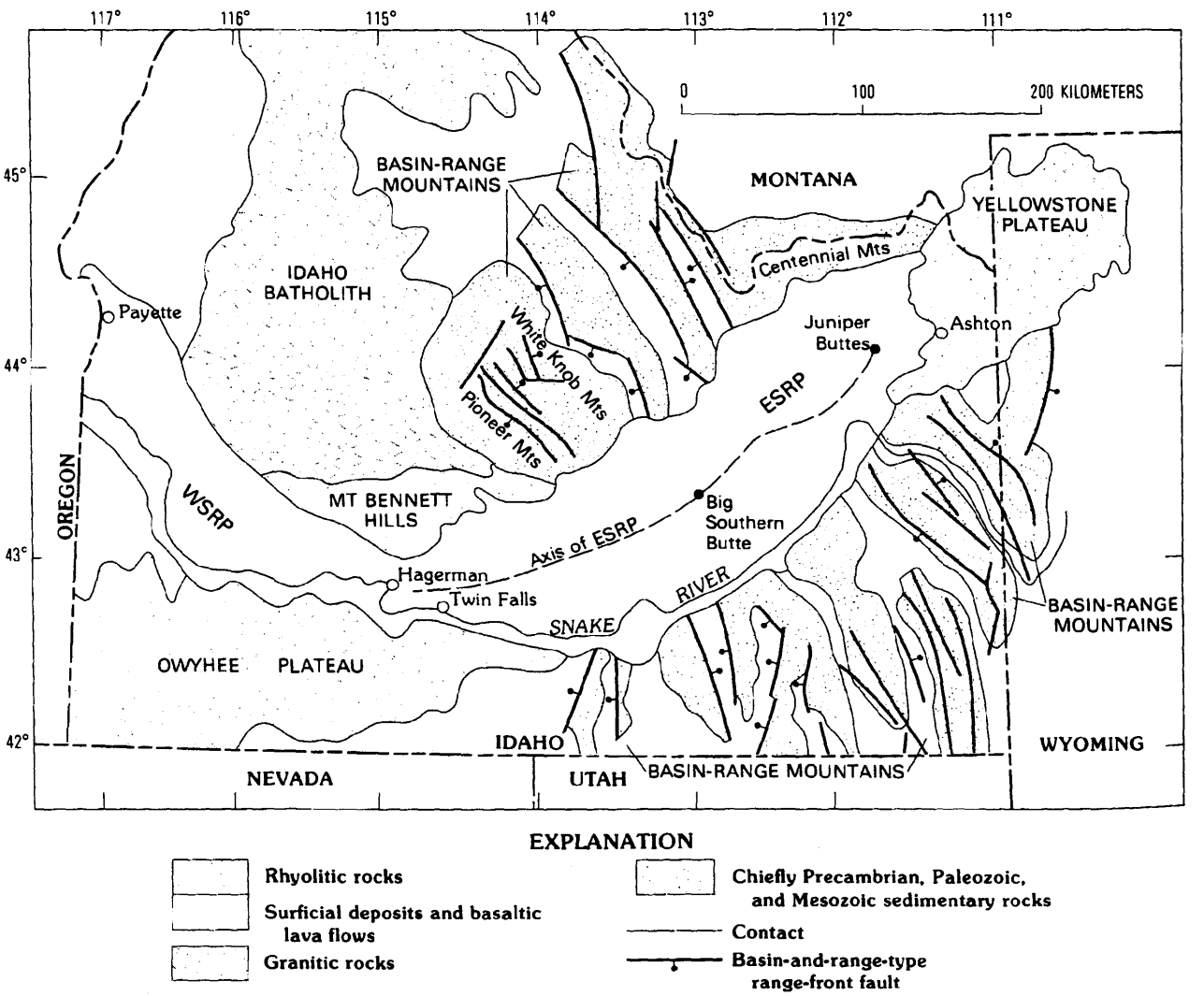

Figure 1. Index map of southern Idaho showing generalized geology, latest Pleistocene-Holocene lava fields, and localities referred to in the text.

lava fields, volcanic rift zones, and the interrelationships between Quaternary basaltic volcanism and Neogene rhyolite calderas. In addition, we describe the volcanic morphology, petrology, petrochemistry, and stratigraphy of the basaltic rocks, the structural control of vents, and magma output rates. We treat only those topics we feel are most important in characterizing basaltic volcanism of the ESRP. The reference section will guide those who wish to investigate these and other topics more completely.

Notes on terminology

Several often-used terms in this chapter are defined here to avoid possible confusion in their meaning. Many of the terms are described by Holcomb (1987) and illustrated in photographs by Takahashi and Griggs (1987). *Lava flow* denotes thin sheets of lava erupted from fissure or pipelike vents. Typical basaltic lava flows of the ESRP are pahoehoe, *slab pahoehoe* (jumbled plates or slabs of broken pahoehoe crust, typically <10 m across), and *shelly pahoehoe* (flows near vents having small open tubes, blisters, and thin crusts that formed from gas-charged lava; Swanson, 1973). *Tube-fed* flows are large-volume pahoehoe flows that advance chiefly by supply of lava through lava tubes; *surface-fed* flows advance by supply of lava in surface conduits such as channels. A'a and block-lava flows are rare; the few that are known in this area are several kilometers wide and several tens of kilometers long and are typically 5 to 15 m thick but as thick as 50 m where ponded.

Flow lobes are nearly contemporaneous discharges of lava that formed during a single eruptive episode. They range from several centimeters to several meters thick. The length of a flow lobe is variable, ranging from local outpourings that moved only a few meters over slightly older surfaces of the same flow to sheets that flowed several kilometers partly or entirely over earlier flow lobes of the same eruption (Wentworth and Macdonald, 1953). In vertical sections and cores in lava flows of the ESRP, it is difficult to determine whether successive flows of similar lava that lack an intervening soil or alluvial horizon are merely different flow lobes of the same major flow or independent flows extruded during different eruptions. *Lava field* refers to a sequence of flows, flow lobes, and associated pyroclastic deposits that accumulated during synchronous eruptions from single or multiple vents along an eruptive fissure. *Volcanic rift zones* are linear arrays of volcanic landforms and structures. The volcanic landforms include eruptive fissures, spatter ramparts, tephra cones, lava cones, shield volcanoes, and dikes at depth. The structures include noneruptive fissures, faults, and grabens.

REGIONAL GEOLOGY AND STRUCTURE

The Snake River Plain

The Snake River Plain is a relatively flat depression, 50 to 100 km wide, that cuts an arcuate swath across southern Idaho. It extends from Payette on the northwest 250 km southeast to Twin Falls and thence 300 km northeast to Ashton (Fig. 1). Elevation of the Snake River Plain rises gradually from 700 m on the west to 2,000 m on the east. The Snake River Plain is bounded on the southeast by folded, thrust-faulted mountains of the Basin and Range province, consisting of upper Precambrian through lower Mesozoic sedimentary rocks that were uplifted along normal faults during Neogene and Quaternary tectonism. The Snake River Plain is bounded on the north by similar basin-and-range type mountains and also by mountains consisting of Mesozoic and lower Tertiary granitic rocks of the Idaho batholith. Southwest of the Snake River Plain are the mid-Miocene rhyolitic and basaltic rocks of the Owyhee Plateau. At the northeast end of the Snake River Plain are the Quaternary rhyolitic and basaltic rocks of the Yellowstone Plateau.

The Snake River Plain is divided into western and eastern parts at about 114° W. longitude. Mabey (1982) defined a central part based chiefly on geophysical characteristics. The eastern and western parts have contrasting structural, geophysical, and geological characteristics, suggesting different modes of origin.

The western Snake River Plain (WSRP) is a late Neogene, fault-bounded graben containing rhyolite and basalt lava flows and thick, interbedded detrital sediments (Malde and Powers, 1962; Malde, 1991). Considerable relief and extensive vertical exposures along the canyons of the Snake River and its tributaries have been important in the geologic study and interpretation of the tectonic history of the western Snake River Plain.

The eastern Snake River Plain (ESRP) is a broad lava plain consisting, at the surface, of mostly Pleistocene and Holocene basaltic lava flows, pyroclastic deposits, and thin, discontinuous deposits of loess, sand dunes, and alluvial sediments. Magnetic polarity determinations and recent radiometric studies (Champion and others, 1988; Kuntz and others, 1992) indicate that most of the surface flows were erupted during the Brunhes Normal-Polarity Chron and thus are younger than 730 ka. Data from wells that penetrate the ESRP to depths as great as 3,500 m (summarized in Embree and others, 1982) show that the lava-flow and sediment sequence is 1 to 2 km thick throughout most of the ESRP. These data also indicate that the thickness of the basaltic volcanic rocks greatly exceeds that of the sedimentary deposits near the center of the ESRP and that the sedimentary deposits are more abundant along the margins.

Drilling and recent field studies (Doherty and others, 1979; Embree and others, 1982; Morgan and others, 1984) show that the basalt-sediment sequence is underlain by rhyolitic lava flows, ignimbrites, and pyroclastic deposits. Volcanologic studies of ignimbrites at localities around the margins of the ESRP indicate the presence of large source calderas beneath the basaltic lava flow and sediment sequence of the ESRP (Pierce and Morgan, this volume; Morgan, this volume).

Available geological and geophysical data suggest that the Snake River Plain has been the site of a northeasterly propagating system of rhyolitic volcanic centers and associated basaltic volcanism (see, for example, Armstrong and others, 1975; Brott and others, 1978, 1981; Mabey, 1982; Malde, 1991; Leeman, 1989;

Pierce and Morgan, this volume). Rhyolitic volcanism began in mid-Miocene time near the southwest corner of Idaho and has migrated northeastward to the site of the most recent volcanism in the Yellowstone Plateau. The volcanic cycle at any one locality is believed to be initiated by generation of basalt magma in the lithospheric mantle. The rise of basalt magma from the mantle produces sufficient heat to cause anatexis of the lower crust and subsequent formation of rhyolitic calderas. Rhyolitic volcanism is generally preceded and followed by basaltic volcanism, thus forming the bimodal basalt-rhyolite volcanic association of the ESRP. Such a volcanic system produces high heat flow, thinning and decreased rigidity of the crust, and progressive formation of a topographic trough along the chain of calderas. The location of the caldera chain in the ESRP may have been governed by a complex interaction between a zone of structural weakness (a crustal "flaw" of Precambrian ancestry) in the crust, an underlying "hot spot" in the mantle, the southwestward drift of the North American plate, and perhaps the major structures of the Basin and Range province.

Major, northeast-southwest–trending faults parallel to the margins of the ESRP have not been identified; thus there is little evidence to support a fault-bounded, rift-valley origin for the ESRP.

Physiography

Mountains north and south of the ESRP are long, narrow, basin-and-range–type mountains, separated by narrow intermontane valleys. Crests of mountain ranges and axes of intermontane valleys are spaced about 35 km apart. Both mountains and valleys trend mostly north or northwest, perpendicular to the long axis of the ESRP, but the Centennial Mountains trend east-west, parallel to the northeast margin of the ESRP (Fig. 1). Most of these ranges are bounded by a single range-front normal-fault system, but others have faults along both margins. The fault-block mountains end abruptly at the margins of the ESRP. The abrupt terminations may reflect their proximity to the walls of calderas that lie within the ESRP.

The Pioneer and White Knob mountains in central Idaho, along the northwest border of the ESRP (Fig. 1), form a broad highland mass consisting of Precambrian rocks of a core complex and Cretaceous and early Cenozoic plutonic rocks of the Idaho batholith. This range has not been broken into distinct basin-and-range–type mountains, even though northwest-trending normal faults in the Big Wood River and Sawtooth valleys suggest incipient basin-and-range deformation (Link and others, 1988).

Drainage in the ESRP is dominated by the Snake River, which flows along the southeast margin of the plain. A topographic ridge of volcanic construction extends from near Hagerman in the western Snake River Plain through Big Southern Butte northeastward to Juniper Buttes near Ashton in the ESRP. The ridge coincides approximately with the long axis of the ESRP (Fig. 1). Rivers entering the ESRP from the north are deflected by the ridge and discharge in closed basins. Because river canyons are absent, little is known of the underlying rocks of the ESRP except from drilling and geophysical data and study of rhyolitic ignimbrites and flows along its margins.

THE STAGES OF BASALTIC ERUPTIONS

Field characteristics of vent areas and lava flows in the ESRP are remarkably similar to those of well-studied volcanoes and volcanic rift zones in Hawaii. By analogy, volcanic processes in the ESRP are assumed to have been similar to Hawaiian volcanic processes, though they may not have occurred at the same rates. Thus, our understanding of ESRP basaltic activity is based partly on Hawaiian studies (for example, Wentworth and Macdonald, 1953; Macdonald and Abbott, 1970; Richter and others, 1970; Swanson and others, 1979; Holcomb, 1987; Peterson and Moore, 1987; Tilling and others, 1987; and Wolfe and others, 1987). From these studies, it is recognized that Hawaiian fissure-fed eruptions generally proceed through four distinct stages, as summarized below.

The *first stage* is characterized by harmonic tremor, ground cracking, and local steam and fume activity. Fissuring is followed by lava fountains, producing a "curtain of fire" that extends for several hundred meters and erupts to heights of as much as 500 m. The early lava is extremely fluid and gas charged. Spatter ramparts typically form along both sides of erupting fissures, and fine tephra is deposited at distances as great as 10 km downwind, depending on lava-fountain height and wind speed. Flows are typically surface-fed, shelly pahoehoe; they accumulate in volumes less than 0.1 km^3 and cover areas less than 5 km^2.

After several days, the *second stage* begins. The erupting fissure system typically diminishes in length, and lava fountains become localized along short segments of a fissure. High fountains form tephra cones over earlier spatter ramparts. Diminished fountaining is typically followed by quiet, more voluminous outpouring of lava over and through tephra-cone walls. Tephra cones may be succeeded by small lava cones or small shields during latter parts of this stage. Flows of the second stage are typically surface-fed pahoehoe, although tube-fed flows form if eruption rates are fairly high.

A *third stage* occurs during long-lived eruptions: Lava fountaining diminishes and is followed by quiet, prolonged, voluminous outpouring of lava for periods of months or a few years, producing a large lava cone or shield volcano. Lava cone or shield summits typically have a crater elongated parallel to the underlying feeder fissure. Large craters may contain a lava lake characterized by pistonlike filling and draining. Proximal flows are largely surface-fed sheets of pahoehoe and slab pahoehoe; medial and distal flows are mostly tube-fed pahoehoe.

The enormous Hawaiian shield volcanoes, such as Mauna Loa and Mauna Kea, represent a *fourth stage* that results from eruptions that take place over thousands or a few million years from a central vent area and from volcanic rift zones. No lava fields of the ESRP correspond to the sustained eruptions of the fourth stage.

During Hawaiian volcanism, long-term eruptions tend to proceed through the four stages, though any one eruptive episode may terminate within the sequence. By inference, some prehistoric volcanic eruptions in the ESRP represent only the first stage of the eruptive sequence, and others proceeded to the second or third stages. Discussions of various lava fields of the ESRP that follow are described in terms of the three-stage eruption sequence.

VOLCANIC LANDFORMS AND LAVA TYPES OF THE ESRP

Shield volcanoes of the ESRP probably began as fissure eruptions, passed through the lava-cone stage, and formed by sustained eruptions lasting several months at a central vent or vent complex. Later-stage eruptive processes typically involved formation of a summit lava lake, pistonlike filling and draining of magma in the vent, collapse of vent walls, and formation of a lava field consisting mainly of tube-fed pahoehoe flows. Shelly-pahoehoe and slab-pahoehoe flows near vents formed from degassed, relatively high viscosity lava by overflow from lava lakes or discharge from rootless vents on lava tubes. Shield volcanoes are distributed widely in the ESRP, although the largest shields are typically located near the plain axis, suggesting that they overlie the main region of magma generation.

Lava flows of shield volcanoes in the ESRP extend as much as 30 km from their vents. Shields cover areas of 100 to 400 km^2 and have volumes of 1 to 7 km^3, the average being about 5 km^3. Dividing this figure into the total volume of basalt in the ESRP ($\sim 4.10^4$ km^3) suggests there may be as many as 8,000 shields in the ESRP. Considering that the ESRP began to form about 10 Ma and assuming a constant eruption rate, the recurrence interval for shield-forming eruptions of the ESRP is about one every 1,000 years.

Lava cones have heights of 10 to 30 m, cover areas of 1 to 50 km^2, and have volumes of 0.05 to 2 km^3. They consist mainly of surface- or channel-fed pahoehoe but have minor amounts of shelly pahoehoe and slab pahoehoe near vents. Tube-fed pahoehoe is present only in some of the larger lava cones. Evidently, sustained eruptions lasting more than several weeks and eruption rates in the range 10^3 to 10^4 kg/sec per meter of eruptive fissure (Kuntz, this volume) were necessary for pahoehoe lava to be distributed by lava tubes.

True a'a flows in the ESRP are found only in lava flows having SiO_2 contents of >50%, but exceptions occur in some flows in the late Pleistocene and Holocene Craters of the Moon (COM) lava field that descended steep slopes, such as the Lava Creek flows (Kuntz and others, 1988).

Although deposits of fissure-type eruptions are widely distributed throughout the ESRP, their contribution to the total volume of basalt lava flows of the ESRP is minimal. Deposits of fissure eruptions are described by Kuntz and others (1988) and are not discussed further here.

Tephra cones in the ESRP occur in two geologic settings: (1) those in the COM lava field formed from lava flows having SiO_2 contents of >50% and (2) cones formed in low areas where surface- or near-surface water played a part in their formation. Tephra cones in the COM lava field are some of the most imposing volcanic features in the ESRP. The largest cone, Big Cinder Butte (refer to Fig. 3), is 240 m high and covers an area of 3 km^2. Most other cones of the COM lava field are ~100 m high and cover areas of ~1 km^2 (Kuntz and others, 1988). Six small cones, each <20 m high and <200 m in diameter, occur within a 15-km^2 area of low elevation near Atomic City (refer to Fig. 4). About a dozen small cones occur at the east end of the Spencer–High Point volcanic rift zone (refer to Fig. 9). At this locality, basalt magma was emplaced in water-bearing sediments ponded between the southern margin of the Centennial Mountains and the Spencer–High Point zone. Tephra cones, like eruptive-fissure deposits, constitute a very small part of the total volume of basalt in the ESRP.

Deposits of hydrovolcanic eruptions are widely scattered in the ESRP. Sand Butte and Split Butte (refer to Fig. 7) consist of deposits of palagonitized sideromelane that surround inner lava lakes, which overlie single, pipelike sources of magma discharge (Womer and others, 1982). The Menan Buttes complex of tuff cones, described by Hackett and Morgan (1988), includes several late Pleistocene tuff cones and tuff rings that form the major part of the northwest-trending, 30-km-long Menan volcanic rift zone (refer to Figs. 7 and 18). The largest tuff cones are North Menan Butte (0.7 km^3) and South Menan Butte (0.3 km^3). Hydrovolcanic deposits, like the eruptive fissure and tephra-cone deposits, are also insignificant in the total volume of basalt in the ESRP.

In a series of three similar papers, Greeley (1977, 1982a, 1982b) described the Snake River Plain as being representative of a distinct type of basaltic volcanism, which he termed "plains volcanism." He suggested that this type is gradational between eruptions of flood lava flows and flows that form shield volcanoes. He also suggested that ESRP flows are emplaced primarily in one of three forms: (1) low shield volcanoes having slopes of less than 1°, (2) fissure flows (eruptive-fissure flows in our terminology), and (3) tube-fed flows. Although we do not disagree with Greeley's conclusions, our mapping suggests a different emphasis on the characteristic volcanic morphologies that make up the bulk of basaltic volcanism of the ESRP. We do not draw a distinction between shield volcanoes and tube-fed flows as does Greeley; we find that tube-fed flows constitute the largest volume of the shield volcanoes and parts of some large lava cones on the ESRP.

We conclude that coalesced shield volcanoes and lava cones, the flows of which are mainly of the tube-fed type, constitute more than 95% of the total volume of basalt in the ESRP. The remainder is made up of eruptive-fissure deposits, tephra cones, and deposits of hydrovolcanic eruptions, in that order.

LATEST PLEISTOCENE AND HOLOCENE LAVA FIELDS OF THE ESRP

Eight basalt or basalt-dominated lava fields in the ESRP appear as dark areas of low reflectance on Landsat images

(Lefebvre, 1975; Champion and Greeley, 1977). Because these fields are relatively young, their original surface morphology is well preserved, except where some are locally covered by thin eolian deposits. Radiocarbon studies (Kuntz, Spiker, and others, 1986) show that these fields are very latest Pleistocene or Holocene in age. These eight lava fields are, from west to east, the Shoshone, Craters of the Moon, Wapi, Kings Bowl, North Robbers, South Robbers, Cerro Grande, and Hells Half Acre fields (Fig. 2). Descriptive data for these fields—length and width of fissures, types of flows, areas and volumes of flows and fields, and stages of basaltic volcanism represented—are summarized in Table 1. The best-studied of these lava fields is the Craters of the Moon field.

Craters of the Moon (COM) lava field

The COM lava field, the largest basaltic, dominantly Holocene lava field in the conterminous United States, has been described by Kuntz and others (1982); Kuntz, Champion, and others (1986); Kuntz, Champion, and Lefebvre (1989); Kuntz, Lefebvre, and Champion (1989a, 1989b); and Champion and others (1989). It is therefore reviewed here only briefly. It contrasts with most other lava fields of the ESRP because it is a composite, polygenetic field composed of at least 60 flows erupted from 25 tephra cones and at least eight eruptive fissure systems aligned along the northern part of the Great Rift volcanic rift zone (Fig. 3). Most other lava fields at the ESRP represent single, monogenetic eruptions from vents that are widely scattered in both space and time.

The COM field covers about 1,600 km^2 and contains about 30 km^3 of lava flows and associated vent and pyroclastic deposits. Stratigraphic relationships, paleomagnetic studies, and radiocarbon ages (Kuntz, Spiker, and others, 1986) show that the COM field formed during eight eruptive periods, designated as H, oldest, to A, youngest. Each eruptive period was several hundred years or less in duration and separated from other eruptive periods by recurrence intervals of several hundred to about 3,000 years. The first eruptive period began about 15,000 years ago, and the latest eruptive period ended about 2,100 years ago. Because the present interval of dormancy has lasted ~2,100 years, it seems likely that another eruptive period will occur within the next 1,000 years.

There is a broad range in the chemical composition of lava flows of the Craters of the Moon, Kings Bowl, and Wapi lava fields along the Great Rift. Kuntz, Champion, and others (1986) defined three magma types based on chemical parameters and petrologic characteristics. The types are (1) a contaminated type that has an SiO_2 range of ~49 to 64% and commonly shows petrographic evidence of crustal contamination, (2) a fractionated type that has an SiO_2 range of ~44 to 54% and chemical and mineralogical variation that can be accounted for mainly by crystal fractionation, and (3) a Snake River Plain type that has an SiO_2 range of ~45 to 48% and shows little evidence of fractionation. The contaminated and fractionated magma types are represented by flows of the COM lava field. The Snake River Plain magma type is represented by flows of the Kings Bowl and Wapi lava fields and by the majority of other lava fields of the ESRP.

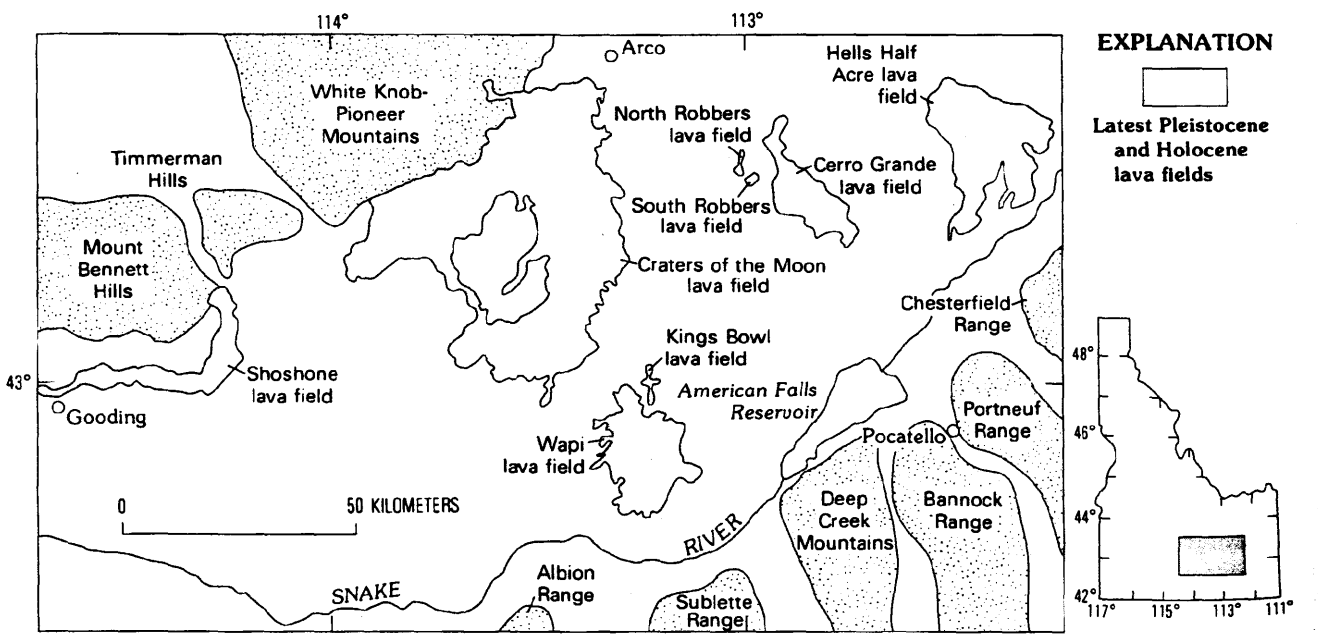

Figure 2. Map showing latest Pleistocene and Holocene lava fields of the eastern Snake River Plain.

Hells Half Acre lava field

The second-largest Holocene lava field in the ESRP is the Hells Half Acre field, a shield volcano about 20 km east of Atomic City (Figs. 2 and 4). The age of the Hells Half Acre lava field is 5,200 ± 150 B.P. (Kuntz, Spiker, and others, 1986). Eruption models (Kuntz, this volume) suggest that the Hells Half Acre field formed over a period of several months. The major study of the field is by Karlo (1977), and most of the field is mapped by Kuntz and others (1992).

The vent area for the Hells Half Acre lava field consists of a flat-floored crater, 0.8 km long and 0.3 km wide, and several spatter cones. A lava lake in the crater floor contains about 10 roughly circular pit craters that are typically <100 m wide and ~5 m deep. Pistonlike draining and filling of the main crater occurred during the last stages of eruptive activity in the crater.

Several small spatter cones and short spatter ramparts lie within the main crater. Five small spatter cones are distributed over a distance of 2 km southwest of the main crater, and two small spatter cones occur about 0.5 km northwest of it. The northwest-southeast–trending eruptive fissure defined by the main crater and spatter cones is about 3 km long.

About 10 km^2 of shelly pahoehoe partly surround and extend out from the main crater for as much as 1.5 km. These flows formed as overflow from the lava lake and from eruptions from spatter cones. As in other latest Pleistocene and Holocene lava fields of the ESRP, lava-tube systems are limited to the proximal and medial parts of the Hells Half Acre lava field; they have not been recognized in distal parts. Two prominent lava-tube systems occur in the proximal parts of the Hells Half Acre lava field. Rootless vents in the tube systems were the sources of some of the youngest pahoehoe flows of the field (Fig. 4).

Slab-pahoehoe flows also partly surround the vent area for distances of several kilometers. In the Hells Half Acre field and other fields in the ESRP, slab pahoehoe formed where partly congealed crust was broken and disturbed as pahoehoe moved over steep, rough topography near vents and also where more viscous degassed lava erupted from lava lakes or rootless vents along lava tubes.

The distal part of the field consists of two major flow lobes, each about 5 km wide and 10 km long. The flows of these lobes moved down the southeast flank of the axis of the ESRP and then extended south and southwest on reaching the flood plain of the Snake River.

Two sets of parallel noneruptive fissures, 1.5 km apart, extend N.50°W. from the Hells Half Acre field (Fig. 4). Each set is about 3.5 km long and consists of en echelon cracks that are 300 m to 1.2 km long. A southeast projection of the noneruptive fissures into the Hells Half Acre lava field forms a three-part fissure system: The eruptive fissure is flanked by noneruptive fissures. This geometry is also present in the Kings Bowl lava field.

Cerro Grande lava field

The Cerro Grande lava field is a small shield volcano fed from a vent that occurs on an extension of a normal fault (down to the east) on the southern flank of Cedar Butte (Fig. 4). The present vent is a shallow depression about 750 m in diameter. An earlier vent was considerably larger, but it was filled by lava that overflowed a late-stage lava lake. Lava tubes occur several kilometers from the vent area, suggesting that near-vent parts of the tubes are filled by lava overflow from the lake. Tephra cones and eruptive fissures characteristic of vent areas of other small shield volcanoes in the ESRP are absent in the Cerro Grande vent area. If originally present, they may also have been covered by overflow from the lava lake. The field was emplaced 13,380 ± 350 B.P. (Kuntz, Spiker, and others, 1986).

The western margin of the southern part of the field is locally indistinct owing to partial cover by eolian sediment. In this respect, the Cerro Grande field is like the North Robbers and South Robbers lava fields, whereas the other latest Pleistocene and Holocene lava fields of the ESRP are essentially free of sediment cover. Porter and others (1983) suggest that Pinedale glacial conditions ended in the ESRP about 11 to 10 ka; thus much of the eolian sediment could have been deposited soon after emplacement.

North and South Robbers lava fields

Two of the smallest late Pleistocene and Holocene lava fields of the ESRP, the North Robbers and South Robbers fields, are a few kilometers west of the Cerro Grande lava field (Fig. 4). The eruptive fissure system for the North Robbers field consists of two segments: The 1-km-long northern segment, which includes both noneruptive and eruptive parts, is offset in alignment about 400 m west from the southern segment, which is 1.2 km long and consists entirely of eruptive fissures. A collinear extension of the northern eruptive fissure, consisting of noneruptive cracks in sediments, extends across the southeast flank of Big Southern Butte for a distance of 700 m. Flows of the North Robbers field were fed mainly by a 2-km-long lava channel that extends from the southern segment of the eruptive fissure system (Fig. 4).

Vents for the South Robbers lava field are aligned along a 1.8-km-long eruptive fissure system. A 150-m-long fissure flanked by spatter ramparts occurs at the south end, and four small tephra cones occur along the north end of the eruptive fissure. A 600-m-long lineation visible on air photos, probably a noneruptive set of cracks, is collinear with and extends northwest from the eruptive fissure system. The South Robbers fissure system lies 1.2 km south and is offset in alignment 600 m west of the eruptive fissures for the North Robbers field. A lava channel that originated at the largest tephra cone was the main distributary for surface-fed flows in the distal part of the South Robbers lava field (Fig. 4).

TABLE 1. CHARACTERISTICS OF FISSURE VENTS AND FLOWS FOR SELECTED ERUPTIONS IN LATEST PLEISTOCENE AND HOLOCENE LAVA FIELDS OF THE EASTERN SNAKE RIVER PLAIN, IDAHO*

Lava Field Flow Name	Length of Eruptive Fissures: Single Fissures (km^2)	Length of Eruptive Fissures: Whole Zone (km^2)	Estimated Width of Fissures (m)	Area of Lava (km^2)	Estimated Flow/Field Volume (km^3)	Flow Type	Comments
Craters of the Moon							
Broken Top	Unknown	<0.3	Unknown	11	0.1	Surface- and tube(?)-fed pahoehoe flows.	Intermediate-volume stage-2 eruption. Flow issued from two obscure vents on east and south sides of Broken Top cinder cone. Vents now largely obscured by colluvium
Blue Dragon	0.6	1	1 to 2	280	3.4	Tube-fed pahoehoe flows.	Large-volume sustained lava-cone eruption of stage 3. Eruptions from southernmost cinder cone in Big Crater complex and from 0.5-km-long fissure south of Big Craters. Spatter cones along fissure have internal diameters of 1 to 3 m. Fissure width estimated from smallest diameters.
Trench Mortar Flat	0.3 to 1.3	6	≤2	6	0.03	Shelly, thin pahoehoe flows.	Small-volume stage-1 fissure eruption. Flows erupted from 0.3- to 1.3-km en echelon segments in 6-km zone of eruptive fissures. Fissure widths estimated where enlargement by erosion seemed minimal.
North Crater	Unknown	Unknown	Unknown	1.5	0.01	Surface-fed pahoehoe.	Small-volume eruption from pipelike vent, which is now covered by colluvial cinders from inner wall of North Crater.
Big Craters	≤0.2	0.9	1 to 2	9	0.05	Surface-fed pahoehoe and slab pahoehoe flows.	Small-volume stage-2 eruption. Two source fissures north of Big Craters cinder cone complex are short (≤0.2 km), but Big Craters cinder cone complex is aligned along fissure system 0.9 km long. Fissure width estimated from deepest part of eastern eruptive fissure.
Serrate, Devils Orchard, and Highway	Unknown	...	Unknown	27†	0.5†	Bulbous, block flows.	Vent area near North Crater largely destroyed by eruptions, also covered by younger North Crater flow. Eruption was explosive because remnants of crater walls are contained in flow. Eruptions may have been from central pipelike vent in North Crater.
Vermillion Chasm	0.6 to 1	2.9	1 to 2	20	0.1	Shelly, thin pahoehoe flows.	Small-volume stage-1 fissure eruption. Eruptive fissures enlarged at most localities by explosive venting. Fissure width estimated at deepest, narrowest part of fissure system. Fissure system is 2.9 km long; consists of 3 fissures that range from 0.6 to 1 km in length.
Deadhorse	0.1 to 0.6	10	≤1.5	8	0.04	Shelly pahoehoe and thin pahoehoe flows.	Small-volume stage-1 fissure eruption. Many thin flows were erupted from numerous (>13) en echelon, right-stepping eruptive fissures that range from 0.1 to 0.6 km in length. The Deadhorse fissure system is the longest known fissure system that was active along the Great Rift volcanic rift zone during a single eruptive pulse.
Devils Cauldron	(>0.3)	...	Unknown	90	0.9	Tube- and surface-fed pahoehoe flows.	Intermediate-volume stage-2 eruption from central vent on lava cone. Lava lakes perched above vents. Fissure and vent are obscured by flows and lava lakes.
Minidoka	Unknown	...	Unknown	250	3.0	Chiefly tube-fed pahoehoe flows.	Large-volume, sustained stage-3 eruption from central vent complex that is now covered by flows.

TABLE 1. CHARACTERISTICS OF FISSURE VENTS AND FLOWS FOR SELECTED ERUPTIONS IN LATEST PLEISTOCENE AND HOLOCENE LAVA FIELDS OF THE EASTERN SNAKE RIVER PLAIN, IDAHO (continued)

Lava Field Flow Name	Length of Eruptive Fissures: Single Fissures (km^2)	Length of Eruptive Fissures: Whole Zone (km^2)	Estimated Width of Fissures (m)	Area of Lava (km^2)	Estimated Flow/Field Volume (km^3)	Flow Type	Comments
Hells Half Acre	Unknown	2	Unknown	400	6	Chiefly tube-fed pahoehoe flows with minor surface-fed shelly, and slab pahoehoe flows near vent area.	Large-volume, sustained stage-3 eruption from central vent complex that contained a large lava lake. Collapse pits, spatter cones, and the main depression define the length of main eruptive fissure.
North Robbers	<0.5	2.9	Unknown	5	0.05	Chiefly surface-fed pahoehoe and minor shelly pahoehoe flows near vents.	Small-volume stage-1 fissure eruption. Eruptive features defined by spatter ramparts and small cinder cones. Noneruptive fissure 0.7 km long extends north of eruptive fissures.
South Robbers	1.1	1.7	Unknown	3	0.03	Chiefly surface-fed pahoehoe and minor shelly pahoehoe flows near vents.	Small-volume stage-1 fissure eruption. Eruptive fissures defined by spatter ramparts and small cinder cones. A 0.6-km-long noneruptive fissure extends north of eruptive fissures.
Cerro Grande	Unknown	Unknown	Unknown	175	2.3	Chiefly tube- and surface-fed pahoehoe flows.	Relatively large-volume stage-3 eruption. Poorly defined vent area filled by a lava lake.
Kings Bowl	0.1 to 0.5	6.2	0.5 to 1§	3.3	0.005	Shelly pahoehoe and thin pahoehoe flows.	Small-volume stage-1 fissure eruption. Eruptions from about a dozen fissures in a zone about 6.5 km long. Dikes ≤1.5 m thick exposed in fissure at Kings Bowl (see Greeley and others, 1977, Figs. 11-14, 11-16; Greeley, 1977, Fig. 3-19).
Wapi	...	>0.6	Unknown	325	6	Surface- and tube-fed pahoehoe flows.	Large-volume stage-3 eruption. Vent complex consists of 11 eruptive centers aligned over a buried eruptive fissure (Champion and Greeley, 1977).
Shoshone	Unknown	Unknown	Unknown	190	1.5	Chiefly tube- and surface-fed pahoehoe flows. Shelly pahoehoe and slab pahoehoe flows near vent.	Relatively large-volume stage-3 eruption. Vent area modified by late-stage lava lake. Lava tubes recognized only in proximal parts of lava field. Lava lake activity with pistonlike draining and filling of vent depression.

*Data from Kuntz, Champion, and others (1986, 1992); Kuntz, Lefebvre, and Champion (1989a, b); Kuntz, Champion, and Lefebvre (1989); and this chapter.
†Total for all three flows.
§Measured width.

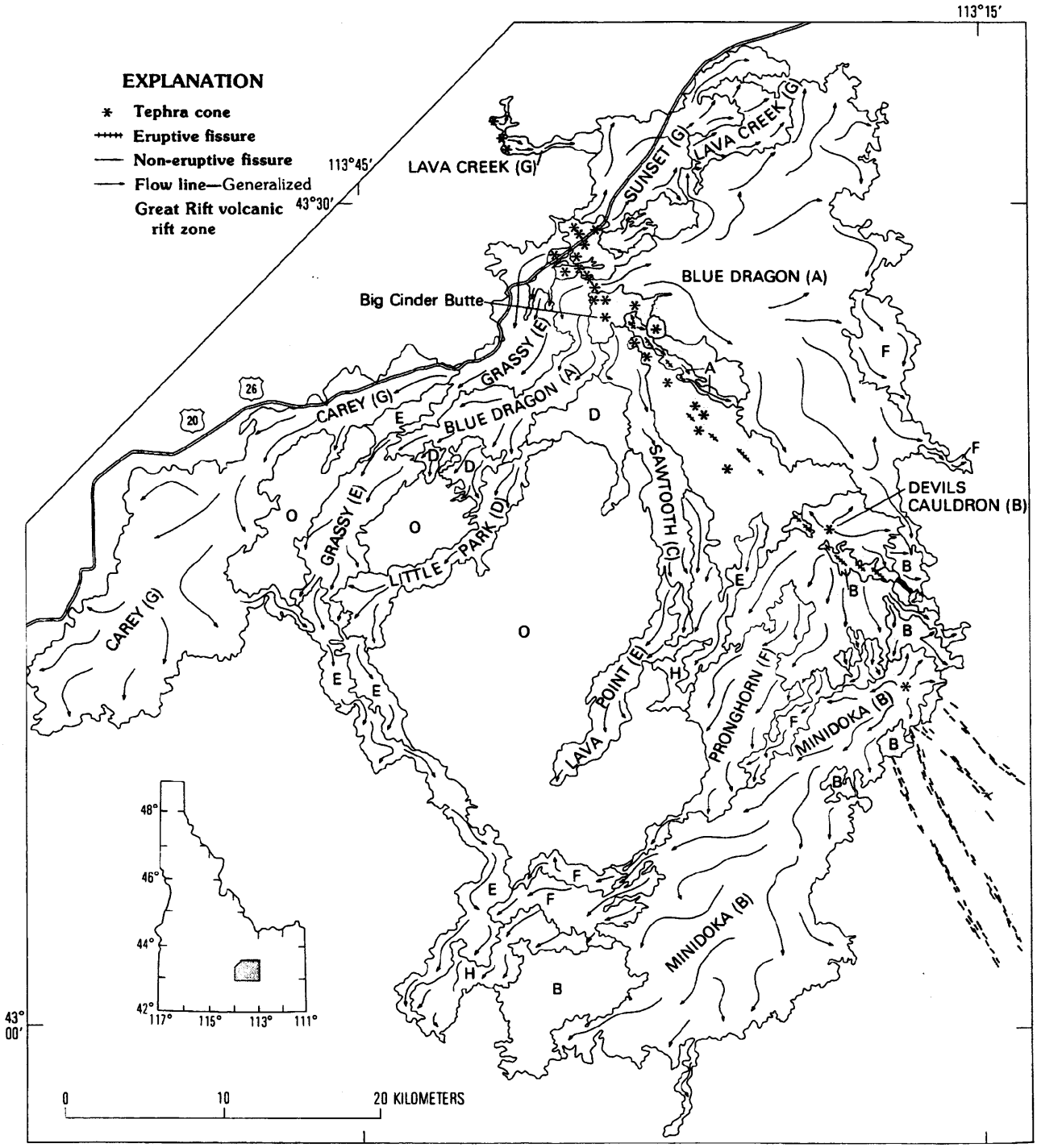

Figure 3. Map of the Craters of the Moon lava field. Map is greatly simplified in area of vents along the Great Rift volcanic rift zone. Some lava flows are shown by name, but most flows are not. However, flow ages are shown by letters that designate eruptive periods from H, oldest, to A, youngest. Several large kipukas within the COM lava field, consisting of flows older than flows of the COM lava field, are designated by the letter O. Adapted from Kuntz and others (1988).

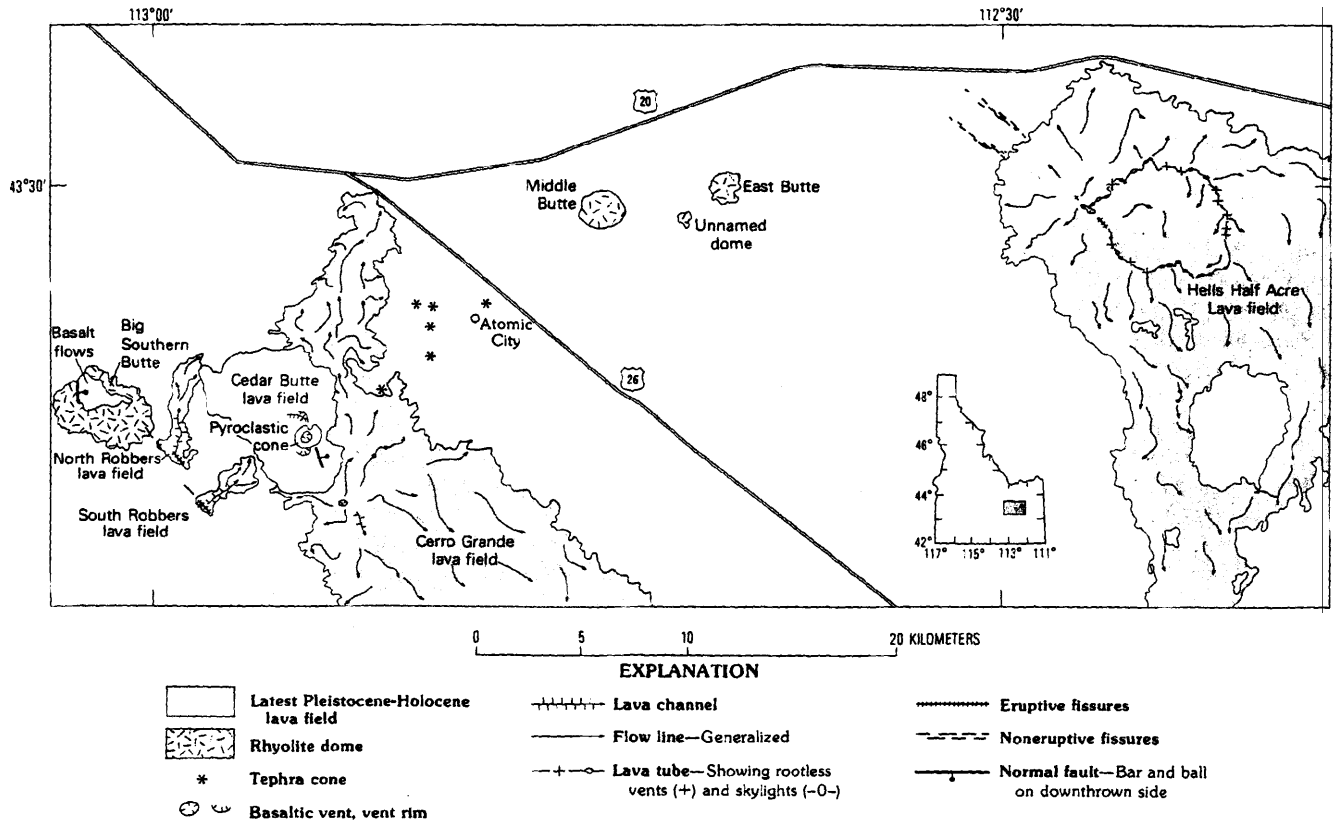

Figure 4. Map of the central part of the eastern Snake River Plain showing parts of the Hells Half Acre and Cerro Grande lava fields and the North Robbers and South Robbers lava fields. Also shown are rhyolite domes (Big Southern Butte, Middle Butte, an unnamed dome, and East Butte) and the Cedar Butte lava field. Adapted from Kuntz and others (1992).

Slab pahoehoe in distal flows and steep flow fronts, as high as 15 m, suggest that flows of the South Robbers field were slightly more viscous and/or were erupted at slower rates than other ESRP basaltic flows.

The North Robbers and South Robbers fields probably formed simultaneously because they are parts of the same eruptive fissure system and have similar paleomagnetic field directions (Champion, 1980). Radiocarbon samples were not obtained for the South Robbers field; the age for the two fields is based on two radiocdarbon ages for the North Robbers field, 11,940 ± 300 and 11,980 ± 300 B.P. (Kuntz, Spiker, and others, 1986).

Flows of the two fields are partly covered by eolian sediment only on their western edges, those closest to sediment sources upwind to the west and southwest. The North and South Robbers fields are mapped by Kuntz and others (1992).

Kings Bowl lava field

The Holocene Kings Bowl lava field lies along the southern part of the Great Rift volcanic rift zone, 12 km southeast of the Craters of the Moon lava field and 1 km north of the Wapi lava field (Figs. 2 and 5; refer also to Fig. 8). The Kings Bowl field has received considerable study (King, 1977; Greeley and others, 1977; Covington, 1977; and Kuntz and others, 1983) because of its small size and easy access. The fissure system in the Kings Bowl area consists of a central eruptive fissure set, about 6.2 km long, trending N.10°W., which is flanked by two subparallel sets of noneruptive fissures that are from 600 to as much as 1,100 m from the main eruptive fissure (Fig. 5). The western noneruptive fissures have a fairly uniform width of about 200 m; the eastern noneruptive fissures have a variable width, ranging from a few meters to 400 m.

The central eruptive fissures consist of discontinuous *en echelon* cracks, 2 to 3 m wide, that are locally filled by breccia and feeder dikes. These short segments, a few meters to 500 m long, are separated by open, noneruptive cracks or by lava that covers eruptive and noneruptive fissures. Feeder dikes, 0.5 to 1 m wide (Figs. 11–14 and 11–16 of Greeley and others, 1977; Fig. 3–19 of Greeley, 1977), are exposed in the central eruptive fissure set, one of the few places where such dikes are exposed in the ESRP.

Small tephra cones, <300 m long and <10 m high, formed

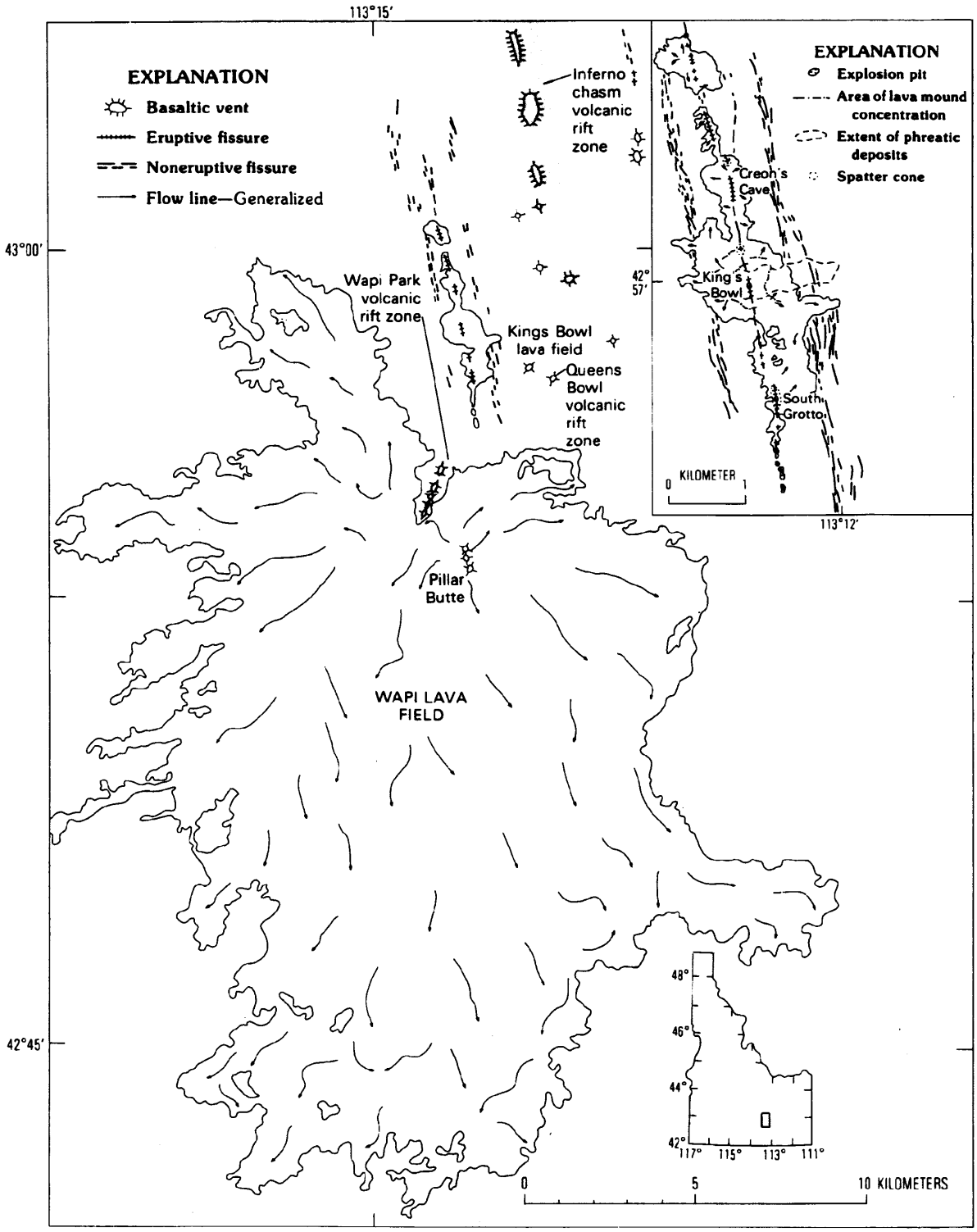

Figure 5. Map of the Wapi and Kings Bowl lava fields. Inset shows greater detail of the Kings Bowl lava field. Also shown are volcanic rift zones discussed in the text. Adapted from King (1977, 1982), Covington (1977), and Kuntz and others (1983, 1988).

along short eruptive fissures at South Grotto and Creons Cave (Fig. 5). Low spatter ramparts occur along a few of the eruptive fissure segments.

The small Kings Bowl lava field possesses excellent examples of certain volcanic landforms that are either poorly developed or simply not present elsewhere in the ESRP. These include explosion pits, lava lakes, squeeze-ups, basalt mounds, and a tephra blanket. The largest explosion pit, Kings Bowl, is 85 m long, 30 m wide, and 30 m deep. A roughly circular lava lake, about 1 km in diameter, surrounded Kings Bowl prior to the explosive eruption. The lake is flat and broken into large plates as a result of subsidence of underlying lava. Basalt mounds several meters wide and <1 m high may be remnants of levees that surrounded the lava lake (King, 1977). A blanket of lapilli tephra east (downwind) of the explosion pit at Kings Bowl is <0.5 m thick, 1.2 km long, and 400 m wide (Fig. 5, inset). King (1977) showed that the volume of the tephra blanket falls short of that needed to occupy the cavity of Kings Bowl, indicating collapse in the vent area subsequent to the explosive event.

The Kings Bowl field represents a single burst of eruptive activity that may have lasted as little as six hours (Kuntz, this volume). A radiocarbon age of 2,222 ± 100 B.P. has been obtained for the Kings Bowl lava field (discussed by Kuntz, Spiker, and others, 1986).

Wapi lava field

Marked contrasts between the Kings Bowl and Wapi fields reflect different styles of eruption. The eruptions that formed the Kings Bowl and Wapi fields probably started simultaneously, but eruption terminated at Kings Bowl after only a few hours and continued at the Wapi site for at least a few months (Kuntz, this volume). The Wapi lava field probably began as a fissure eruption and, with more prolonged activity, progressed to a sustained eruption from a central vent complex, forming a low shield volcano typical of a third-stage eruption.

The vent area for the Wapi field is 4 km south of the southernmost vents of the Kings Bowl lava field (Fig. 5). The Wapi vents are part of the Great Rift volcanic rift zone, but they do not lie on an extension of the fissures of the Kings Bowl rift system. A complex of five major vents and six smaller vents, covering an area of ~0.5 km^2, constitutes the vent area. The vents are steep-sided, roughly circular depressions typically 100 m in diameter and 10 m deep. The largest depression contains several pit craters that display the ledges of lava lakes that filled the crater. Lava tubes are exposed in walls of some of the depressions. Flows of the summit area are chiefly shelly pahoehoe and minor slab pahoehoe. Pillar Butte, a mass of agglutinate and layered flows, rises 18 m above the south side of the largest vent. The origin of Pillar Butte is unclear; its relief is due either to inflation by injection of dikes or to deflation of the area around it (Champion, 1973).

Most flows in the medial and distal parts of the field are tube-fed pahoehoe composed of numerous flow units piled side by side and atop one another, forming a type of lava flow described by Walker (1972) as compound. Exposures in many kipukas along the south and west sides of the lava field show that the flows there have an aggregate thickness of 5 to 10 m. Flow thicknesses near the center of the field are 15 to 25 m except at the vent area, where the total thickness may be 100 m (Champion, 1973). Near the margins of the field, the flow units are larger, tend to have greater local relief (as much as 10 m), and are characterized by large pressure plateaus, flow ridges, and collapse depressions. The transition in size of the flows from the periphery to the interior of the field is apparently a function of proximity to the vent area; thus, closer to the vent, many small pahoehoe flows have filled depressions in earlier flow units and generally leveled the local relief.

A radiocarbon age of 2,270 ± 50 B.P. was obtained for charcoal from a tunnel excavated beneath the Wapi lava field (Champion and Greeley, 1977; Kuntz, Spiker, and others, 1986). Within limits of analytical error, the ages of the Kings Bowl and Wapi lava fields are identical.

Shoshone lava field

The Shoshone lava field is the westernmost of the latest Pleistocene and Holocene lava fields of the ESRP (Fig. 6). Its vent area, Black Butte Crater, is on the northern margin of the ESRP about 20 km northwest of Richfield at the eastern end of the Mt. Bennett Hills. Flows from Black Butte Crater filled parts of the alluvial valleys of the Big Wood and Little Wood rivers, thus forming a lava field that extends 60 km south and west and ranges in width from 2 to 5 km. The Big Wood and Little Wood rivers joined about 10 km southwest of Richfield prior to eruption of the Shoshone flow. At present, the Big Wood River follows the north margin and the Little Wood River follows the south margin of the Shoshone field. These two rivers now join 10 km west of Gooding, 40 km west of their original junction (Fig. 6).

The summit vent area is a complex lava lake that forms a six-petal, flower-shaped depression. The lake has an area of 2 km^2, and its steep walls are as high as 30 m. The lava lake shows evidence of pistonlike filling and draining and extensive overflow by degassed lava. The overflow formed broken shelly-pahoehoe and slab-pahoehoe flows that are distributed in a radial pattern around the lava-lake vents.

There are no obvious features in the vent area, such as eruptive fissures, spatter ramparts, or small cones, that might indicate the length of the original eruptive fissure system. Evidence is also lacking for any structural control for the orientation of the original fissure system, but faults in the Mt. Bennett Hills and the elongation of vents for nearby older volcanoes trend N.35–50°W. (Fig. 6).

A 5-km-long lava tube-channel system extends southeast from the vent area (Fig. 6). The tube system had both roofed and unroofed sections during formation of the field. Many of the formerly roofed parts have collapsed, leaving open trenches that

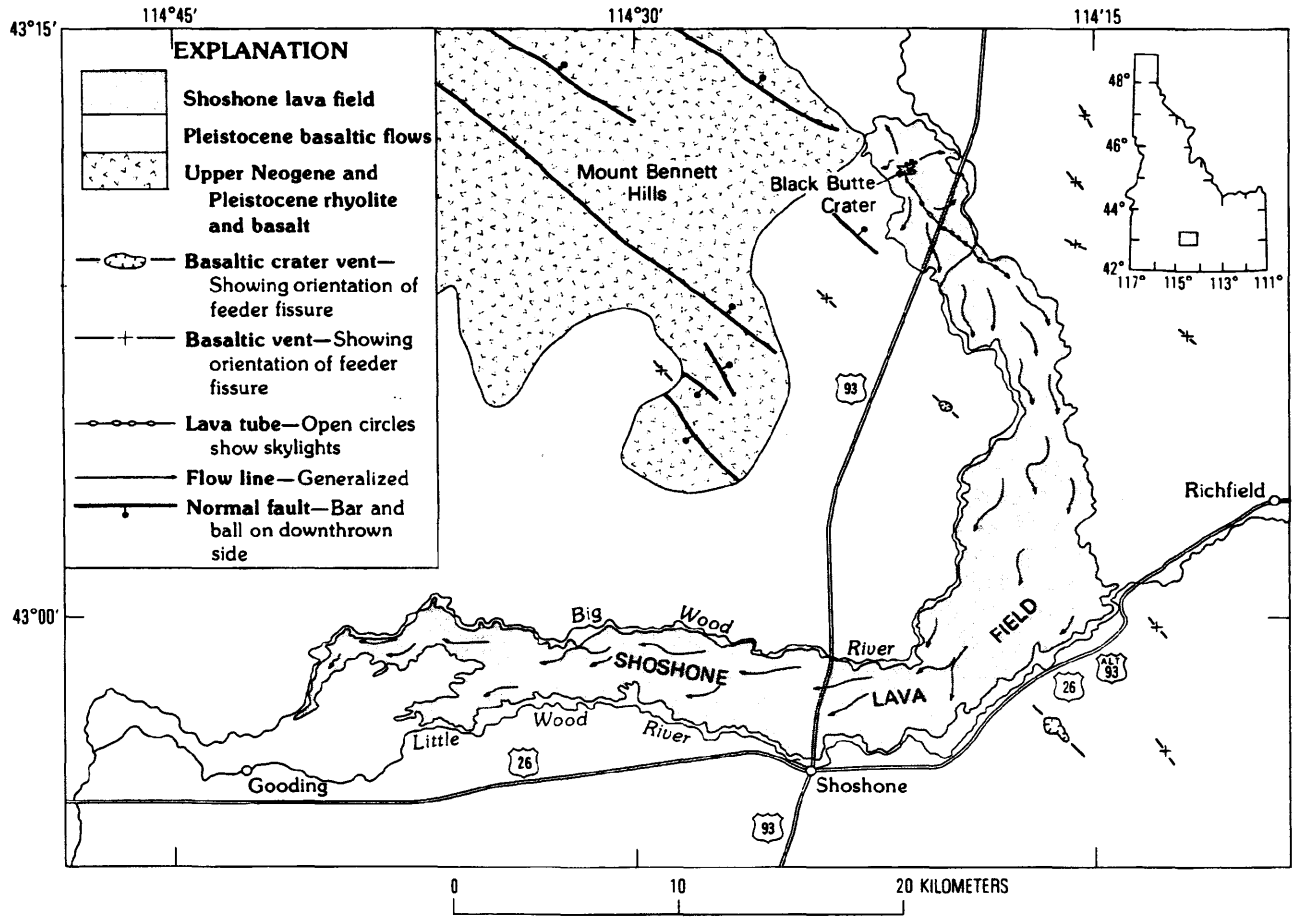

Figure 6. Map of the Shoshone lava field. Based on LaPoint (1977) and unpublished mapping by M. A. Kuntz.

are continuous with the unroofed sections. Smaller distributary tubes that branch from the main tube are still preserved (Greeley, 1977).

The medial and distal parts of the Shoshone lava field consist of pahoehoe flows and flow units that have an average thickness of 6 m. Whether these flows are tube- or surface-fed is not clear. Lava tube systems have not been recognized in medial and distal parts of the lava field, but fields of this size and volume are typically formed of tube-fed pahoehoe. The age of the Shoshone field is 10,130 ± 350 B.P. (Kuntz, Spiker, and others, 1986).

Summary of Holocene and latest Pleistocene basaltic lava fields

The eight latest Pleistocene and Holocene lava fields of the ESRP represent the entire span of lava-field types, eruption processes, and eruption durations described in the section on stages of basaltic eruptions. The fields include short-duration, low-volume eruptions from a long eruptive-fissure system (Kings Bowl, North Robbers, South Robbers fields); intermediate-volume and intermediate-duration eruptions that formed lava cones or small shields (for example, the Holocene Devils Cauldron flow of the COM lava field; see Kuntz, Champion, and Lefebvre, 1989; Fig. 3); and large-volume, relatively long duration eruptions from central vents (Hells Half Acre and Wapi fields).

Individual eruptive fissures range in length from 0.1 km to slightly more than 1 km and average about 0.5 km. The data are highly skewed toward small-volume, eruptive-fissure-dominated eruptions, because those eruptions tend to leave eruptive fissures unburied, whereas large-volume eruptions do not.

Eruptive fissure zones vary in length from <0.3 km to about 10 km; the average is about 3 km. The shorter zones produced small-volume eruptive-fissure eruptions, and the longer ones generated large-volume lava-cone or shield-building eruptions. Sustained eruptions occurred from central vents overlying pipe-like conduits along eruptive fissures. However, the elongation of

most vents in lava cones and shield volcanoes shows that eruptive fissures still influenced the location and shape of these central vents.

The areas, volumes, and types of lava fields of the ESRP are functions chiefly of the eruptive stage at which the eruption terminated. Stage-1 fissure eruptions are characterized by flow areas of 2 to 20 km^2, flow volumes of 0.005 to 0.1 km^3, and surface-fed pahoehoe, much of which is shelly pahoehoe near vents. In stage-2 eruptions, lava cones cover areas of 10 to 100 km^2, have volumes of 0.05 to 2 km^3, and consist mostly of surface- and channel-fed pahoehoe. Some large lava cones consist chiefly of tube-fed pahoehoe. Shield volcanoes of stage-3 eruptions cover areas of 100 to 400 km^2, have volumes of 1 to 7 km^3, and consist mainly of tube-fed pahoehoe.

Among these latest Pleistocene and Holocene lava fields (Table 1), the aggregate volume from the stage-1 fissure eruptions (North Robbers, South Robbers, and Kings Bowl) is only 0.085 km^3, whereas the stage-3 shield and lava-cone eruptions (Craters of the Moon, Hells Half Acre, Cerro Grande, Wapi, and Shoshone) produced about 45 km^3. The contrast between these figures illustrates the predominance of the latter type of volcanism in contributing to the total basalt volume of the ESRP (Table 1). The latest Pleistocene and Holocene lava fields cover about 2,600 km^2 (13%) of the 20,000 km^2 area of the ESRP.

VOLCANIC RIFT ZONES

Basaltic volcanism occurs as fissure eruptions within volcanic rift zones in many parts of the world, including Hawaii (Macdonald and Abbott, 1970), Iceland (Macdonald, 1972), and the ESRP (Kuntz, 1977a). The volcanism of the ESRP is concentrated in volcanic rift zones, though it is not confined to them.

In the ESRP, most volcanic rift zones are roughly perpendicular to the axis of the ESRP and roughly parallel to the major basin-and-range structures in mountains that bound the plain. Kuntz (1977a) noted that most of the volcanic rift zones appear to be continuations onto the ESRP of basin-and-range-type, range-front faults and older structures, such as thrust faults, which occur in the bedrock of the mountains outside the ESRP (Figs. 7 and 11). It is important to note that the term *volcanic rift zone,* as applied here, merely designates linear arrays of volcanic landforms and structures; it does not imply that these features have origins, histories, or structures like those of rift valleys.

Some volcanic rift zones of the ESRP are well-defined, narrow, linear to curvilinear belts that contain numerous, geologically young volcanic structures and landforms. These zones illustrate vigorous, relatively concentrated eruptive activity. Examples are the Great Rift and Spencer–High Point volcanic rift zones (Fig. 7; also refer to Figs. 8 and 9). Other volcanic rift zones are less well defined; their presence is indicated by fissure-controlled elongated vents and noneruptive fissures aligned in belts. These zones illustrate sporadic, dispersed eruptive activity. For example, the Lava Ridge–Hells Half Acre zone and other volcanic rift zones in the central part of the ESRP are belts that consist of fewer, relatively older structures and volcanic landforms (Fig. 7).

Radiometric data currently available for ESRP lava flows (Kuntz and others, 1992) suggest that the volcanic activity in the well-defined zones occurred over a period of a few tens or hundreds of thousands of years and that repose intervals between eruptions are on the order of 10^4 to 10^5 years. The radiometric data further suggest that the less well defined volcanic rift zones formed from eruptions that occurred over periods of several hundred thousand to a few million years and that repose intervals between eruptions are on the order of 10^5 to 10^6 years.

Volcanic rift zones of the ESRP typically are 5 to 20 km wide and 50 to 100 km long, are spaced roughly 35 km (range of 20 to 40 km) apart, and trend northwest (Fig. 7). The spacing between rift zones is similar to the 35-km spacing between Basin and Range mountains and their intervening valleys north and south of the ESRP. Two exceptions to the general northwest trend are the Rock Corral Butte and Spencer–High Point volcanic rift zones (Fig. 7; also refer to Figs. 8 and 9).

Some of the major volcanic rift zones of the ESRP are described below in order from west to east.

The Great Rift volcanic rift zone

The Great Rift (Russell, 1902; Stearns, 1928; Murtaugh, 1961; Prinz, 1970; Kuntz and others, 1982, 1983, 1988; Kuntz, Champion, and others, 1986) is the most important volcanic rift zone in the Snake River Plain. It is an 85-km-long, 2- to 15-km-wide system of fractures that extends nearly across the width of the Snake River Plain (Figs. 7 and 8). The Great Rift is defined by an array of tephra cones, shield volcanoes, lava cones, eruptive fissures, and noneruptive fissures. The latest Pleistocene and Holocene Craters of the Moon, Kings Bowl, and Wapi lava fields are aligned along the Great Rift volcanic rift zone (Kuntz and others, 1988; Fig. 8).

The vents of the COM field define the northern 45 km of this volcanic rift zone. These vents include about 25 tephra cones and more than eight eruptive-fissure systems (Figs. 3 and 8). The Great Rift volcanic rift zone extends northwest into the Pioneer Mountains; the tephra-cone vents of the Lava Creek flows of the COM field occur about 10 km beyond the topographic margins of the ESRP (Fig. 3).

The Great Rift continues from the southeastern margin of the Craters of the Moon lava field as two groups of noneruptive fissures (Figs. 3 and 8). The northeastern group consists of individual fissures 150 to 600 m long. This group of fissures is oriented N.45°W. and extends about 8 km beyond the southeast margin of the COM lava field. The southwestern group consists of fissures 100 to 1,000 m long, oriented N.25°W., that extend for about 15 km beyond the southeast margin of the COM field. The eastern and western groups of fissures constitute the open crack rift set of Prinz (1970). The Kings Bowl eruptive and noneruptive fissures, described previously in the discussion of the Kings Bowl lava field, constitute the main part of the Great Rift volcanic rift zone just south of the open crack rift set (Figs. 5 and 8).

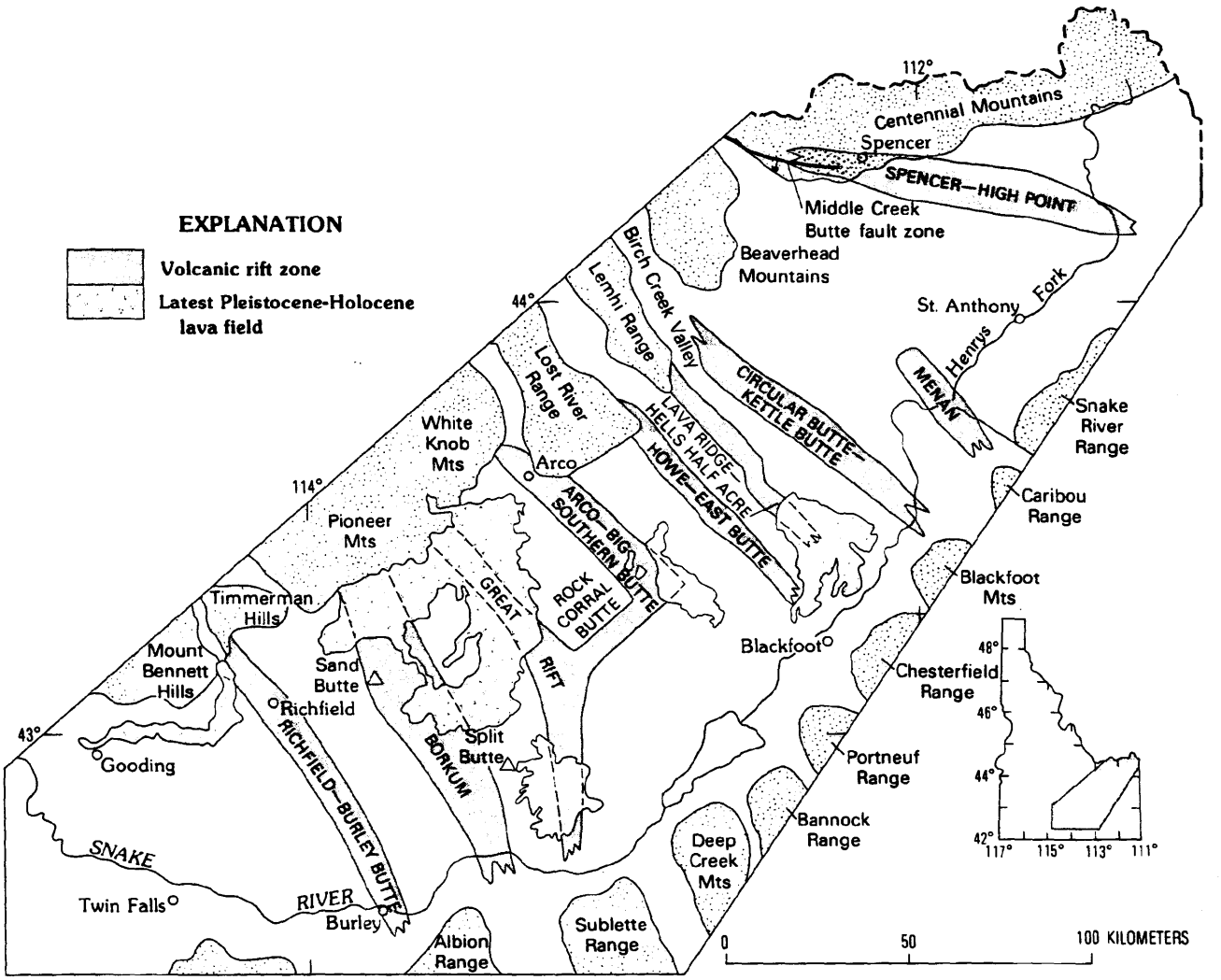

Figure 7. Map of the eastern Snake River Plain showing volcanic rift zones and other geologic and geographic features discussed in the text. Also shown are two hydrovolcanic features—Sand Butte and Split Butte—and latest Pleistocene and Holocene lava fields.

The Inferno Chasm volcanic rift zone (Greeley and King, 1975; King, 1982) is a narrow, 10-km-long, N.10°W.-trending belt that is parallel to and lies 3 km east of the Kings Bowl volcanic rift zone (Fig. 5). The Inferno Chasm zone is marked by six aligned lava cones and shield volcanoes. Flows from vents on the Inferno chasm zone are covered by significantly greater amounts of eolian sediment and vegetation than flows from other latest Pleistocene and Holocene vents on the Great Rift, showing that the Inferno Chasm segment is older than other nearby segments of the Great Rift volcanic rift zone. Greeley and King (1975) and King (1982) identify two other short (<2 km), N.10°E.-trending volcanic rift zones in the Kings Bowl area: the Wapi Park and Queens Bowl zones (Fig. 5). They suggest that both of these north-northeast–trending volcanic rift zones formed before the northwest-trending eruptive and noneruptive fissures of the Great Rift volcanic rift zone.

The Arco–Big Southern Butte volcanic rift zone

The Arco–Big Southern Butte volcanic rift zone extends 50 km southeast from the northwest margin of the ESRP at Arco to the long axis of the ESRP southeast of the Cedar Butte lava field (Figs. 7 and 8). This zone is a locus of extensional faults, grabens, eruptive fissures, and noneruptive fissures. Volcanic features of the volcanic rift zone include fissure-fed basalt flows, the rhyolite dome complex of Big Southern Butte, the andesite volcano at Cedar Butte, and the cones and eruptive-fissure vents of the North

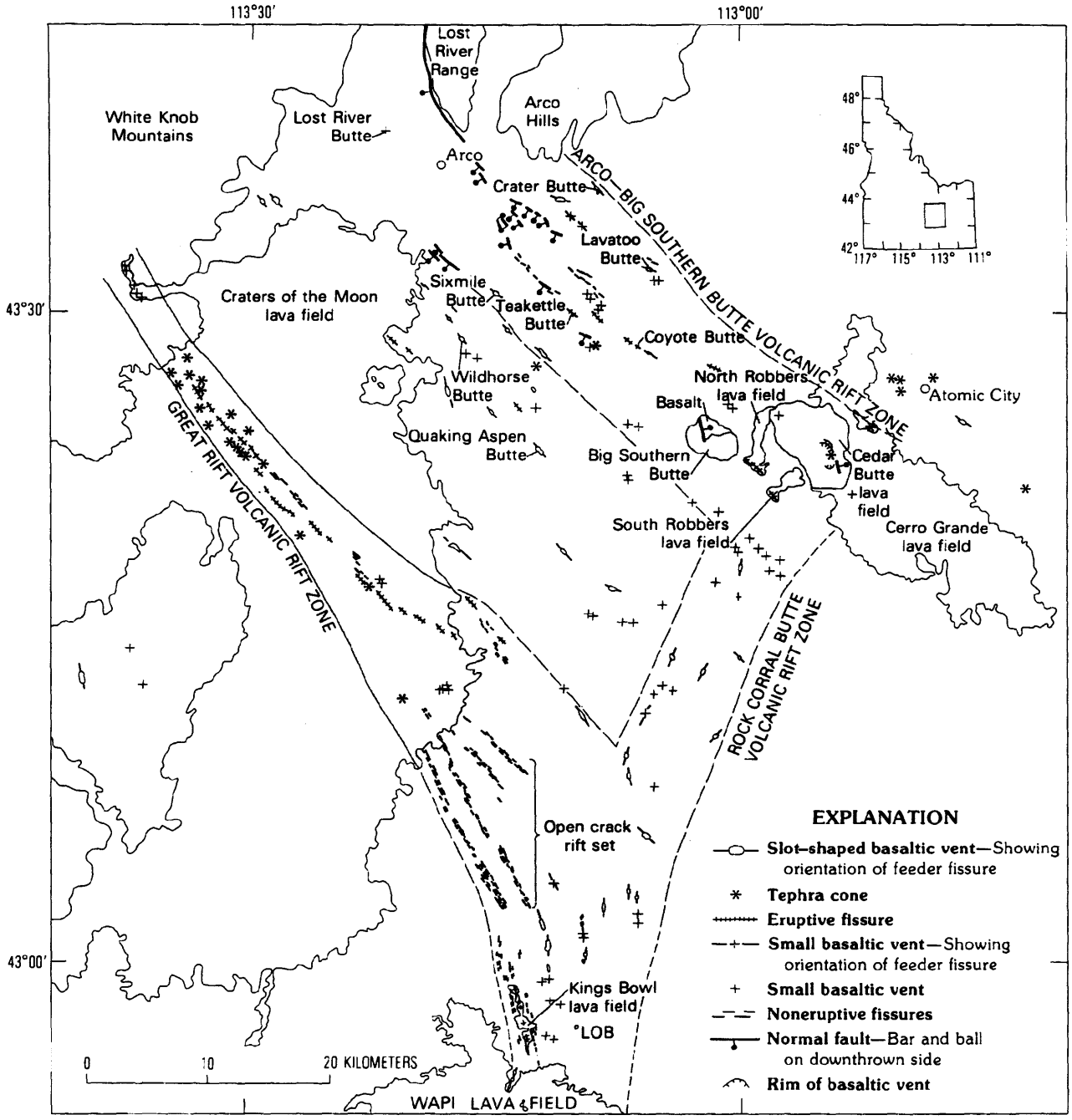

Figure 8. Simplified map showing volcanic and structural features of the Great Rift, Arco–Big Southern Butte, and Rock Corral Butte volcanic rift zones. Adapted from Kuntz and others (1988, 1992).

Robbers, South Robbers, and Cerro Grande lava fields (Spear, 1977; Spear and King, 1982; Kuntz, 1977b; Kuntz and others, 1992). The Arco–Big Southern Butte zone terminates at the vent for the Cerro Grande field, where it joins the northeast-trending Rock Corral Butte volcanic rift zone (Figs. 7 and 8).

Faults, noneruptive fissures, and air-photo lineaments are abundant and well developed along the Big Lost River 3 to 10 km southeast of Arco (Smith and others, 1989; Kuntz and others, 1992; Fig. 8). At that locality, extensional faults having as much as 10 m vertical displacement formed a graben that controls the

course of the Big Lost River. Most of these faults show good scarps. At the ends of some faults, however, the surface basalt is unbroken but shows substantial drag across the linear extensions of surface ruptures. The faults range in length from several tens of meters to as much as 4 km. Most scarps are relatively fresh, and the few slickensides observed suggest a purely dip-slip component of movement. Displacements on faults generally decrease to the southeast, and 15 km southeast of Arco, the faults are replaced by open fissures that have purely tensional displacement. Between Arco and Big Southern Butte, northeast-trending lineaments, apparent on aerial photographs, reflect eolian features and prairie-fire scars. Some lineaments having northwest trend, however, are obvious continuations of fissures and faults. Other northwest-trending lineaments are elongated depressions in surficial sediments that are parallel to nearby fissures and faults. Still other northwest-trending features are defined only by luxuriant growth of grass or sagebrush and lack a surface depression or other obvious relation to bedrock deformation. However, all lineaments of the latter type parallel known faults and fissures, suggesting that they too are the surface expressions in sediments of underlying faults and fissures.

Volcanoes in the Arco–Big Southern Butte volcanic rift zone represent all stages of basaltic volcanism. Fissure-fed lava flows occur southeast of Big Southern Butte in the North Robbers and South Robbers lava fields and at Coyote Butte northwest of Big Southern Butte. Small lava cones (Lavatoo Butte, Teakettle Butte, and Lost River Butte) occur at the northwest end of the volcanic rift zone (Fig. 8). These cones are 1 to 5 km in diameter and 50 to 350 m high. Their summits are indented by craters elongated parallel to the long axis of the volcanic rift zone. The largest volcanoes in the Arco–Big Southern Butte volcanic rift zone are shield volcanoes along the margins of the zone. These are the Quaking Aspen Butte, Crater Butte, Sixmile Butte, Wildhorse Butte, and Cerro Grande shield volcanoes (Fig. 8).

Although rhyolitic volcanism and rhyolitic rocks are not the focus of this paper, the Big Southern Butte dome complex must be mentioned because it is an integral part of the Arco–Big Southern Butte volcanic rift zone (Fig. 8). Big Southern Butte consists of two coalesced cumulo domes, both about 300 ka (Spear and King, 1982; Kuntz and others, 1992). The dome complex is 6.5 km in diameter, rises 760 m above the relatively flat surface of the surrounding ESRP, and has an exposed volume of about 8 km^3. Spear and King (1982) suggest that Big Southern Butte formed in several stages, including initial sill and laccolithic stages at depth, followed by extrusion and growth of two endogenous domes on the surface. The southeastern dome consists of spherulitic, flow-banded rhyolite in the core and autoclastic breccias and sugary rhyolite that represent deformed crust above the core. The northwestern dome consists of massive, aphyric rhyolite that formed along the northwest margin of the earlier dome.

A 350-m-thick section of basalt that dips N.45°E. is exposed on the north flank of Big Southern Butte (Fig. 8). Spear and King (1982) suggest that this section is an uplifted and tilted flap of basalt flows of the pre-dome surface of the ESRP. Fifteen to 20 individual flows and flow units are present in the flap. Most flows are olivine basalts and evolved olivine basalts; the uppermost flow is ferrolatite from Cedar Butte volcano.

Cedar Butte, a steep-sided shield volcano, is between Big Southern Butte and the vent area for the Cerro Grande lava field (Figs. 4 and 8). The summit of the shield is defined by several arcuate ridges that outline a vent area 3 km long and 2 km wide. The elongated vent trends N.40°W. A younger pyroclastic cone consisting of rhyolite and obsidian blocks occupies the center of the vent complex. A 2-km-long, northeast-facing scarp of a normal fault extends across the southeast flank of Cedar Butte toward the vent area of the Cerro Grande lava field (Figs. 4 and 8).

Volcanic rift zones in the central part of the ESRP

Volcanic rift zones in the central part are less well defined than zones elsewhere in the ESRP. Because most lava fields in this area are older (300 to 600 ka; Kuntz and others, 1992) than other ESRP fields, many features of these volcanic rift zones have been covered by lava flows and eolian deposits (Pierce and others, 1982).

The Lava Ridge–Hells Half Acre zone is a good example of volcanic rift zones in the central part of the ESRP. This zone extends 50 km southeast across the ESRP from the southern end of the Lemhi Range to the Hells Half Acre lava field (Fig. 7). The southeast end of the zone is well defined by open fissures and the vent complex of the Hells Half Acre lava field. The central part is defined by several small- to medium-sized shield volcanoes near the axis of the ESRP. Vents for these volcanoes are elongated north-south; thus the rift zone is offset in a right-lateral sense in its central part (refer to Fig. 17). The northwest end of the zone is ill defined: Poorly exposed flows of reversed magnetic polarity (older than 730 ka) are mantled by relatively thick fluvial and lacustrine deposits and eolian sediment. Volcanic activity on the Lava Ridge–Hells Half Acre volcanic rift zone is oldest (mostly more than 730 ka) at the northwest end, of intermediate age in the central part (200 to 500 ka), and youngest (about 5 ka) at the southeast end of the zone at the Hells Half Acre lava field (Kuntz and others, 1992).

Spencer–High Point volcanic rift zone

The Spencer–High Point (S-HP) volcanic rift zone occupies the northeastern end of the ESRP (Figs. 7 and 9). The zone extends 70 km from Indian Creek Buttes to High Point, a basaltic vent on Big Bend Ridge. Indian Creek Buttes are rhyolite domes (4.14 ± 0.085 Ma; G. B. Dalrymple, U.S. Geological Survey, written communication, 1979), each about 2 km in diameter, along the Middle Creek Butte fault zone at the western end of the S-HP zone. A few small basalt vents lie along the fault zone near the rhyolite domes (Fig. 9). The main part of the S-HP volcanic rift zone begins where the Middle Creek Butte fault zone enters the ESRP near Spencer (Figs. 7 and 9). There, faults, grabens, a few open fissures, and the feeder fissures for tephra cones, spatter

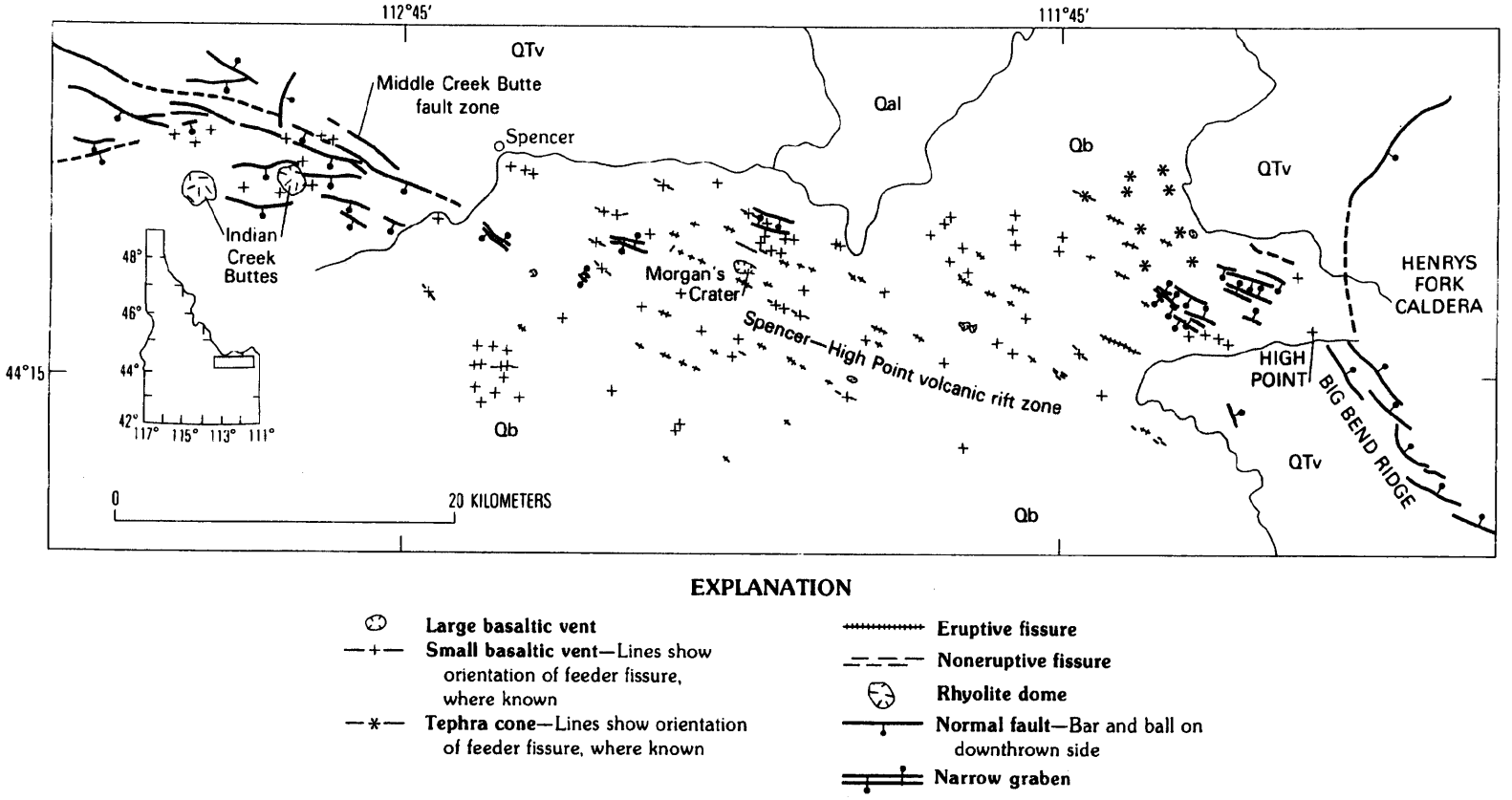

Figure 9. Simplified map showing volcanic and structural features of the Spencer–High Point volcanic rift zone. Abbreviations: QTv, Quaternary and Tertiary rhyolitic and basaltic volcanic rocks; Qb, Quaternary basalt; Qal, Quaternary alluvium. Adapted from Christiansen (1982) and unpublished mapping by M. A. Kuntz, G. F. Embree, and H. J. Prostka.

ramparts, and small shield volcanoes all trend about N.60°W. These structures occur in an east-trending zone about 15 km wide and 55 km long.

The vents and lava fields of the S-HP zone are smaller than other vents and fields in the ESRP. Lava fields in the S-HP zone are mainly of eruptive-fissure and lava-cone types. The flows are typically long and narrow because they moved chiefly south down relatively steep slopes (1 to 2°). Most lava fields cover areas of 10 to 100 km^2 and have volumes of 0.05 to 1 km^3. The larger areas and the higher volumes represent a few lava cones and small shields at the eastern end of the zone. Some of the youngest lava fields of the S-HP zone are believed to be latest Pleistocene or Holocene (<15 ka) in age based on their youthful surface morphology. Suitable material for radiocarbon dating of these fields has been sought but not obtained.

About a half-dozen tephra cones occur near the eastern end of the zone between Morgan's Crater and High Point (Fig. 9). Two factors may explain the restriction of the cones to this locality: (1) Magmas that fed the tephra cones are slightly more siliceous and probably were more viscous than other basalts of the S-HP volcanic rift zone, and (2) magmas in this area passed through alluvial, water-bearing sediments deposited by streams that ponded north of the topographic barrier created by the volcanic rift zone.

The S-HP volcanic rift zone is unique in several respects: (1) It contains the highest concentration of volcanic vents in the ESRP (Fig. 10); (2) it is a wide volcanic rift zone when compared to its length (15 km wide in the 55-km-long stretch between Spencer and High Point); (3) its east-west trend is unlike that of the other volcanic rift zones in the ESRP, most of which trend northwest-southeast; and (4) the vents and structures within the zone have a trend (northwest-southeast) different from that of the zone itself (Fig. 9).

The northwest trend of en echelon volcanic structures in the

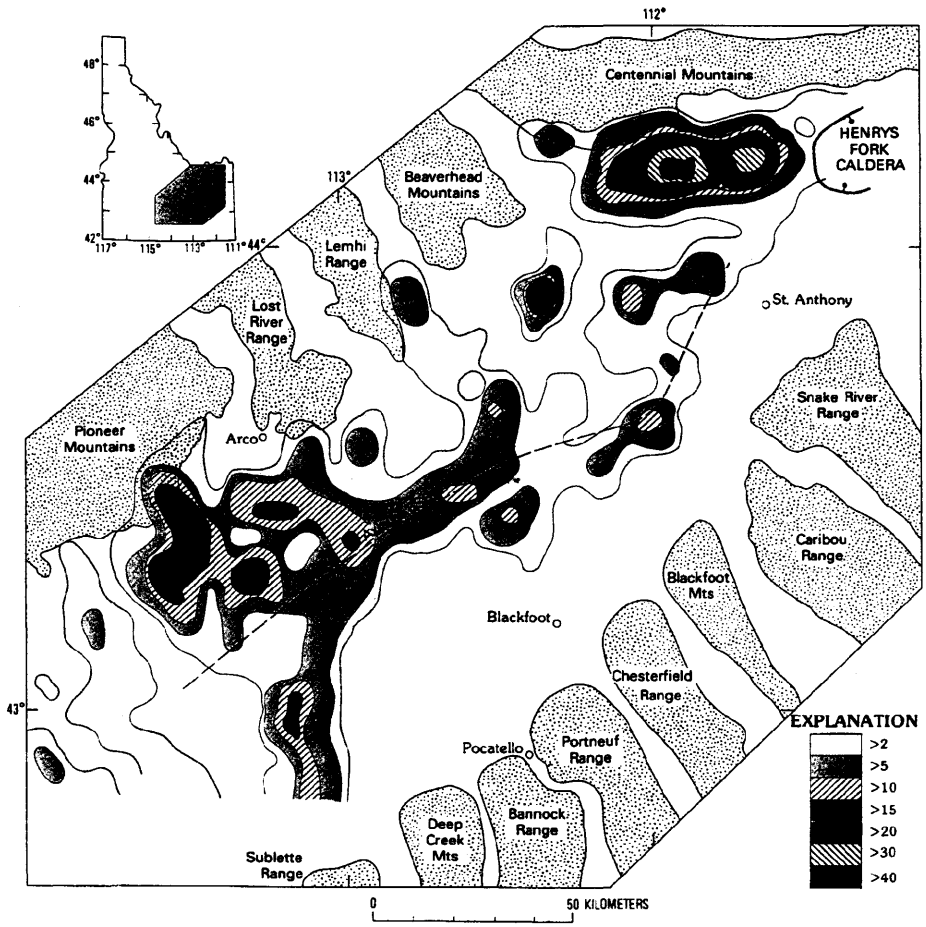

Figure 10. Number of volcanic vents per 140 km^2 (approximate area of a 7½-minute quadrangle) in eastern Snake River Plain.

S-HP volcanic rift zone may result from a component of right-lateral movement on the Middle Creek Butte fault, which produced extension fractures in a broad zone in the overlying flows.

Axis of the ESRP

The axis of the ESRP, from Big Southern Butte to Juniper Buttes, is a broad topographic ridge formed by the accumulation of basaltic lava flows from vents concentrated along it and from local uplift that accompanied emplacement of rhyolite domes. However, the axis of the ESRP is not a volcanic rift zone because the orientations of fissures that control the location and trend of the fissure-dominated vents are perpendicular, rather than parallel, to the axis. Local concentrations of basaltic vents occur along the axis where it crosses volcanic rift zones.

The axis is a belt of basaltic volcanoes and several rhyolite domes in an area about 10 km wide and 100 km long (Fig. 10). The domes and their ages, from west to east, are: Big Southern Butte (300 ka), Middle Butte (<1 Ma), an unnamed dome (1.4 Ma), and East Butte (580 ka) (Kuntz and others, 1992; refer to Fig. 17).

Magnetotelluric soundings (Stanley and others, 1977) and Curie isotherm maps for the ESRP (Bhattacharya and Mabey, 1980) indicate that a ridge of high temperature at shallow depth is roughly parallel to the axis of the ESRP (D. Mabey, oral communication, 1979). Evidently, excess heat resulting from the formation and upward transfer of basalt magma is still present in the deep crust beneath the axis of the ESRP. However, the movement to the surface generally follows fractures oriented perpendicular to the axis. The vertical transfer of heat may also be responsible for melting the deep crust and producing rhyolitic magmas and the rhyolite domes (e.g., Leeman, 1982d).

REGIONAL RELATIONSHIPS OF VOLCANIC RIFT ZONES

Relationships between volcanic rift zones and structures beyond the margins of the ESRP

Based on ideas developed by Stearns (1928), Stearns and others (1938), Prinz (1970), LaPoint (1977), and H. J. Prostka (unpublished) and on his own fieldwork, Kuntz (1977a, 1977b, 1978) suggested that most volcanic rift zones of the ESRP are collinear continuations onto the ESRP of range-front faults in mountains beyond the margins of the plain (Fig. 11). The outlying range-front faults are normal and listric faults that produce fault scarps and steep mountain fronts. Within the ESRP, the continuations of these faults are represented by the structures and volcanic landforms of volcanic rift zones, including normal faults, eruptive and noneruptive fissures, grabens, volcanic vents at the surface, and dikes at depth (Figs. 8 and 9). It is not clear that the range-front faults continue onto the ESRP in bedrock beneath the basaltic lava flows. The three-dimensional relationship between the range-front faults and the structures of the volcanic rift zones can only be inferred from the surface expression of these structures and their inferred arrangement and attitudes at depth. What seems clear at present is that regional extensional strain is manifested in basin-and-range faulting and topography in mountains north and south of the ESRP, but within the ESRP it is expressed only in minor normal faulting, emplacement of dikes, formation of fissure-controlled basaltic eruptions, and development of structures related to eruptions (e.g., faults, grabens, noneruptive fissures) in volcanic rift zones.

Examples of volcanic rift zones as collinear continuations of range-front faults are the Arco–Big Southern Butte, Lava Ridge–Hells Half Acre, and Menan volcanic rift zones, which are collinear with range-front faults of the Lost River, Lemhi, and Caribou Ranges, respectively (Fig. 11). The Spencer–High Point volcanic rift zone is collinear with the Middle Creek Butte fault zone along the southwest margin of the Centennial Mountains (Figs. 9 and 11).

Relations between regional extension, volcanic rift zones, and magma production

Kuntz (this volume) proposes that strain release in the form of basin-and-range faulting and concomitant concentrated extension in volcanic rift zones leads to greater amounts of magma production in the lithospheric mantle, perhaps by decompression melting, which in turn increases the number of suitable fractures for the rise of magma to the surface. The mechanical-thermal feedback nature of this mechanism suggests that volcanic rift zones of the ESRP are long-lived, self-perpetuating zones of volcanism that result from regional extensional tectonics.

We suspect that major periods of faulting near the margins of the ESRP correlate with major periods of volcanism on collinear volcanic rift zones. Two general conclusions support this relationship. (1) The youngest sites of volcanism on the northern margin of the ESRP (Great Rift and Spencer–High Point volcanic rift zones) are near sites of major Quaternary faulting (Pierce and Morgan, this volume; Fig. 11). (2) The area that has only a few, very old volcanic vents and poorly defined volcanic rift zones, along the southeast margin of the ESRP, is adjacent to Belt IV of Pierce and Morgan (this volume), defined by them as an area having range-front faults that were active in late Tertiary time but that show little or no evidence of Quaternary activity (Fig. 11). We conclude that strain release at various times along various basin-and-range faults near the margins of the ESRP also contributed to approximately contemporaneous formation of magma by decompression melting and basaltic volcanism in adjacent volcanic rift zones. Thus, volcanic rift zones may serve as strain recorders that mark the approximate times of basin-and-range–type faulting along the margins of the ESRP and of subsequent volcanism concentrated within the zones. Unfortunately, currently available ages of faulting and volcanism are not yet sufficiently accurate to allow us to investigate this relationship more fully.

Volcanic rift zones and regional tectonic stress

Basin-and-range faults beyond the margins of the ESRP and volcanic rift zones within the ESRP formed in the same regional

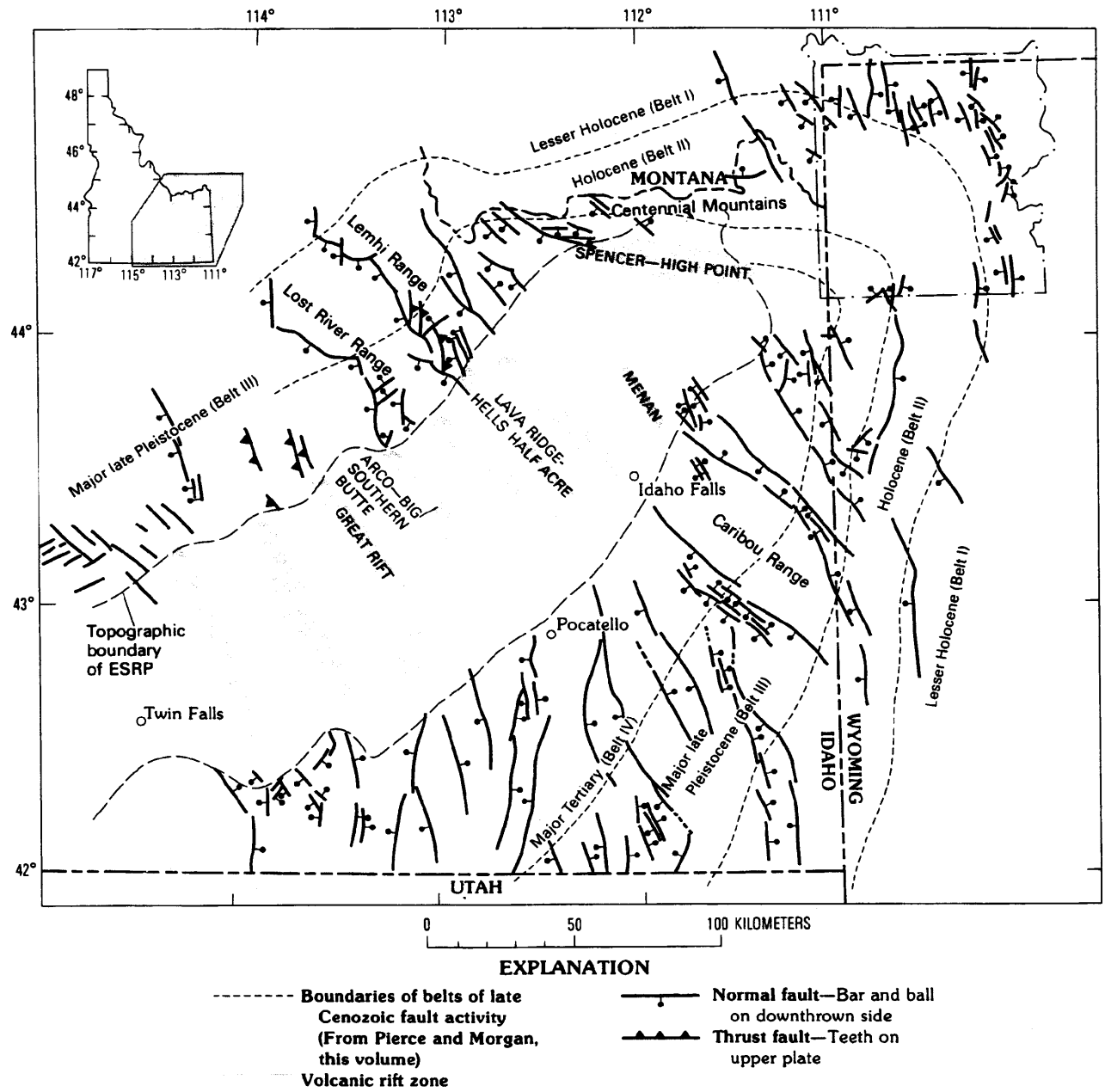

Figure 11. Map of the eastern Snake River Plain, showing the relationship between range-front faults and other structures beyond the margins of the ESRP and volcanic rift zones within the ESRP. Compiled from many sources.

stress system. The axis of least principal (extensional) stress in the region is presently oriented S.45°W. (Stickney and Bartholomew, 1987), which is consistent with regional stress directions identified by Zoback and Zoback (1980). Volcanic rift zones have acted as extensional strain concentrators in the ESRP, just as basin-and-range faults are the loci of regional strain in adjacent regions.

An important feature of the distribution of volcanic vents and volcanic rift zones in the ESRP is the absence of fissure-controlled, elongated vents and volcanic rift zones aligned parallel

to and near the margins of the ESRP. If the ESRP were a fault-bounded rift valley, as suggested by some (see, for example, Corbett, 1975; Hamilton, 1987), basaltic vents and volcanic rift zones could be expected to be concentrated along and elongated parallel to boundary faults. On the contrary, volcanic rift zones of the ESRP cut at right angles to the postulated boundary-rift faults (Figs. 7 and 11). Although this observation does not preclude the existence of boundary faults along the margins of the ESRP, it makes their existence unlikely. Faults parallel to the margins of the ESRP have been described from several localities (see, for example, Rodgers and Zentner, 1988). These faults lack regional continuity and basaltic vents are not aligned along them, thus they do not qualify as boundary faults.

AGE OF BASALTIC VOLCANISM OF THE ESRP

Radiometric studies of basaltic lava flows of the ESRP have been undertaken only recently. Radiocarbon study of young lava fields has been an arduous, time-consuming task fraught with many difficulties (see Kuntz, Spiker, and others, 1986). K-Ar dating has been hampered by the low K_2O contents of the basaltic flows (typically less than 0.8%), the relative youth of the flows, and until recently, mass spectrometric and electronic limitations. In spite of these difficulties, about 30 reliable radiocarbon ages and 70 reliable K-Ar ages are presently available for surface and near-surface flows of the ESRP (summarized in Kuntz, Spiker, and others, 1986; Champion and others, 1988; Kuntz and others, 1992).

Field- and laboratory-determined paleomagnetic directions, combined with available radiometric ages, indicate that about 95% of the ESRP is covered by basaltic lava flows that are younger than 730 ka. Most flows have normal polarity and, therefore, were erupted in the Brunhes Normal-Polarity Chron. Surface flows known to be older than 730 ka occur near the mouth of Birch Creek Valley on the northwestern margin of the ESRP and along the northern part of the Lava Ridge–Hells Half Acre volcanic rift zone (refer to Fig. 17). Most flows in the central part of the ESRP are between 200 and 700 ka (Kuntz and others, 1992).

In general, the radiometric data suggest that eruptive activity was earlier and more sporadic near the margins and was later and more persistent near the center of the ESRP. Vents for the latest Pleistocene and Holocene basaltic volcanism are scattered along the entire length of the ESRP and most of them are concentrated near the plain axis. However, vents for the mostly Holocene COM lava field are concentrated near the intersection of the Great Rift volcanic rift zone and the northern margin of the ESRP.

Because vertical exposures are scarce and few core samples of flows have been dated radiometrically, little is known about the age of basalt flows at depth or about the rates at which flows accumulate in various parts of the ESRP. At each locality in the ESRP, all major basalt flows are considered to be younger than the rhyolitic rocks and their associated calderas. This relationship and the known ages of surface and near-surface basaltic flows indicate that most of the basaltic volcanism of the ESRP is Pliocene and younger.

PETROLOGY, PETROCHEMISTRY, AND PETROGENESIS OF BASALTIC LAVA FLOWS OF THE ESRP

Petrologic variability

Stone (1967, 1970) was the first to accurately assess the mineralogical and chemical variability of basaltic rocks of the Snake River Plain. He concluded that (1) they are highly uniform in field, textural, mineralogical, and chemical characteristics; (2) they are mainly olivine tholeiites in terms of mineralogical and chemical character; (3) they constitute a primary magma suite because of their great volume and comparatively uniform composition; (4) they were only slightly affected by magmatic evolution; (5) their minor diversity may reflect small differences in composition of parental magmas as a result of variation in depths of magma genesis; and (6) local compositional variations were produced by contamination by crustal rocks. Subsequent studies have modified but not changed Stone's basic conclusions.

At present, two major types of basaltic rocks are recognized in the Snake River Plain. The majority of lava flows of the Snake River Plain are *olivine basalts* that show little evidence of differentiation or contamination. Most consist of normative olivine and hypersthene (Fig. 12) and are olivine tholeiites in the classification of Yoder and Tilley (1962), but some are alkali olivine basalts based on mineralogical and thermodynamic classifications (Stout, 1975; Stout and Nicholls, 1977). Most basalts shown in Tables 3 and 4 and Figure 12 are olivine tholeiites (normative ol and hy); however, three of the most mafic COM rocks (Table 2), two of 22 analyzed samples from latest Pleistocene and Holocene lava fields (Table 3), and four of 24 olivine basalts of Pleistocene lava fields (Table 4) are slightly nepheline-normative (<3 molecular percent Ne) alkali olivine basalts (Fig. 12).

The second major type of rock is *evolved basaltic* rocks that have SiO_2 contents as high as 65%. Evolved basaltic rocks are now known from at least nine areas on or near the Snake River Plain (Leeman, 1982c). The major areas in the ESRP are the Craters of the Moon lava field, the Cedar Butte field, and the Spencer–High Point area. The most evolved rocks of the COM lava field are quartz normative (<10 molecular percent Q; Table 2 and Fig. 12).

Kuntz, Champion, and others (1986) distinguish three types of basaltic rocks in the COM, Kings Bowl, and Wapi lava fields on the Great Rift volcanic rift zone. The Snake River Plain type (SRPT), represented by rocks of the Kings Bowl and Wapi lava fields, comprises the undifferentiated, uncontaminated olivine basalts discussed above. A fractionated type is represented by COM rocks having an SiO_2 range of 44 to 54%. These rocks are fractionated with respect to SRPT olivine basalts, they mostly lack disequilibrium minerals and textures, and their chemical and

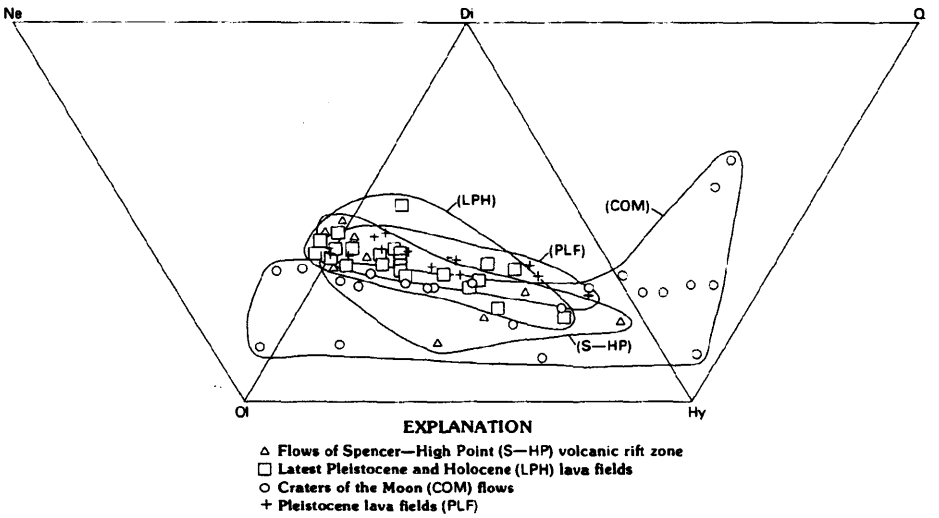

Figure 12. Normative Q-Hy-Di-Ol-Ne for the 70 analyses listed in Tables 2, 3, and 4.

mineralogical variation can be accounted for mainly by fractionation of observed mineral phases. A contaminated type is represented by COM rocks that have an SiO_2 range of 49 to 64%. These rocks commonly contain rhyolitic pumice inclusions that range from microscopic to several meters across, xenoliths of gneissic granulite, and xenocrysts of disequilibrium minerals.

Our field studies indicate that mantle xenoliths are absent in olivine basalts of the ESRP. Karlo (1977) found olivine gabbro xenoliths in rocks of the Hells Half Acre lava field, but these are probably cumulates of phenocryst phases common in Hells Half Acre rocks. Xenoliths and xenocrysts derived from Precambrian gneiss beneath the ESRP are present locally in olivine basalts (Leeman and Manton, 1971; Leeman and others, 1976; Menzies and others, 1984; Leeman and others, 1985; Futa and others, 1988) but are uncommon. The abundant inclusions of rhyolitic rocks in evolved rocks of the COM lava field are absent or extremely rare in olivine basalts of the ESRP. The absence of xenoliths of Upper Precambrian, Paleozoic, and Mesozoic sedimentary rocks (or their metamorphic equivalents) in all basaltic rocks of the ESRP suggests, but does not prove, that these sedimentary and metamorphic rocks do not underlie large tracts of the ESRP.

Petrography

The petrography of the varieties of basaltic rocks of ESRP has been described in detail elsewhere (e.g., Stone, 1967; Leeman, 1974, 1982b, 1982c; Stout and Nicholls, 1977; Kuntz, Champion, and others, 1986) and is reviewed here only briefly. Olivine basalts consist of olivine (Fo_{80-90}), a single clinopyroxene (augite to ferroaugite), plagioclase (An_{70-50}), titanomagnetite, ilmenite, and brown glass. Most samples have a coarse, intergranular texture: Crystals are typically 0.5 to 3 mm long. Other textures range from ophitic and subophitic to intergranular and diktytaxitic. Some samples are inequigranular and consist of 0.5- to 5-mm-long, euhedral and subhedral olivine and plagioclase crystals in a diktytaxitic, subophitic matrix of olivine, plagioclase, clinopyroxene, and opaque minerals <0.2 mm in largest dimension.

Evolved rocks of the contaminated type are typically hypocrystalline, and most of their crystals are <0.5 mm long. They generally contain crystals of olivine (Fo_{60-25}), plagioclase ($An_{\sim 25-60}$), clinopyroxene, titanomagnetite, and ilmenite in a matrix of brown glass. The rocks typically show some evidence of contamination in the form of disequilibrium textures (resorbed plagioclase, clinopyroxene, and anorthoclase crystals), disequilibrium minerals (hypersthene, anorthoclase), inclusions of rhyolitic pumice and gneissic granulite, and xenocrysts of clinopyroxene, zircon, anorthoclase, and apatite. Xenoliths and xenocrysts are far more abundant in evolved rocks than in olivine basalts, suggesting that the inclusions may be important factors in the chemical and mineralogical diversity of the evolved rocks.

Petrochemistry and petrogenesis

Olivine basalts. Olivine basalts of the ESRP have a fairly narrow range in major-element and minor-element chemistry, as shown in Tables 3 and 4. Covariation between various oxides and Mg value [MgO/(MgO+FeO*)] and between total alkalies and SiO_2 illustrates the chemical diversity of olivine basalts of the ESRP (Figs. 13 and 14). The diagrams also aid in recognizing mechanisms that may have played a role in creating the limited chemical diversity. Note that a coherent covariation trend characterizes the olivine basalts in Figure 13 and that olivine basalts form a tight cluster in Figure 14.

Petrochemical and experimental studies suggest that SRPT olivine basalts were derived by partial melting of spinel lherzolite

mantle at depths of 40 to 60 km and that little fractionational crystallization occurred prior to or during eruption. The minor chemical variation in the olivine basalts (Figs. 13 and 14) can be accounted for by fractionation of olivine and plagioclase, which are phenocryst phases in these rocks. Varying degrees of partial melting of peridotite source rocks of the mantle have also been advocated to explain part of the variation in the olivine basalt suite (Stone, 1967). Tilley and Thompson (1970), Thompson (1975), Leeman and Vitaliano (1976), Stout and Nicholls (1977), Leeman (1982b), and Menzies and others (1984) summarize experimental and petrochemical data that support these conclusions.

Rocks from the Spencer–High Point area have affinities with olivine basalts and evolved basalts. The more evolved rocks occur at the low-Mg-value end of the coherent covariation trends for olivine basalts (Fig. 13), suggesting that they may have formed by higher degrees of olivine and plagioclase fractionation than most other SRPT olivine basalts.

Evolved basalts. Evolved basaltic rocks of the ESRP show large variations in major-element and minor-element chemistry (Table 2). The different slopes in the covariation diagrams (Figs. 13 and 14) for the array defined by the three sets of olivine basalts (latest Pleistocene and Holocene lava fields—LPH, Pleistocene lava fields—PLF; and most S-HP) and the array defined by rocks of the COM lava field suggest that fractionation of olivine and plagioclase alone, which accounts for the chemical variation in olivine basalts, is not the same process that accounts for the chemical variation of COM rocks. The different slopes also suggest that significant amounts of crystal fractionation—of olivine, plagioclase, and perhaps other minerals—would be required to derive even the least evolved COM basalts from SRPT olivine basalt.

Studies by Leeman and others (1976), Leeman (1982c), Kuntz, Champion, and others (1986), Futa and others (1988), and Stout and others (1989) identify two mechanisms for the derivation of the evolved basalts from parental SRPT magmas: (1) fractionation of observed phenocryst phases at pressures of ~8 to 10 kb, corresponding to depths of ~30 km, and (2) contamination of primary basalt by mineral components from deep crustal rocks or by partial melts of deep crustal rocks. Either or both of these mechanisms could account for most of the evolved basalts. Stout and others (1989) showed that coherent trends and nonzero intercepts on Pearce element-ratio plots suggest derivation of the evolved COM magmas from basalt by crystal fractionation and by assimilation of pumiceous rhyolite by basalt. Stout and others (1989) also suggested that chemical variations in COM rocks cannot be explained by fractionation of olivine and plagioclase alone but must include augite and Fe-Ti oxide accumulation and/or fractionation as well.

The character of parental magma for the varied COM rocks is problematic. The Kings Bowl and Wapi olivine basalts appear to be likely parental magmas for COM basaltic rocks because they erupted almost simultaneously with the youngest COM rocks along the Great Rift volcanic rift zone. However, Kuntz and others (1985) and Kuntz, Champion, and others (1986) showed that the most mafic basaltic rocks of the COM lava field have a significantly different major-element composition than the Wapi and Kings Bowl basalts. The most mafic COM rocks have rare-earth contents 1.3 to 8 times those of the olivine basalts, represented by latest Pleistocene and Holocene lava rocks (Fig. 15). These geochemical relations suggest that COM basaltic rocks were not derived by fractional crystallization from olivine basalt parental magmas; rather, they were derived from fundamentally different parental magmas.

Petrogenetic schemes to account for the significant enrichment of large-ion-lithophile (LIL) and rare-earth elements (REE) in COM basaltic rocks relative to SRPT olivine basalts might include varying degrees of partial melting of mantle peridotite, crystal fractionation, and interaction of magma with wall rocks in either the crust or the mantle, as suggested by Jamieson and Clarke (1970). In our opinion, the most significant factor that bears on this point is that a 10-km-thick granitic body probably underlies the COM lava field (see Kuntz, this volume). This relatively low density body or the partially melted lower- or middle-crustal rocks beneath it may have inhibited the ascent of magma through the crust and may have promoted enrichment processes such as magma-wall rock interaction and/or crystal fractionation.

Leeman (1982c) and Futa and others (1988) noted that Sr isotopic compositions of COM rocks trend toward typical lower-crustal values with increasing degrees of differentiation and decreasing time, suggesting that progressive assimilation of rhyolitic xenoliths and/or addition of partial melts of lower-crustal granulites may partly account for the compositional variability of the COM suite. Menzies and others (1984) suggest that less than 20% contamination is required to produce the most highly evolved rocks of the COM field.

In summary, the chemical diversity of most SRPT olivine basalts is due to variable degrees of partial melting of mantle source rocks at various depths and minor, subsequent crystal fractionation of olivine and plagioclase. Fractionation of olivine, plagioclase, clinopyroxene, and Fe-Ti oxides and crustal contamination are factors only in formation of more evolved basaltic magmas, such as those of the COM lava field.

MAGMA OUTPUT RATES

Magma output rate (MOR) is the long-term, time-averaged discharge rate of a volcano or volcanic region. Baksi and Watkins (1973) and Nakamura (1974) have shown that the MOR of volcanoes is related to their tectonic environment: It is greatest for intraplate oceanic volcanoes, intermediate for volcanoes at convergent plate margins, and least for intraplate continental volcanoes.

Analyses of volumes and ages of lava flows in the COM lava field show that the MOR was fairly constant at ~1.5 km^3/1,000 yr for the period from 15,000 to 7,000 B.P. and that the rate increased to ~2.8 km^3/1,000 yr from 7,000 to 2,100 B.P.,

TABLE 2. MAJOR-ELEMENT AND TRACE-ELEMENT ANALYSES AND MOLECULAR NORMS OF SELECTED LAVA FLOWS OF THE CRATERS OF THE MOON LAVA FIELD, IDAHO*

Eruptive Period	H	G	G	G	F	F	E	E	D	D	D
Flow	Kimama	Lava Creek	Sunset	Carey	Bottleneck Lake	Pronghorn	Lava Point	Grassy Cone	Little Park	Carey Kipuka	Silent Cone
Age (ka)	15.1	12.8	12.0	12.0	11.0	10.2	7.8	7.3	6.5	6.6	6.5
Sample No.	79K99	79K85	78K184	78K61	78K72	78K73	78K68	78K183	78K65	78K147A	78K150
Major Oxides (percent)											
SiO_2	45.24	43.50	49.65	47.22	46.58	45.52	45.64	47.25	49.46	50.54	52.78
TiO_2	3.28	3.83	2.44	3.09	3.33	3.20	3.63	3.23	2.55	2.42	1.86
Al_2O_3	14.23	14.20	14.50	13.46	13.42	13.81	13.39	12.49	14.28	14.16	14.06
Fe_2O_3	1.27	2.16	4.53	0.89	1.35	1.20	1.79	8.62	1.14	1.22	0.78
FeO	15.11	14.78	10.47	14.93	14.71	14.96	14.28	7.45	13.55	13.18	11.55
MnO	0.28	0.27	0.24	0.26	0.27	0.24	0.23	0.25	0.24	0.22	0.22
MgO	4.53	5.21	3.14	3.91	4.21	4.10	4.67	3.82	3.08	2.95	1.90
CaO	7.50	8.13	6.47	8.24	8.78	7.48	8.18	8.40	6.49	6.28	5.39
Na_2O	3.50	3.47	4.50	3.47	3.39	4.02	3.55	3.07	4.28	4.28	3.51
K_2O	1.75	1.60	2.35	1.94	1.83	1.92	1.65	1.82	2.30	2.38	2.71
H_2O^+	0.33	0.38	0.12	0.24	0.23	0.32	0.37	0.19	0.43	0.46	0.61
H_2O^-	0.08	0.08	0.16	0.10	0.06	0.09	0.11	0.05	0.14	0.15	0.16
P_2O_5	2.64	2.78	1.56	2.29	2.46	2.18	2.13	2.33	1.60	1.46	1.13
Total	99.74	100.39	100.13	100.04	100.62	99.04	99.62	98.97	99.54	99.70	96.66
Molecular Norms											
Ap	5.71	5.98	3.34	4.94	5.28	4.73	4.62	5.14	3.45	3.14	2.53
Il	4.73	5.49	3.48	4.44	4.76	4.63	5.24	4.75	3.66	3.47	2.77
Mt	1.95	2.00	1.73	1.89	1.90	1.93	1.91	1.87	1.75	1.71	1.52
Or	10.70	9.73	14.20	11.83	11.10	11.77	10.11	11.35	14.01	14.48	17.11
Ab	32.52	30.91	39.77	32.17	31.26	33.18	33.04	29.10	39.62	39.56	33.69
An	18.57	18.98	12.70	15.92	16.43	14.50	16.31	15.76	13.36	12.76	15.61
Di	1.66	3.06	7.75	8.67	9.44	7.39	9.07	9.73	7.24	7.59	4.06
Hy	6.68	0	0	8.02	5.96	0	1.84	19.97	2.68	6.63	18.42
Ol	17.48	23.16	16.11	12.11	13.85	19.31	17.86	2.33	14.24	10.65	0
Ne	0	0.69	0.92	0	0	2.57	0	0	0	0	0
Q	0	0	0	0	0	0	0	0	0	0	4.29
Trace Elements (parts per million)											
Ba	1,180	1,100	1,600	1,290	1,160	1,300	944	1,200	1,740	1,490	1,720
Be	3	4	5	3	3	4	2	3	5	4	4
Ce	224	200	250	215	207	230	174	210	274	230	250
Co	35	45	29	35	37	37	40	39	33	28	21
Cr	4	<1	<1	3	4	<1	15	5	4	3	2
Cu	41	29	22	45	50	27	62	46	59	42	38
Eu	nd	8	9	nd	nd	8	nd	nd	nd	nd	nd
Ga	28	28	32	25	26	30	22	26	33	26	29
Ho	nd	5	5	nd	nd	5	nd	nd	nd	nd	nd
La	114	100	130	110	108	110	90	110	143	122	134
Li	21	19	25	20	20	21	16	15	26	23	23
Mo	<2	<2	<2	<2	<2	<2	<2	<2	3	<2	<2
Nb	98	13	<4	107	94	<4	90	108	122	112	126
Nd	nd	120	140	nd	nd	130	nd	nd	nd	nd	nd
Ni	<2	10	<2	<2	<2	3	17	<2	<2	<2	<2
Pb	21	14	17	20	21	15	21	21	30	21	26
Rb	48	50	73	56	52	58	43	48	36	70	84
Sc	28	23	24	29	28	24	30	32	35	30	28
Sr	352	350	330	340	345	353	313	335	373	311	290
V	95	130	45	97	116	98	177	146	84	64	25
Y	114	100	120	109	108	110	92	109	134	113	117
Yb	12	11	13	9	9	11	10	9	15	13	13
Zn	236	230	250	228	224	200	198	225	271	229	229
Zr	994	842	1,228	980	940	965	795	990	1,165	1,170	1,362

TABLE 2. MAJOR-ELEMENT AND TRACE-ELEMENT ANALYSES AND MOLECULAR NORMS OF SELECTED LAVA FLOWS OF THE CRATERS OF THE MOON LAVA FIELD, IDAHO* (continued)

Eruptive Period	C	C	C	C	C	B	B	A	A	A	A	A
Flow	Sentinel	Fissure Butte	Sheep Trail	Sawtooth	Indian Wells N.	Minidoka	Devils Cauldron	Highway	Serrate	Big Craters	Trench Mortar Flat	Blue Dragon
Age (ka)	6.0	6.0	6.0	6.0	6.0	4.5	4.5	2.4	2.4	2.4	2.2	2.1
Sample No.	78K118	78K129	78K92	78K67	78K95A	79K94	78K81	78K151	78K99	78K120	78K126	78K52
Major Oxides (percent)												
SiO_2	44.65	49.58	44.33	55.37	57.20	48.40	48.73	62.88	59.91	52.04	51.08	49.01
TiO_2	3.70	2.41	3.65	1.70	1.29	2.96	2.93	0.67	0.95	2.54	2.57	2.87
Al_2O_3	12.97	14.40	13.77	14.67	15.11	14.06	13.62	14.49	13.94	13.91	13.29	13.41
Fe_2O_3	1.70	16.24	5.06	1.55	1.04	1.09	1.35	0.88	2.94	1.33	1.72	0.77
FeO	14.55	0.02	11.31	11.21	10.23	14.44	13.90	7.58	7.44	13.40	12.16	14.50
MnO	0.27	0.25	0.25	0.20	0.21	0.26	0.22	0.17	0.18	0.24	0.23	0.24
MgO	4.90	2.82	5.57	1.94	1.45	3.83	3.54	0.27	0.52	2.68	3.05	3.34
CaO	9.60	6.36	8.33	4.95	4.12	6.92	7.12	2.94	3.55	6.76	6.82	6.93
Na_2O	3.04	3.86	3.36	4.12	3.97	3.58	4.21	4.20	4.00	3.57	3.55	3.61
K_2O	1.56	2.26	1.50	3.04	3.40	1.96	2.00	4.64	3.91	2.31	2.39	2.03
H_2O^+	0.37	0.32	0.18	0.16	0.43	0.26	0.23	0.14	0.11	0.18	0.13	0.20
H_2O^-	0.06	0.17	0.08	0.04	0.10	0.06	0.08	0.03	0.01	0.03	0.06	0.14
P_2O_5	2.87	1.51	2.77	0.87	0.62	2.12	1.88	0.14	0.29	1.47	1.44	1.77
Total	100.24	100.20	100.16	99.82	99.17	99.94	99.81	99.03	97.75	100.46	98.49	98.82
Molecular Norms												
Ap	6.21	3.29	5.97	1.86	1.34	4.57	4.04	0.30	0.63	3.16	3.15	3.87
Il	5.34	3.50	5.24	2.42	1.85	4.25	4.20	0.96	1.38	3.63	3.74	4.18
Mt	1.93	1.77	1.90	1.50	1.34	1.85	1.81	1.00	1.23	1.74	1.66	1.84
Or	9.54	13.93	9.13	18.39	20.73	11.94	12.15	28.10	24.17	14.02	14.75	12.53
Ab	28.26	36.16	31.09	37.88	36.78	33.16	38.86	38.65	37.57	32.93	33.30	33.85
An	17.74	15.96	18.61	12.86	13.80	17.03	12.71	7.16	8.93	15.52	13.87	15.03
Di	9.72	5.34	4.26	5.17	2.49	3.28	8.78	5.49	6.01	7.25	9.33	7.04
Hy	6.53	12.76	4.00	17.79	16.54	16.53	3.00	8.64	11.30	20.47	19.63	16.97
Ol	14.73	7.28	19.80	0	0	7.39	14.46	0	0	0	0	4.69
Ne	0	0	0	0	0	0	0	0	0	0	0	0
Q	0	0	0	2.12	5.13	0	0	9.72	8.78	1.27	0.57	0
Trace Elements (parts per million)												
Ba	959	1,470	948	1,850	2,180	1,300	1,300	1,900	2,600	1,600	1,500	1,310
Be	3	4	3	5	6	3	4	6	6	5	5	3
Ce	190	244	181	262	276	218	230	270	257	240	240	210
Co	42	24	41	18	16	32	36	22	9	30	32	31
Cr	11	2	19	3	<1	4	<1	<1	<1	<1	8	3
Cu	60	37	64	34	29	54	25	27	26	23	23	42
Eu	nd	nd	nd	nd	nd	nd	8	8	nd	8	8	nd
Ga	26	29	26	31	28	25	30	31	29	31	30	24
Ho	nd	nd	nd	nd	nd	nd	5	5	nd	5	5	nd
La	98	127	95	137	147	112	120	150	142	130	130	109
Li	16	26	17	26	31	20	22	30	30	25	25	20
Mo	<2	<2	<2	<2	<2	<2	<2	3	4	<2	<2	<2
Nb	89	1,284	95	140	136	111	6	22	nd	17	23	110
Nd	nd	nd	nd	nd	nd	nd	130	150	nd	140	130	nd
Ni	8	<2	12	<2	<2	<2	5	<2	<2	<2	10	<2
Pb	21	24	22	25	24	22	18	23	26	19	18	15
Rb	47	50	40	82	77	55	56	90	nd	64	72	53
Sc	31	29	31	28	25	29	25	22	30	25	24	32
Sr	343	338	336	282	256	321	320	270	209	310	290	334
V	172	40	175	15	5	117	110	11	<1	66	99	106
Y	100	122	97	119	124	105	110	120	121	120	110	107
Yb	11	14	9	14	15	12	11	14	15	12	12	12
Zn	209	244	203	231	226	220	210	260	232	250	240	215
Zr	789	1,284	774	1,401	1,344	992	948	1,482	nd	1,113	290	979

See Kuntz and others (1985) for sample localities. nd = no data. USGS analysts: J. Crock, A. Bartel, E. Brandt, J. Carr, M. Elsheimer, L. Espos, L. Jackson, P. Klock, R. Mays, V. McDaniel, R. Moore, J. Rivielle, D. Siems, and K. Wong.

TABLE 3. MAJOR-ELEMENT AND TRACE-ELEMENT ANALYSES AND MOLECULAR NORMS OF LATEST PLEISTOCENE AND HOLOCENE LAVA FIELDS OF THE EASTERN SNAKE RIVER PLAIN, IDAHO*

	Hells Half Acre Lava Field							North Robbers Lava Field		South Robbers Lava Field	
Sample No.	84KS4	6-16-6	6-24-4B	HHA-W	HHA-8D	SRV72-2	SRV72-4	84KS2	75K173	84KS1	84KS3
					Major Oxides (percent)						
SiO_2	47.10	48.40	46.27	46.77	45.72	47.21	47.44	46.40	47.00	44.60	45.20
TiO_2	3.42	2.90	3.02	3.22	3.37	3.44	2.65	2.10	2.30	3.10	3.49
Al_2O_3	14.60	15.30	14.99	13.94	14.87	14.14	14.58	15.40	15.50	14.90	14.70
Fe_2O_3	1.90	2.90	1.06	1.67	1.99	4.12	3.70	1.20	3.70	9.10	2.00
FeO	12.80	12.60	12.66	12.48	13.82	10.53	9.12	11.20	9.20	6.26	12.50
MnO	0.22	0.22	0.20	0.18	0.16	0.22	0.18	0.20	0.16	0.23	0.23
MgO	6.47	6.50	6.54	7.10	5.84	6.40	8.33	9.27	8.80	7.17	6.32
CaO	9.30	8.50	9.12	9.40	9.28	9.60	9.37	10.80	10.10	9.71	9.60
Na_2O	2.60	2.50	2.57	2.40	2.56	2.84	2.83	2.48	2.60	2.93	2.88
K_2O	0.82	0.82	0.83	0.84	0.83	0.87	0.77	0.40	0.43	0.66	0.89
H_2O^+	0.19	0.25	0.17	0.30	0.18	0.10	0.23	0.14	0.23	0.25	0.20
H_2O^-	0.02	0.03	nd	nd	nd	0.12	0.11	0.02	0.06	0.04	0.03
P_2O_5	0.57	0.54	0.68	0.82	0.99	0.11	0.39	0.56	0.67	1.00	1.29
Total	100.01	101.46	98.11	99.12	99.61	99.70	99.70	100.17	100.75	99.95	99.33
					Molecular Norms						
Ap	1.22	1.14	1.48	1.77	2.14	0.24	0.83	1.17	1.40	2.15	2.78
Il	4.88	4.09	4.37	4.63	4.85	4.92	3.74	2.93	3.21	4.43	5.01
Mt	1.73	1.79	1.64	1.68	1.87	1.70	1.47	1.43	1.46	1.72	1.71
Or	4.96	4.90	5.10	5.13	5.07	5.28	4.61	2.37	2.55	4.00	5.42
Ab	23.92	22.72	23.98	22.26	23.75	26.20	25.78	22.31	23.40	25.50	26.64
An	26.38	28.45	27.97	25.60	27.52	23.91	25.17	29.77	29.43	26.22	25.29
Di	13.66	8.53	11.55	13.63	10.70	19.43	15.53	16.21	13.13	13.20	2.07
Hy	13.41	22.18	12.93	16.91	12.47	3.89	5.29	1.84	7.55	0	4.25
Ol	9.84	6.19	10.99	8.40	11.62	14.43	17.59	21.97	17.87	21.88	6.84
Ne	0	0	0	0	0	0	0	0	0	0.89	0
					Trace elements (parts per million)						
Rb	nd	nd	nd	nd	nd	nd	nd	nd	nd	10	15
Sr	341	nd	nd	nd	nd	nd	nd	227	nd	324	336
Zr	243	nd	nd	nd	nd	nd	nd	215	nd	377	428
Nb	21	nd	nd	nd	nd	nd	nd	15	nd	29	44
Y	40	38	nd	nd	nd	nd	nd	32	nd	42	59
La	23	22	nd	nd	nd	nd	nd	20	nd	nd	51
Ce	52	51	nd	nd	nd	nd	nd	44	nd	nd	110
Nd	35	32	nd	nd	nd	nd	nd	27	nd	nd	63
Sm	8.1	7.7	nd	nd	nd	nd	nd	6.10	nd	nd	13
Eu	3.2	2.9	nd	nd	nd	nd	nd	2.4	nd	nd	4.6
Gd	9.9	9.0	nd	nd	nd	nd	nd	7.7	nd	nd	14.3
Tb	1.5	1.4	nd	nd	nd	nd	nd	1.0	nd	nd	2.2
Dy	8.3	3.9	nd	nd	nd	nd	nd	6.5	nd	nd	12.4
Er	4.4	4.0	nd	nd	nd	nd	nd	3.5	nd	nd	6.6
Tm	0.59	0.65	nd	nd	nd	nd	nd	0.49	nd	nd	0.89
Yb	3.89	3.68	ne	nd	nd	nd	nd	3.23	nd	nd	5.89
Lu	0.55	0.51	nd	nd	nd	nd	nd	0.45	nd	nd	0.85

TABLE 3. MAJOR-ELEMENT AND TRACE-ELEMENT ANALYSES AND MOLECULAR NORMS OF LATEST PLEISTOCENE AND HOLOCENE LAVA FIELDS OF THE EASTERN SNAKE RIVER PLAIN, IDAHO* (continued)

	Cerro Grande Lava Field		Kings Bowl Lava Field			Wapi Lava Field			Shoshone Lava Field		
Sample No.	75K166A	SRV72-21	K-KB	IV71-14	IV71-13	K-WAPI	P46HRC	K-SHOS	84KS6	84KS5	SRV72-9
					Major Oxides (percent)						
SiO_2	46.50	45.37	45.80	45.70	45.86	46.20	46.39	46.10	46.40	46.40	46.26
TiO_2	3.20	3.32	2.48	2.29	2.29	2.36	2.17	2.84	2.54	2.68	2.66
Al_2O_3	14.50	14.57	14.70	14.76	14.66	15.00	15.43	14.40	15.00	14.80	14.36
Fe_2O_3	2.40	2.01	1.50	1.78	4.25	1.60	1.05	1.50	1.90	1.70	1.52
FeO	11.60	12.35	11.60	11.03	8.78	11.00	11.03	11.70	11.30	11.70	11.51
MnO	0.17	0.19	0.21	0.18	0.17	0.20	0.19	0.21	0.21	0.21	0.18
MgO	6.80	7.25	9.48	9.86	10.04	8.98	8.34	7.72	8.27	8.14	8.52
CaO	8.90	9.23	10.40	10.13	10.18	10.60	10.77	9.85	10.00	10.10	9.84
Na_2O	2.80	2.92	2.31	2.56	2.56	2.30	2.65	2.52	2.57	2.59	2.88
K_2O	0.89	0.88	0.45	0.41	0.42	0.50	0.61	0.85	0.68	0.69	0.78
H_2O^+	0.45	0.16	0.12	0.10	0.14	0.20	0.14	0.32	0.19	0.25	0.19
H_2O^-	0.13	0.19	nd	0.06	0.10	nd	0.06	nd	0.03	0.03	0.23
P_2O_5	1.40	1.03	0.60	0.55	0.60	0.60	0.67	1.21	0.90	0.95	0.91
Total	99.74	99.47	99.65	99.41	100.05	99.54	99.50	99.22	99.99	100.24	99.84
					Molecular Norms						
Ap	3.01	2.21	1.27	1.16	1.26	1.27	1.42	2.59	1.90	2.01	1.93
Il	4.58	4.74	3.49	3.22	3.21	3.33	3.05	4.05	3.58	3.78	3.75
Mt	1.64	1.69	1.52	1.48	1.47	1.46	1.41	1.55	1.53	1.55	1.51
Or	5.40	5.33	2.69	2.44	2.49	2.99	3.64	5.15	4.07	4.12	4.66
Ab	25.83	26.86	20.96	23.19	23.10	20.92	23.92	23.19	23.35	23.52	26.17
An	25.04	24.64	28.72	27.82	27.41	29.51	28.71	26.10	27.71	27.02	24.24
Di	8.75	12.30	15.58	15.41	15.53	15.84	16.69	12.70	13.23	13.90	15.32
Hy	15.26	1.89	4.88	0.35	0.57	6.33	0	10.47	6.76	6.51	0.17
Ol	10.48	20.35	20.90	24.94	24.96	18.34	21.08	14.19	17.86	17.59	22.26
Ne	0	0	0	0	0	0	0.07	0	0	0	0
					Trace elements (parts per million)						
Rb	25	nd	14	nd	nd	13	nd	21	11	14	nd
Sr	363	nd	264	nd	nd	281	nd	317	304	325	nd
Zr	407	nd	205	nd	nd	211	nd	361	271	288	nd
Nb	40	nd	18	nd	nd	16	nd	36	32	28	nd
Y	nd	nd	35	nd	nd	35	nd	53	40	41	nd
La	nd	nd	22	nd	nd	23	nd	46	33	nd	nd
Ce	nd	nd	47	nd	nd	50	nd	97	71	nd	nd
Nd	nd	nd	28	nd	nd	30	nd	56	41	nd	nd
Sm	nd	nd	6.60	nd	nd	6.3	nd	12	8.6	nd	nd
Eu	nd	nd	2.5	nd	nd	2.5	nd	3.9	3.1	nd	nd
Gd	nd	nd	8.6	nd	nd	9.3	nd	13.1	10.1	nd	nd
Tb	nd	nd	1.4	nd	nd	1.6	nd	1.8	1.4	nd	nd
Dy	nd	nd	6.9	nd	nd	6.9	nd	10.5	8.1	nd	nd
Er	nd	nd	3.9	nd	nd	3.8	nd	5.6	4.3	nd	nd
Tm	nd	nd	0.54	nd	nd	0.51	nd	0.80	0.56	nd	nd
Yb	nd	nd	3.16	nd	nd	3.56	nd	5.19	3.93	nd	nd
Lu	nd	nd	0.50	nd	nd	0.49	nd	0.73	0.54	nd	nd

See Kuntz and others (1985) for sample localities. nd = no data. USGS analysts: J. Crock, B. Anderson, A. J. Bartel, S. Botts, M. Cremer, L. Kapos, Z. A. Hamlin, L. L. Jackson, G. Mason, H. G. Neiman, K. Stewart, C. Stone, and J. Taggart.

TABLE 4. MAJOR-ELEMENT ANALYSES AND MOLECULAR NORMS OF SELECTED PLEISTOCENE LAVA FIELDS, EASTERN SNAKE RIVER PLAIN, IDAHO*

	Central ESRP											
Sample No.	76K50	76K107	75K229A	76K68	76K12	76K11	76K66	76K99	76K176	76K177	76K133	6-14-6
						Major Oxides (percent)						
SiO_2	47.41	46.25	46.50	46.78	45.71	47.10	48.11	46.34	46.24	46.38	47.47	47.50
TiO_2	1.65	3.44	3.70	2.59	2.37	1.26	2.35	2.96	3.48	3.48	3.46	3.20
Al_2O_3	16.42	14.11	14.30	15.59	15.48	16.55	15.59	15.04	14.73	14.78	13.56	15.50
Fe_2O_3	1.54	2.26	3.40	3.30	2.48	1.75	2.22	3.67	3.92	2.94	0.91	2.90
FeO	9.34	12.95	11.90	10.15	10.81	7.38	10.42	10.35	11.63	12.41	13.64	11.60
MnO	0.17	0.20	0.17	0.19	0.21	0.18	0.19	0.21	0.21	0.21	0.23	0.22
MgO	8.78	6.09	6.10	7.79	8.10	9.50	7.67	7.04	6.57	6.61	7.37	4.90
CaO	11.53	9.28	9.40	10.21	11.41	11.00	10.06	10.33	9.38	9.39	10.07	9.50
Na_2O	2.40	2.89	2.50	2.74	2.48	2.36	2.63	2.83	2.73	2.62	2.53	2.70
K_2O	0.32	0.75	0.70	0.49	0.32	0.26	0.66	0.62	0.72	0.73	0.54	0.74
H_2O^+	0.15	0.26	0.48	0.22	0.22	0.44	0.32	0.27	0.30	0.40	0.36	0.35
H_2O^-	0.05	0.10	0.18	0.10	0.12	0.14	0.10	0.10	0.15	0.06	0.06	0.15
P_2O_5	0.33	0.95	0.90	0.58	0.54	0.28	0.57	0.84	0.78	0.81	1.18	1.10
Total	100.09	99.53	100.23	100.73	100.25	98.20	100.89	100.60	100.84	100.82	101.38	100.36
						Molecular Norms						
Ap	0.69	2.05	1.95	1.22	1.14	0.59	1.20	1.78	1.66	1.73	2.50	2.37
Il	2.30	4.95	5.33	3.63	3.34	1.78	3.29	4.18	4.95	4.95	4.88	4.59
Mt	1.25	1.80	1.80	1.53	1.53	1.06	1.45	1.61	1.80	1.79	1.70	1.70
Or	1.89	4.58	4.27	2.92	1.91	1.56	3.92	3.72	4.34	4.40	3.23	4.50
Ab	21.56	26.80	23.20	24.77	21.90	21.53	23.73	25.78	25.02	24.01	22.98	24.97
An	33.11	24.08	26.60	29.00	30.50	34.34	28.93	26.89	26.35	26.96	24.34	28.83
Di	17.58	13.65	12.42	14.56	18.54	15.40	13.99	15.63	12.76	12.15	14.73	9.85
Hy	3.76	9.54	18.21	4.11	0	6.69	10.76	2.80	8.81	11.57	18.65	20.64
Ol	17.86	12.57	6.22	18.25	20.78	17.06	12.73	17.62	14.32	12.45	6.99	2.55
Ne	0	0	0	0	0.37	0	0	0	0	0	0	0

mainly because output of contaminated magma was added to the nearly constant output rate of fractionated magma (Kuntz, Champion, and others, 1986).

The MOR for the entire ESRP for the last 15,000 years, calculated from estimated volumes of the latest Pleistocene and Holocene lava fields, is 3.3 km^3/1,000 yrs. This MOR, when compared to the rate for the COM lava field, indicates that about 75% of the volume of lava erupted in the ESRP in the last 15,000 years has been from the Great Rift volcanic rift zone.

Because there is no reason to assume that the MOR has increased or waned during the history of basaltic volcanism of the ESRP, the latest Pleistocene and Holocene MOR is used to represent the ESRP in Table 5. This value is approximately the same as that for other intraplate-continental, dominantly basaltic lava fields, such as the Springerville and San Francisco volcanic fields in Arizona on the western margin of the Colorado Plateau. These intraplate-continental volcanoes generally have lower MOR values than either intraplate-oceanic or convergent-plate-margin volcanoes, probably because less magma is produced in these regions and/or because they have higher intrusion-extrusion ratios.

RELATIONSHIPS BETWEEN BASALTIC VOLCANISM AND CALDERAS OF THE ESRP

Kuntz and Covington (1979) suggested that the lengths and orientations of volcanic rift zones, the areal density and types of basaltic vents, and subtle topographic features in the ESRP are partly controlled by underlying buried calderas. In addition, they proposed that (1) the orientations of some volcanic rift zones may be controlled by buried ring fractures of underlying calderas, (2) other zones terminate at caldera margins, (3) areas that have few or no vents on the ESRP may overlie areas of low-density rocks within calderas, and (4) subtle arcuate depressions on the ESRP may reflect collapsed parts of underlying calderas. All of these relationships were highly speculative when originally proposed because little was known then about the rhyolite calderas.

Kuntz and Covington used these relationships to predict the size and location of underlying calderas. In hindsight, our ideas about the size and location of the calderas were quite inaccurate when compared to what is presently known or inferred about the calderas. However, we feel that many of the relationships we developed in 1979 remain viable.

TABLE 4. MAJOR-ELEMENT ANALYSES AND MOLECULAR NORMS OF SELECTED PLEISTOCENE LAVA FIELDS, EASTERN SNAKE RIVER PLAIN, IDAHO* (continued)

	Central ESRP			Spencer-High Point Volcanic Rift Zone								
Sample No.	76K119	76K127	76K134	76K28	76K178	76K192	76K205	76K210	76K240	76K196	76K315	77K51
						Major Oxides (percent)						
SiO_2	47.28	46.17	46.35	47.49	46.78	47.78	47.38	47.33	46.17	52.21	50.24	47.34
TiO_2	2.36	3.16	2.58	1.93	2.94	2.87	3.02	1.22	1.74	1.98	1.94	1.21
Al_2O_3	15.21	15.33	15.65	16.25	15.28	15.79	15.24	16.54	16.30	15.89	16.15	16.25
Fe_2O_3	1.70	2.43	3.57	1.86	1.37	3.79	4.40	1.09	1.48	2.74	3.24	0.83
FeO	11.13	12.11	9.89	10.17	12.25	9.84	10.07	9.12	10.37	8.90	8.09	9.52
MnO	0.19	0.20	0.20	0.19	0.19	0.22	0.25	0.17	0.18	0.21	0.17	0.17
MgO	8.10	7.30	7.79	7.90	7.00	4.01	4.05	10.27	9.64	2.88	6.66	9.92
CaO	10.14	9.89	10.03	10.14	9.85	8.44	7.80	11.02	10.28	6.38	8.74	11.10
Na_2O	2.67	2.83	2.92	2.98	3.06	3.63	3.80	2.48	2.48	3.75	3.16	2.72
K_2O	0.67	0.56	0.67	0.54	0.60	1.29	1.51	0.39	0.35	2.71	0.99	0.36
H_2O^+	0.42	0.30	0.46	0.08	0.09	0.27	0.16	0.06	0.08	0.41	0.13	0.27
H_2O^-	0.10	0.08	0.12	0.09	0.08	0.23	0.17	0.11	0.09	0.24	0.11	0.13
P_2O_5	0.58	0.74	0.65	0.60	0.62	1.85	2.12	0.30	0.34	1.06	0.67	0.40
Total	100.55	101.10	101.08	100.22	100.11	100.01	99.97	100.10	99.50	99.36	100.29	100.22
						Molecular Norms						
Ap	1.22	1.56	1.36	1.26	1.31	3.97	4.56	0.62	0.71	2.28	1.41	0.83
Il	3.31	4.44	3.61	2.69	4.15	4.11	4.32	1.68	2.43	2.84	2.72	1.67
Mt	1.48	1.68	1.53	1.38	1.59	1.58	1.68	1.16	1.36	1.36	1.29	1.18
Or	3.99	3.34	3.97	3.20	3.59	7.83	9.17	2.28	2.08	16.48	5.88	2.11
Ab	24.15	25.63	24.80	26.81	27.82	33.49	35.07	21.90	22.35	34.67	28.54	22.23
An	27.74	27.71	27.72	29.43	26.51	23.61	20.63	32.54	32.44	19.07	27.12	30.81
Di	15.29	13.52	14.37	13.64	15.09	5.59	3.93	15.74	13.23	5.11	9.68	16.97
Hy	5.27	3.18	0	1.63	1.33	10.99	8.79	0	1.30	17.11	16.08	0
Ol	17.54	18.94	21.74	19.97	18.62	8.82	11.86	23.98	24.10	1.07	7.29	23.01
Ne	0	0	0.91	0	0	0	0	0.09	0	0	0	1.19

*USGS analysts: S. Botts, L. Espos, Z. A. Hamlin, D. Hopping, P. Klock, S. Morgan, and M. Villareal.

Sample Localities

76K50 = Quaking Aspen Butte
76K107 = Taber Butte
75K229A = Table Legs Butte
76K68 = Crater vent
76K12 = Sixmile Butte
76K11 = Teakettle Butte
76K66 = AEC Butte
76K99 = State Butte
76K176 = Topper Butte
76K177 = Dome Butte
76K133 = Circular Butte
6-14-6 = Kettle Butte
76K119 = Antelope Butte
76K127 = Lava Ridge
76K134 = Teat Butte
76K28 = Morgans Crater
76K178 = Davis Butte
76K192 = Crystal Butte
76K205 = Laird's Butte
76K210 = Big Crater
76K240 = Experimental Crater
76K196 = Red Top Butte
76K315 = Snowshoe Butte
77K51 = Youngest vent, Split Rock Quadrangle

Since that time, much has been learned about the calderas. The Twin Falls and Picabo volcanic fields are described by Pierce and Morgan (this volume); the Taber caldera was originally described and illustrated by Kuntz and Covington (1979); the Blue Creek, Blacktail, and Kilgore calderas are described by Embree and others (1982), Morgan (1988), Morgan and others (1984, 1989), Pierce and Morgan (this volume), and Morgan (this volume); and the Henrys Fork and Yellowstone calderas are described by Christiansen (1982).

The known or inferred location and size of the calderas has been determined mainly from geophysical signatures and also from exposures around the margins of the ESRP. It should be noted that more is known about the calderas in the northeastern part of the ESRP because they are mostly or partly exposed; less is known about calderas farther to the southwest because they are mostly or completely covered by basaltic lava flows. What is presently known or inferred about the location, size, and extent of the rhyolitic calderas and the volcanic rift zones in the ESRP is summarized in Figure 16.

Here, we describe and attempt to evaluate critical field relations of the basaltic volcanism of the ESRP that may be related to underlying calderas. Many of the relationships remain speculative and abstract because of uncertainties about the size, location, and character of the calderas.

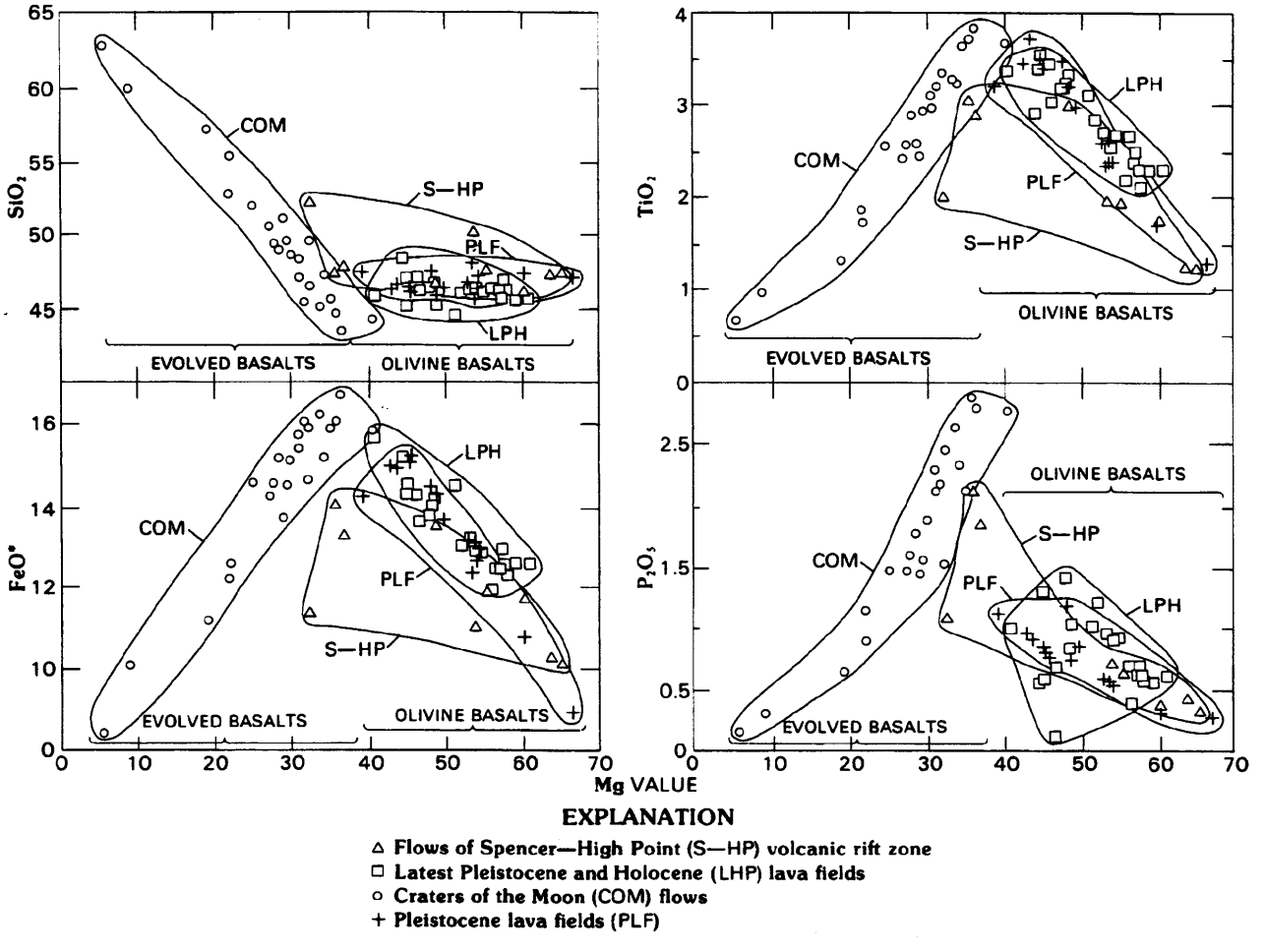

Figure 13. SiO_2, FeO^*, TiO_2, and P_2O_5 vs. Mg value [MgO/(MgO+FeO*)] (wt. percent) for the 70 analyses listed in Tables 2, 3, and 4. FeO^* is FeO + $0.9Fe_2O_3$.

Relationships between the orientations of volcanic rift zones and underlying calderas

The orientation and distribution of basaltic vents and volcanic rift zones are controlled mainly by regional stress directions and belts of strain concentration, the range-front faults. However, the influence of buried rhyolitic calderas on the orientation and distribution of volcanic vents and volcanic rift zones is important locally within the ESRP.

Several critical observations illustrate the variety and complexity of the influence of buried rhyolitic calderas on the orientation and distribution of basaltic vents and volcanic rift zones. (1) The Rock Corral Butte volcanic rift zone lies on the probable northwest boundary of the Taber caldera (Figs. 16 and 17). (2) Fracture-controlled basaltic vents in the central part of the Lava Ridge–Hells Half Acre volcanic rift zone are elongated north-south, whereas fracture-controlled vents in the northwestern and southeastern parts are elongated northwest-southeast (Fig. 17). (3) Fracture-controlled vents are elongated northeast-southwest between the central parts of the Lava Ridge–Hells Half Acre and Circular Butte–Kettle Butte volcanic rift zones (Fig. 17). (4) The Arco–Big Southern Butte volcanic rift zone terminates at the northern boundary of the Taber caldera (Figs. 16 and 17). (5) Linear concentrations of basaltic vents within calderas in the ESRP occur chiefly where well-developed volcanic rift zones, as collinear continuations of major range-front faults, extend into or cross calderas; major examples are seen where the Spencer–High Point volcanic rift zone crosses the Kilgore caldera and where the Menan volcanic rift zone extends 15 km into but does not completely traverse the Kilgore caldera (Fig. 18). Several concepts may partly explain these field relationships.

1. The regional stress direction in the ESRP (N.45°E.) is evidently deflected and reoriented by the northwest margin of the Taber caldera, producing fracture-controlled basaltic vents within

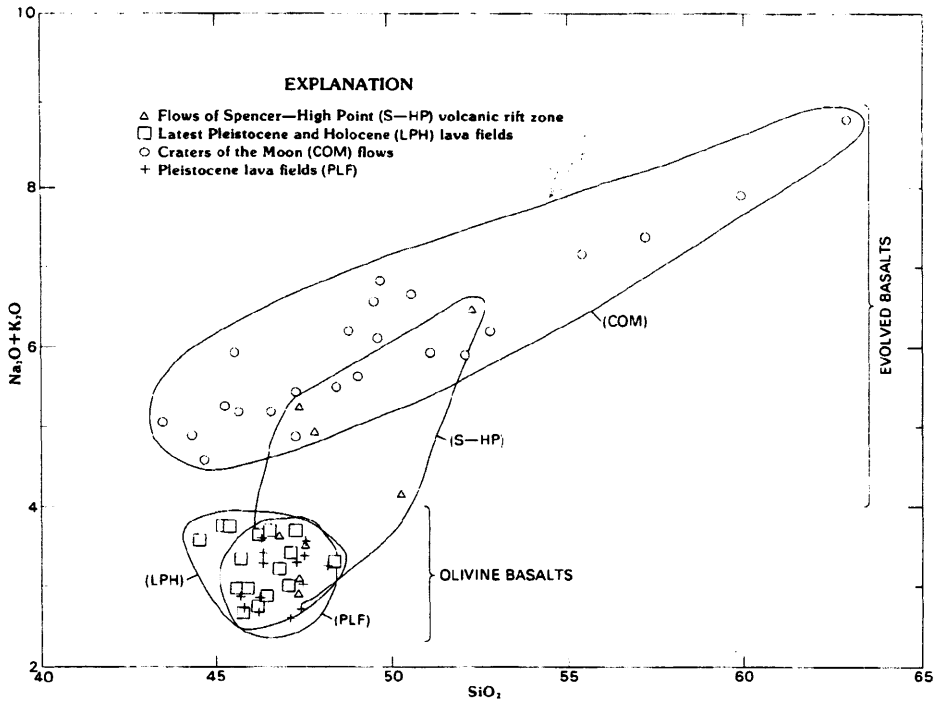

Figure 14. $Na_2O + K_2O$ vs. SiO_2 (wt. percent) for the 70 analyses listed in Tables 2, 3, and 4.

the Rock Corral Butte volcanic rift zone that are oriented nearly parallel to the regional stress direction and, presumably, above and parallel to the caldera margin.

2. The anomalous north-south and northeast-southwest orientation of fracture-controlled basaltic vents occurs at the intersection of the southeast boundary of the Blue Creek caldera and the center of the Lava Ridge–Hells Half Acre volcanic rift zone (Fig. 17). We suggest that regional stress patterns are deflected near the intersection to cause the north-south–trending vents and that the boundary (ring fractures?) of the Blue Creek caldera has controlled the orientation of the northeast-southwest–trending vents.

3. Low-density rocks in calderas may be barriers to the ascent and eruption of basaltic magmas to the surface. As described by Kuntz (this volume), this relationship may explain the termination of the Arco–Big Southern Butte volcanic rift zone at the northwest margin of the Taber caldera (Figs. 16 and 17).

4. Fracture pathways for magma ascent are most abundant in volcanic rift zones that extend into or cross the calderas. The two volcanic rift zones that cross or partly cross the Kilgore caldera are extensions into the caldera of the two major range-front fault systems near its borders (Fig. 19).

5. Calderas may be affected by basaltic eruptions only after subcaldera plutons have cooled and solidified sufficiently that regional stresses can create faults in the plutons (Christiansen, 1982). The time span for the cycle of caldera formation, cooling of subcaldera plutons, subsequent fracturing, and basaltic volcan-

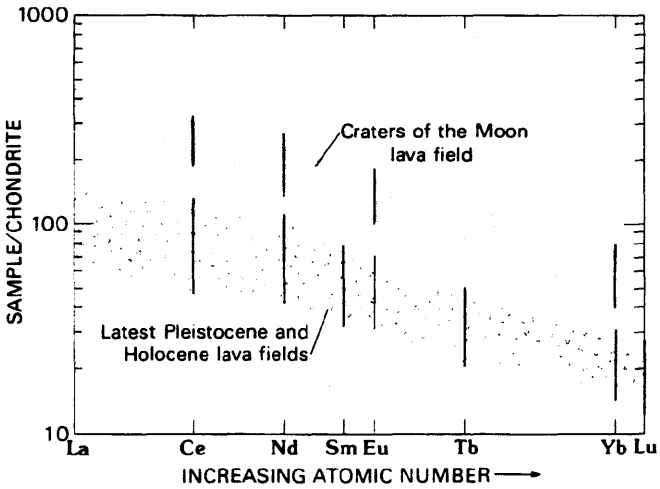

Figure 15. Chondrite-normalized rare-earth element (REE) plot of samples from 23 lava flows from the Craters of the Moon lava field and eight lava flows from latest Pleistocene and Holocene lava fields of the ESRP. Data from Tables 2 and 3. Chondritic abundances used to normalized REE are those of Haskin and others (1969).

TABLE 5. MAGMA OUTPUT RATES FOR VARIOUS VOLCANOES, LAVA FIELDS, AND VOLCANIC REGIONS*

Volcano or volcanic region	Magma Output Rate (km^3/1,000 yr)
CONTINENTAL, DOMINANTLY BASALTIC LAVA FIELDS	
Craters of the Moon lava field, eastern Snake River Plain (15 to 2 ka)	2.4
Entire eastern Snake River Plain (15 to 2 ka)	3.3
San Francisco volcanic field, Arizona (5 Ma to present)	0.2 to 3.3†
Springerville volcanic field, Arizona:	
Peak activity (2 to 1 Ma)	2.5
Average 2 to 0.3 Ma	1.5
CENTRAL VOLCANOES	
Etna, Italy (1759 to 1974)	9.5
Piton de la Fournaise, Reunion Island (1972 to 1981)	9.5
Fuego, Chile	16
Kilauea, Hawaii (1823 to 1975)	22
Mauna Loa, Hawaii (1823 to 1975)	22
LARGE VOLCANIC REGIONS	
Iceland (last 10,000 years)	500
Columbia Plateau, USA	1,000

*Data from Kuntz, Champion, and others, 1986; Tanaka and others, 1986; and Condit and others, 1989.
†Range for various time intervals.

ism can be estimated from radiometric data for rocks in and near the 4.3-Ma Kilgore caldera and the 1.3-Ma Henrys Fork caldera (Figs. 9 and 18). Gerritt Basalt flows that cover the floor of the Henrys Fork caldera were erupted at 200 ka from vents in the southwest part of the caldera (Christiansen, 1982). The Morgans Crater lava field, erupted from one of the oldest vents in the central part of the Spencer–High Point volcanic rift zone, has a K-Ar age of 365 ± 68 ka (G. B. Dalrymple, U.S. Geological Survey, written communication, 1980). These ages suggest that the Spencer–High Point volcanic rift zone had formed and was the locus of eruptions within the Kilgore caldera before 350 ka and extended into Henrys Fork caldera about 200 ka, when the caldera was 1.1 million years old. From this we conclude that roughly one million years was necessary for sufficient cooling to take place before subcaldera plutons were cut by faults.

Relationships between low density or absence of basaltic vents and underlying calderas

Various parts of the ESRP, even within volcanic rift zones, contain few or no basaltic vents (Figs. 10, 17, and 18). Notable examples are: (1) the area within the inferred boundaries of the Taber caldera, (2) the area of the sinks of the Big Lost River, Little Lost River, and Birch Creek along the northwest margin of the ESRP, (3) near the northwest end of the Circular Butte–Kettle Butte volcanic rift zones, (4) the southeast margin of the ESRP between Idaho Falls and Pocatello, (5) an area northwest of Terreton, (6) an area between Idaho Falls and the Menan volcanic rift zone, and (7) the region between the Spencer–High Point volcanic rift zone and Juniper Buttes.

These areas of sparse or no basaltic vents are within the known or inferred boundaries of buried rhyolitic calderas (Figs. 17 and 18). The concept that fill of low-density rocks in calderas created density barriers to the intrusion of basalt magma may partly explain the distribution of sparse or no basaltic vents in some parts of the ESRP. For example, Kuntz (this volume) suggests that the lack of basaltic vents in the area west of Blackfoot may be due to a thick accumulation of low-density rocks throughout the deep, piston-shaped Taber caldera.

The spatial relationship between the sparseness or absence of basaltic vents and low-density rocks in underlying calderas elsewhere in the ESRP is more speculative. Morgan (1988) and Morgan and others (1989) suggest that the Blacktail, Blue Creek, and Kilgore calderas are shallow structures less than 1 km deep and that relatively deep structures, possibly filled by low-density ejecta and/or colluvial materials, occur as separate, grabenlike rhyolitic vents along the margins of these calderas. If the relationship between thick fill of low-density rocks and sparsity of basaltic vents holds, then we propose that elongated, grabenlike rhyolitic vents may occur along the northwest margin of the Blue Creek caldera in the vicinity of the sinks area of the Big Lost River, Little Lost River, and Birch Creek (Fig. 17). A possible caldera-margin rhyolitic vent or vents at this locality may also explain the absence of basaltic vents near the northwest end of the Circular Butte–Kettle Butte volcanic rift zone (Fig. 17).

The absence of basaltic vents along the southeast margin of the ESRP between Idaho Falls and Pocatello (Figs. 10 and 17) may reflect a real lack of basaltic vents or may result from the concealment of older vents by alluvial sediments along the Snake and Henrys Fork rivers. As discussed above, this part ofthe ESRP lies adjacent to Belt IV of Pierce and Morgan (this volume), defined by them as an area having range-front faults that were active in late Tertiary time but show no evidence of Quaternary activity (Fig. 11). By assuming that basaltic volcanism in the ESRP is roughly coeval with basin-and-range deformation along its margins, as discussed above, we conclude that basaltic vents in this region may have formed several million years ago and may be covered by younger alluvial sediments.

Subtle topographic lows generally coincide with areas of sparse or no basaltic vents at four localities in the ESRP: (1) the area northwest of Terreton, (2) the area between Idaho Falls and the Menan volcanic rift zone, (3) the area between the Spencer–High Point volcanic rift zone and Juniper Buttes, and (4) the Taber caldera (Figs. 17 and 18). We suggest that these four regions may be areas of sparse basaltic vents and low elevation because they are adjacent to basaltic vents concentrated in high-

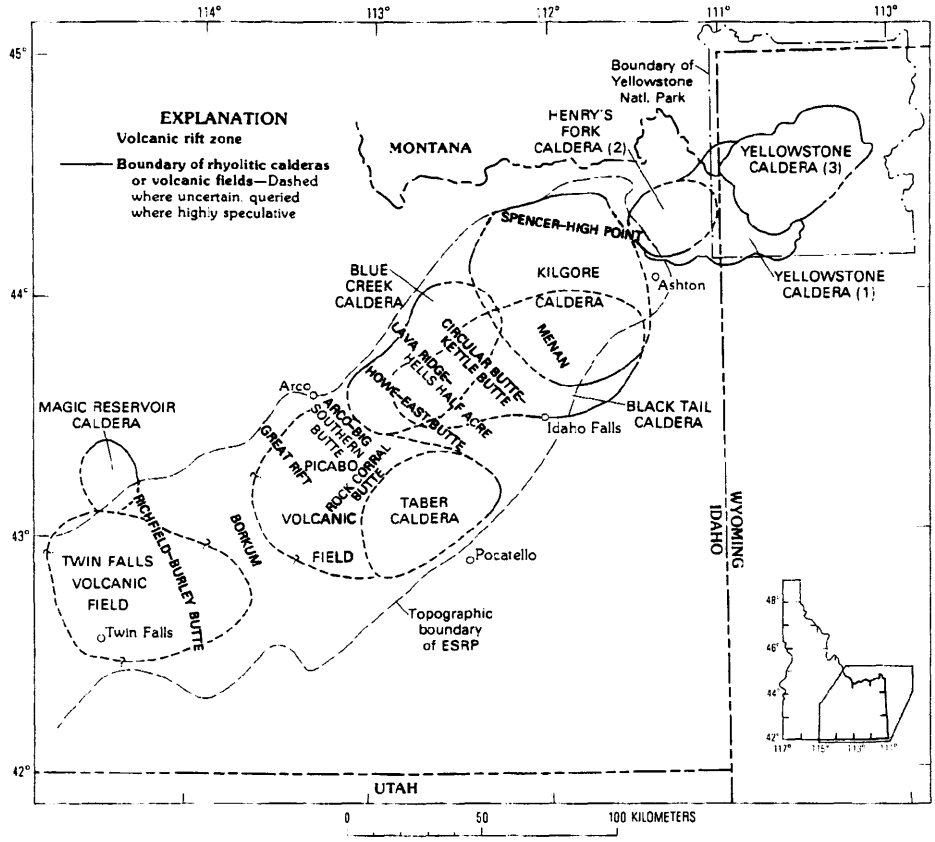

Figure 16. Map of eastern Snake River Plain showing boundaries of known and inferred rhyolitic calderas and volcanic rift zones. (1), (2), and (3) are designations from Christiansen (1982) for the order in which the three calderas formed. Compiled from Embree and others (1982), Christiansen (1982), Morgan (1988), Morgan and others (1984, 1989), Pierce and Morgan (this volume), and Morgan (this volume).

standing volcanic rift zones. Alternatively, these areas may overlie parts of underlying calderas that were once filled with low-density materials and have since compacted, leaving collapsed parts of calderas unrelated to caldera-forming eruptions.

Relationships between high density of basaltic vents, rhyolite domes, and underlying calderas

Within the Arco–Big Southern Butte and Howe–East Butte volcanic rift zones, the highest concentration of basaltic vents occurs near their centers where they intersect the western and southern boundary of the Blue Creek caldera (Fig. 17). This relationship suggests that interaction between fractures of the rift zones and the caldera boundary (ring fractures?) has localized basaltic vents. The rhyolite domes that form Big Southern Butte, Middle Butte, East Butte, and an associated, unnamed dome also are located along this same segment of the Blue Creek caldera boundary (Fig. 17). The Arco–Big Southern Butte and Howe–East Butte volcanic rift zones and the southwestern boundary of the Blue Creek caldera may have concentrated heat for partial melting of deep crustal rocks, which would have led to formation of rhyolite magma and emplacement of the domes (see Leeman, 1982d, for details of this process). This concept is supported by the general correlation between the ages of the rhyolite domes (300 ka to <1.0 Ma) and the ages (200 to 700 ka) of most nearby surface basaltic lava flows (Kuntz and others, 1992).

The rhyolite dome complex at Juniper Buttes (Figs. 18 and 19; Kuntz, 1979) is distinctly different from the rhyolite domes of Big Southern Butte, Middle Butte, East Butte and the unnamed dome in several respects: (1) it is much larger, (2) it is cut by a ditinctive pattern of rectilinear faults, (3) it contains a modified crestal graben, and (4) it does not lie on a volcanic rift zone. With respect to factors 1, 2, and 3, the Juniper Buttes dome complex is similar to resurgent domes of cauldron complexes (compare

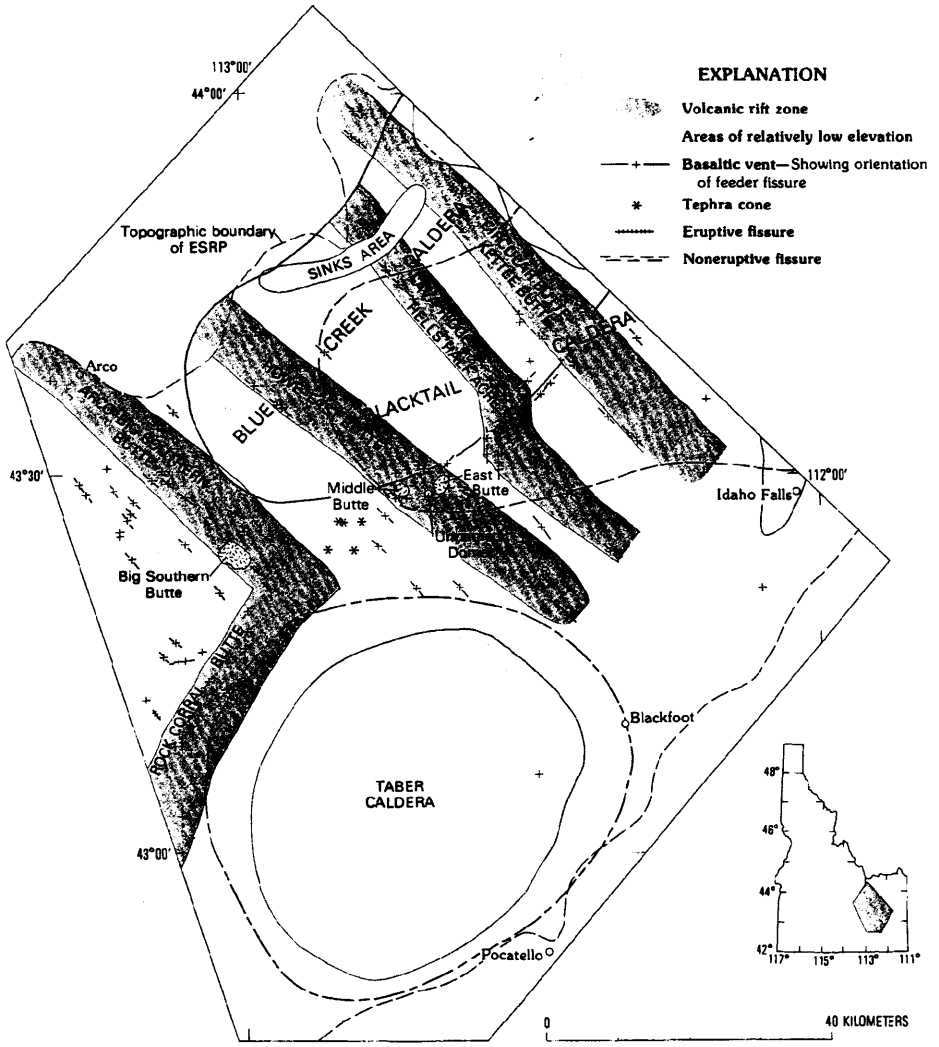

Figure 17. Simplified map of central part of eastern Snake River Plain showing basaltic vents, volcanic rift zones, boundaries of buried calderas, and other features referred to in text. Compiled from Kuntz and others (1992), LaPoint (1977), Pierce and Morgan (this volume), and Morgan (this volume). Map in this figure overlaps southwest boundary of map shown in Fig. 18.

Smith and Bailey, 1968). Morgan (1988) suggested that Juniper Buttes represents a resurgent dome or uplifted fault block in the Kilgore caldera.

Relatively high densities of basaltic vents unrelated to volcanic rift zones occur at several localities within or along the margins of the Kilgore caldera: at Table Butte, Lewisville Knolls, and northeast of Hamer (Fig. 18). The basaltic vents at Table Butte and Lewisville Knolls are not obviously elongated; thus they are probably not related to regional fracture patterns, and they do not lie on volcanic rift zones. The basaltic vents northeast of Hamer are elongated east-west, parallel to one of the fracture sets in the Juniper Buttes dome complex. At present, we have no explanation for the high concentration of basaltic vents at these three localities that might relate to structures or other features of the Kilgore caldera except to note that these vent concentrations occur along inferred caldera margins (Lewisville Knolls, Hamer) or at the intersection of caldera boundaries (Table Butte).

CONCLUDING REMARKS

The formation and petrologic evolution of the ESRP involves extremely complex, large-scale volcano-tectonic processes that have been described in detail only recently (see, for example, Leeman, 1982a, 1989; and Pierce and Morgan, this volume). From these studies, it is clear that the physiographic depression of

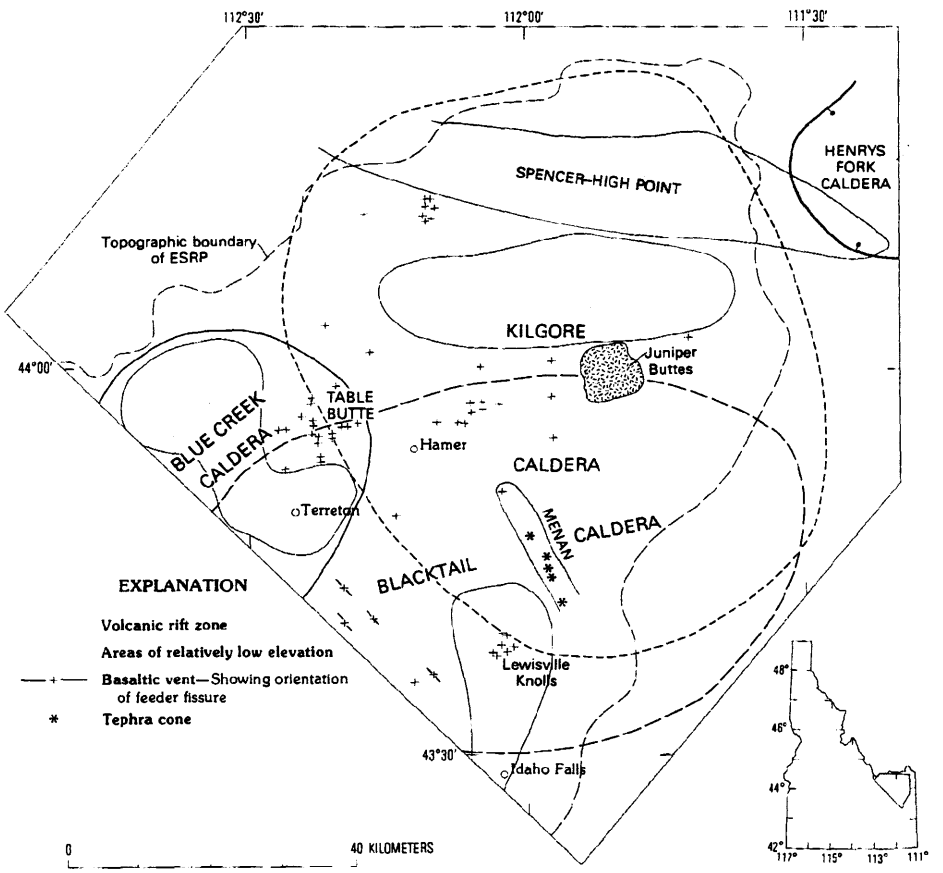

Figure 18. Simplified map of northeastern part of eastern Snake River Plain showing basaltic vents, volcanic rift zones, boundaries of buried calderas, and other features referred to in text. Compiled from unpublished mapping by M. A. Kuntz and G. F. Embree and from LaPoint (1977), Kuntz (1979), Pierce and Morgan (this volume), and Christiansen (1982). For simplicity, basaltic vents and structures in the Spencer–High Point volcanic rift zone are omitted in this figure but are shown in Figure 9. Map in this figure overlaps northeast boundary of map shown in Figure 17.

the ESRP formed initially as a result of earlier rhyolitic volcanism. The rhyolitic volcanism caused high heat flow, thinning and decreased rigidity of the crust, and progressive formation of a topographic trough along the chain of calderas.

The ESRP has been the site of dominantly shield-building basaltic eruptions for the last 4 m.y.; basaltic volcanism followed rhyolitic volcanism after subcaldera plutons first cooled and then fractured in response to regional northeast-southwest extension. Regional extensional strain has been concentrated in basin-and-range faults beyond the margins of the ESRP and in volcanic rift zones within the ESRP. Concentrated extension in volcanic rift zones has resulted in greater amounts of magma production, perhaps by decompression melting. Both of these processes, in turn, increased the number of suitable fractures for intrusion and extrusion of magma. The mechanical-thermal feedback nature of the mechanism created volcanic rift zones that were long-lived and self-perpetuating zones of dike emplacement and surface volcanism.

The ESRP is a unique basalt province in a tectonic sense: Eruptive fissures and volcanic rift zones are oriented essentially perpendicular to the long axis of the physiographic depression of the ESRP, and thus the ESRP is not an intracontinental, fault-bounded, volcanic-rift province, such as the African rift valleys and the Rio Grande rift. Rather, the ESRP is an intracontinental basalt province created through a combination of an earlier history dominated by rhyolitic volcanism that formed the ESRP depression and a more recent history that consists chiefly of basaltic volcanism. The origin of basalt magmas may be due to decompression melting controlled by the timing of strain release, and the location of basaltic vents is controlled by the orientation of contemporary regional stress patterns and resulting fracture pathways.

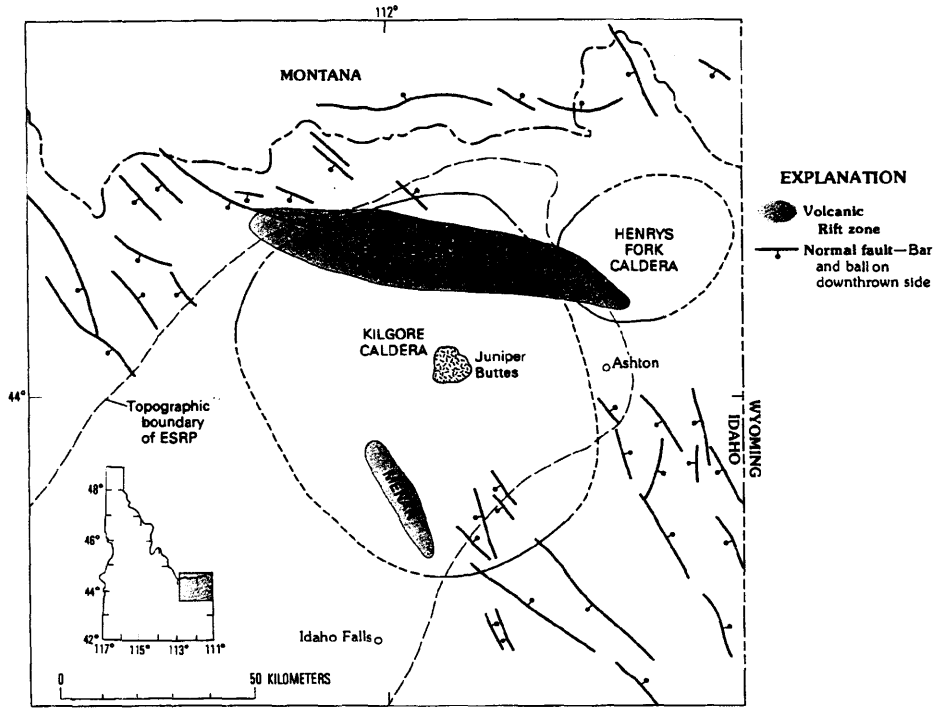

Figure 19. Simplified map of northeastern part of eastern Snake River Plain showing normal faults along margins of the plain, volcanic rift zones, boundaries of calderas, and other features referred to in text. Compiled from unpublished mapping by M. A. Kuntz and G. F. Embree and from Pierce and Morgan (this volume) and Christiansen (1982).

ACKNOWLEDGMENTS

Many people contributed to our studies and interpretations of basaltic volcanism of the ESRP, including U.S.G.S. colleagues D. E. Champion, R. T. Holcomb, S. R. Anderson, and P.J.I. LaPoint; academic colleagues R. H. Lefebvre (Grand Valley State College), W. P. Leeman (Rice University), J. S. King (SUNY-Buffalo), Ronald Greeley (Arizona State University), and W. R. Hackett (Idaho State University); David Clark of Craters of the Moon National Monument; R. P. Smith of EG&G Idaho, Inc., and others. Most of our conclusions and speculations were reached with naive neglect of their views. We thank L. D. Nealey, W. R. Hackett, S. H. Wood, and especially P. L. Martin for helpful reviews of the manuscript and Wayne Hawkins for his skillful preparation of the figures.

Our field studies were conducted under the aegis of the late Steven S. Oriel in his capacity as leader of the U.S. Geological Survey's Snake River Plain project. The guidance, encouragement, and patience that Steve rendered as project leader are deeply appreciated.

REFERENCES CITED

Armstrong, R. L., Leeman, W. P., and Malde, H. E., 1975, K-Ar dating and Quaternary and Neogene volcanic rocks of the Snake River Plain, Idaho: American Journal of Science, v. 275, p. 225–257.

Baksi, A. K., and Watkins, N. D., 1973, Volcanic production rates—Comparison of oceanic ridges, islands, and the Columbia Plateau basalts: Science, v. 180, p. 493–495.

Bhattacharya, B. K., and Mabey, D. R., 1980, Interpretation of magnetic anomalies over southern Idaho using generalized multibody methods: U.S. Geological Survey Open-File Report 80-457, 49 p.

Brott, C. A., Blackwell, D. D., and Mitchell, J. C., 1978, Tectonic implications of heat flow of the western Snake River Plain, Idaho: Geological Society of America Bulletin, v. 89, p. 1697–1707.

Brott, C. A., Blackwell, D. D., and Ziagos, J. P., 1981, Thermal and tectonic implications of heat flow in the eastern Snake River Plain, Idaho: Journal of Geophysical Research, ser. B, v. 86, p. 11709–11734.

Champion, D. E., 1973, The relationship of large-scale surface morphology to lava flow direction, Wapi lava field, southeast Idaho [M.S. thesis]: Buffalo, State University of New York, 44 p.

——, 1980, Holocene geomagnetic secular variation in the western United States: Implications for global geomagnetic field: U.S. Geological Survey Open-File Report 80-824, 326 p.

Champion, D. E., and Greeley, R., 1977, Geology of the Wapi lava field, Snake River Plain, Idaho, *in* Greeley, R., and King, J. S., eds., Volcanism of the eastern Snake River Plain, Idaho: A comparative planetary geology guidebook: Washington, D.C., National Aeronautics and Space Administration, p. 133–152.

Champion, D. E., Lanphere, M. A., and Kuntz, M. A., 1988, Evidence for a new geomagnetic reversal from lava flows in Idaho: Discussion of short polarity reversals in the Brunhes and late Matuyama polarity chrons: Journal of Geophysical Research, v. 93, p. 11667–11680.

Champion, D. E., Kuntz, M. A., and Lefebvre, R. H., 1989, Geologic map of the North Laidlaw Butte quadrangle, Blaine and Butte Counties, Idaho: U.S. Geological Survey Geologic Quadrangle Map GQ-1634, scale 1:24,000.

Christiansen, R. L., 1982, Late Cenozoic volcanism of the Island Park area, eastern Idaho, *in* Bonnichsen, B., and Breckenridge, R. M., eds., Cenozoic geology of Idaho: Idaho Bureau of Mines and Geology Bulletin 26, p. 345–368.

Condit, C. D., Crumpler, L. S., Aubele, J. C., and Elston, W. E., 1989, Patterns of volcanism along the southern margin of the Colorado Plateau: The Springerville field: Journal of Geophysical Research, v. 94, p. 7975–7986.

Corbett, M. K., 1975, Structural development of the eastern Snake River Plain, Idaho, as an intracontinental rift: Geological Society of America Abstracts with Programs, v. 7, p. 599–600.

Covington, H. R., 1977, Preliminary geologic map of the Pillar Butte, Pillar Butte NE, Pillar Butte SE, and Rattlesnake Buttes quadrangles, Bingham, Blaine, and Power Counties, Idaho: U.S. Geological Survey Open-File Report 77-779, scale 1:48,000.

Doherty, D. J., McBroome, L. A., and Kuntz, M. A., 1979, Preliminary geological interpretation and lithologic log of the exploratory geothermal test well (INEL-1), Idaho National Engineering Laboratory, eastern Snake River Plain, Idaho: U.S. Geological Survey Open-File Report 79-1248, 9 p.

Embree, G. F., McBroome, L. A., and Doherty, D. J., 1982, Preliminary stratigraphic framework of the Pliocene and Miocene rhyolite, eastern Snake River Plain, Idaho, *in* Bonnichsen, B., and Breckenridge, R. M., eds., Cenozoic geology of Idaho: Idaho Bureau of Mines and Geology Bulletin 26, p. 333–343.

Futa, K., Kuntz, M. A., and Stout, M. Z., 1988, Major- and trace-element geochemistry and Sr and Nd isotopic characteristics of flows from Craters of the Moon lava field: Geological Society of America Abstracts with Programs, v. 20, p. 415.

Greeley, R., 1977, Basaltic "plains" volcanism, *in* Greeley, R., and King, J. S., eds., Volcanism of the eastern Snake River Plain, Idaho: A comparative planetary geology guidebook: Washington, D.C., National Aeronautics and Space Administration, p. 23–44.

—— , 1982a, The style of basaltic volcanism in the eastern Snake River Plain, Idaho, *in* Bonnichsen, B., and Breckenridge, R. M., eds., Cenozoic geology of Idaho: Idaho Bureau of Mines and Geology Bulletin 26, p. 407–422.

—— , 1982b, The Snake River Plain, Idaho: Representative of a new category of volcanism: Journal of Geophysical Research, v. 87, p. 2705–2712.

Greeley, R., and King, J. S., 1975, Geologic field guide to the Quaternary volcanics of the south-central Snake River Plain, Idaho: Idaho Bureau of Mines and Geology Pamphlet 160, 49 p.

Greeley, R., Theiling, E., and King, J. S., 1977, Guide to the geology of Kings Bowl lava field, *in* Greeley, R., and King, J. S., eds., Volcanism of the eastern Snake River Plain, Idaho: A comparative planetary geology guidebook: Washington, D.C., National Aeronautics and Space Administration, p. 171–188.

Hackett, W. R., and Morgan, L. A., 1988, Explosive basaltic and rhyolitic volcanism of the eastern Snake River Plain, *in* Link, P. K., and Hackett, W. R., eds., Guidebook to the geology of central and southern Idaho: Idaho Geological Survey Bulletin 27, p. 283–301.

Hamilton, W., 1987, Plate-tectonic evolution of the western U.S.A.: Episodes, v. 10, p. 271–276.

Haskin, L. A., Haskin, M. A., Frey, F. A., and Wildeman, T. R., 1969, Relative and absolute terrestrial abundances of the rare earth elements, *in* Ahrens, L. H., ed., Origin and distribution of the elements: New York, Pergamon Press, p. 889–912.

Holcomb, R. T., 1987, Eruptive history and long-term behavior of Kilauea Volcano: U.S. Geological Survey Professional Paper 1350, p. 261–350.

Jamieson, B. G., and Clarke, D. B., 1970, Potassium and associated elements in tholeiitic basalts: Journal of Petrology, v. 11, p. 183–204.

Karlo, J. F., 1977, The geology and Bouguer gravity of the Hells Half Acre area and their relation to volcano-tectonic processes within the Snake River Plain rift zone, Idaho [Ph.D. thesis]: Buffalo, State University of New York, 152 p.

King, J. S., 1977, Crystal Ice Cave and Kings bowl Crater, eastern Snake River Plain, Idaho, *in* Greeley, R., and King, J. S., eds., Volcanism of the eastern Snake River Plain, Idaho: A comparative planetary geology guidebook: National Aeronautics and Space Administration, p. 153–163.

—— , 1982, Selected volcanic features of the south-central Snake River Plain, Idaho, *in* Bonnichsen, B., and Breckenridge, R. M., eds., Cenozoic geology of Idaho: Idaho Bureau of Mines and Geology Bulletin 26, p. 439–454.

Kuntz, M. A., 1977a, Rift zones of the Snake River Plain, Idaho, as extensions of basin-range and older structures: Geological Society of America Abstracts with Programs, v. 9, p. 1061–1062.

—— , 1977b, Extensional faulting and volcanism along the Arco rift zone, eastern Snake River Plain, Idaho: Geological Society of America Abstracts with Programs, v. 9, p. 740–741.

—— , 1978, Geologic map of the Arco–Big Southern Butte area, Butte, Blaine, and Bingham Counties, Idaho: U.S. Geological Survey Open-File Report 78-302, scale 1:62,500.

—— , 1979, Geologic map of the Juniper Buttes area, eastern Snake River Plain, Idaho: U.S. Geological Survey Miscellaneous Investigations Series Map I-1115, scale 1:48,000.

Kuntz, M. A., and Covington, H. R., 1979, Do basalt structures and topographic features reflect buried calderas in the eastern Snake River Plain (ESRP)?: EOS, Transactions of the American Geophysical Union, v. 60, p. 945.

Kuntz, M. A., Champion, D. E., Spiker, E. C., Lefebvre, R. H., and McBroome, L. A., 1982, The Great Rift and the evolution of the Craters of the Moon lava field, Idaho, *in* Bonnichsen, B., and Breckenridge, R. M., eds., Cenozoic geology of Idaho: Idaho Bureau of Mines and Geology Bulletin 26, p. 423–437.

Kuntz, M. A., Lefebvre, R. H., Champion, D. E., King, J. S., and Covington, H. R., 1983, Holocene basaltic volcanism along the Great Rift, central and eastern Snake River Plain, Idaho: Utah Geological and Mineral Survey Special Studies 61, Guidebook, pt. 3, p. 1–34.

Kuntz, M. A., Elsheimer, N. H., Espos, L. F., and Klock, P. R., 1985, Major-element analyses of latest Pleistocene–Holocene lava fields of the Snake River Plain, Idaho: U.S. Geological Survey Open-File Report 85-593, 64 p.

Kuntz, M. A., Champion, D. E., Spiker, E. C., and Lefebvre, R. H., 1986, Contrasting magma types and steady-state, volume-predictable basaltic volcanism along the Great Rift, Idaho: Geological Society of America Bulletin, v. 97, p. 579–594.

Kuntz, M. A., Spiker, E. C., Rubin, M., Champion, D. E., and Lefebvre, R. H., 1986, Radiocarbon studies of latest Pleistocene and Holocene lava flows of the Snake River Plain, Idaho; data, lessons, interpretations: Quaternary Research, v. 25, p. 163–176.

Kuntz, M. A., Champion, D. E., Lefebvre, R. H., and Covington, H. R., 1988, Geologic map of the Craters of the Moon, Kings Bowl, and Wapi lava fields and the Great Rift volcanic rift zone, south-central Idaho: U.S. Geological Survey Miscellaneous Investigations Series Map I-1632, scale 1:100,000.

Kuntz, M. A., Champion, D. E., and Lefebvre, R. H., 1989, Geologic map of the Fissure Butte quadrangle, Blaine and Butte Counties, Idaho: U.S. Geological Survey Geologic Quadrangle Map GQ-1635, scale 1:24,000.

Kuntz, M. A., Lefebvre, R. H., and Champion, D. E., 1989a, Geologic map of the Inferno Cone quadrangle, Butte County, Idaho: U.S. Geological Survey Geologic Quadrangle Map GQ-1632, scale 1:24,000.

—— , 1989b, Geologic map of The Watchman quadrangle, Butte County, Idaho: U.S. Geological Survey Geologic Quadrangle Map GQ-1633, scale 1:24,000.

Kuntz, M. A., and twelve others, 1992, Geologic map of the Idaho National Engineering Laboratory and adjoining areas, eastern Idaho: U.S. Geological Survey Miscellaneous Investigations Series Map I-2330, scale 1:100,000.

LaPoint, P.J.L, 1977, Preliminary photogeologic map of the eastern Snake River Plain, Idaho: U.S. Geological Survey Miscellaneous Field Studies Map MF-850, scale 1:250,000.

Leeman, W. P., 1974, Part 1: Petrology of basalt lavas from the Snake River Plain, Idaho. Part 2: Experimental determination of partioning of divalent cations between olivine and basaltic liquid [Ph.D. thesis]: Eugene, University of Oregon, 337 p.

—— , 1982a, Development of the Snake River Plain–Yellowstone Plateau province, Idaho and Wyoming: An overview and petrologic model, *in* Bonnichsen, B., and Breckenridge, R. M., eds., Cenozoic geology of Idaho: Idaho Bureau of Mines and Geology Bulletin 26, p. 155–177.

—— , 1982b, Olivine tholeiitic basalts of the Snake River Plain, Idaho, *in* Bonnichsen, B., and Breckenridge, R. M., eds., Cenozoic geology of Idaho: Idaho Bureau of Mines and Geology Bulletin 26, p. 181–191.

—— , 1982c, Evolved and hybrid lavas from the Snake River Plain, Idaho, *in* Bonnichsen, B., and Breckenridge, R. M., eds., Cenozoic geology of Idaho: Idaho Bureau of Mines and Geology Bulletin 26, p. 193–202.

—— , 1982d, Rhyolites of the Snake River Plain–Yellowstone Plateau province, Idaho and Wyoming: A summary of petrogenetic models, *in* Bonnichsen, B., and Breckenridge, R. M., eds., Cenozoic geology of Idaho: Idaho Bureau of Mines and Geology Bulletin 26, p. 203–212.

—— , 1989, Origin and development of the Snake River Plain (SRP), Idaho, *in* Ruebelmann, K. L., ed., Snake River Plain–Yellowstone volcanic province: International Geological Congress, 28th, Guidebook T305: Washington, D.C., American Geophysical Union, p. 4–12.

Leeman, W. P., and Manton, W. I., 1971, Strontium isotopic composition of basaltic lavas from the Snake River Plain, southern Idaho: Earth and Planetary Science Letters, v. 11, p. 420–434.

Leeman, W. P., and Vitaliano, C. J., 1976, Petrology of McKinney basalt, Snake River Plain, Idaho: Geological Society of America Bulletin, v. 87, p. 1777–1792.

Leeman, W. P., Vitaliano, C. J., and Prinz, M., 1976, Evolved lavas from the Snake River Plain, Craters of the Moon National Monument, Idaho: Contributions to Mineralogy and Petrology, v. 56, p. 35–60.

Leeman, W. P., Menzies, M. A., Matty, D. J., and Embree, G. F., 1985, Strontium, neodymium, and lead isotopic compositions of deep crustal xenoliths from the Snake River Plain; evidence for Archean basement: Earth and Planetary Science Letters, v. 75, p. 354–368.

Lefebvre, R. H., 1975, Mapping in Craters of the Moon volcanic field, Idaho, with LANDSAT (ERTS) imagery: Proceedings, Ann Arbor, University of Michigan, 10th International Symposium on Remote Sensing of the Environment: v. 2, no. 10, p. 951–957.

Link, P. K., Skipp, B., Hait, M. H., Jr., Janecke, S. U., and Burton, B. R., 1988, Structural and stratigraphic transect of south-central Idaho; a field guide to the Lost River, White Knob, Pioneer, Boulder, and Smoky Mountains, *in* Link, P. K., and Hackett, W. R., eds., Guidebook to the geology of central and southern Idaho: Idaho Geological Survey Bulletin 27, p. 5–42.

Mabey, D. R., 1982, Geophysics and tectonics of the Snake River Plain, Idaho, *in* Bonnichsen, B., and Breckenridge, R. M., eds., Cenozoic geology of Idaho: Idaho Bureau of Mines and Geology Bulletin 26, p. 139–153.

Macdonald, G. A., 1972, Volcanoes: Englewood Cliffs, N.J., Prentice-Hall, 510 p.

Macdonald, G. A., and Abbott, A. T., 1970, Volcanoes in the sea: Honolulu, University of Hawaii Press, 441 p.

Malde, H. E., 1991, Quaternary geology and structural history of the Snake River Plain, Idaho and Oregon, *in* Morrison, R. B., ed., Quaternary nonglacial geology; Conterminous U.S.: Boulder, Colorado, Geological Society of America, The geology of North America, v. K-2, p. 252–281.

Malde, H. E., and Powers, H. A., 1962, Upper Cenozoic stratigraphy of the western Snake River Plain, Idaho: Geological Society of America Bulletin, v. 73, p. 1197–1220.

Menzies, M. A., Leeman, W. P., and Hawkesworth, C. J., 1984, Geochemical and isotopic evidence for the origin of continental flood basalts with particular reference to the Snake River Plain, Idaho, U.S.A.: Transactions of the Royal Society of London, v. A310, p. 643–660.

Morgan, L. A., 1988, Explosive volcanism on the eastern Snake River Plain [Ph.D. thesis]: Manoa, University of Hawaii, 191 p.

Morgan, L. A., Doherty, D. J., and Leeman, W. P., 1984, Ignimbrites of the eastern Snake River Plain: Evidence for major caldera-forming eruptions: Journal of Geophysical Research, v. 89, p. 8665–8678.

Morgan, L. A., Doherty, D. J., and Bonnichsen, B., 1989, Evolution of the Kilgore caldera: A model for caldera formation on the Snake River Plain–Yellowstone Plateau volcanic province; Continental magmatism abstracts: New Mexico Bureau of Mines and Mineral Resources Bulletin 131, p. 195.

Murtaugh, J. G., 1961, Geology of Craters of the Moon National Monument, Idaho [M.S. thesis]: Moscow, University of Idaho, 99 p.

Nakamura, K., 1974, Preliminary estimate of global volcanic production rate, *in* Colp, J. L., ed., The utilization of volcano energy: Albuquerque, N.M., Sandia National Laboratories, p. 273–285.

Peterson, D. W., and Moore, R. B., 1987, Geologic history and evolution of concepts, Island of Hawaii: U.S. Geological Survey Professional Paper 1350, p. 149–190.

Pierce, K. L., Fosberg, M. A., Scott, W. E., Lewis, G. C., and Colman, S. M., 1982, Loess deposits of southeastern Idaho: Age and correlation of the upper two loess units, *in* Bonnichsen, B., and Breckenridge, R. M., eds., Cenozoic geology of Idaho: Idaho Bureau of Mines and Geology Bulletin 26, p. 717–725.

Porter, S. C., Pierce, K. L., and Hamilton, T. D., 1983, Late Pleistocene glaciation in the western United States, *in* Porter, S. C., ed., The late Pleistocene, v. 1 *of* Wright, H. E., Jr., ed., Late Quaternary environments of the United States: Minneapolis, University of Minnesota Press, p. 71–111.

Prinz, M., 1970, Idaho rift system, Snake River Plain, Idaho: Geological Society of America Bulletin, v. 81, p. 941–947.

Richter, D. H., Eaton, J. P., Murata, K. J., Ault, W. U., and Krivoy, H. L., 1970, Chronological narrative of the 1959–1960 eruption of Kilauea Volcano, Hawaii: U.S. Geological Survey Professional Paper 539-E, 73 p.

Rodgers, D. W., and Zentner, N. C., 1988, Fault geometries along the northern margin of the eastern Snake River Plain, Idaho: Geological Society of America Abstracts with Programs, v. 20, p. 465–466.

Russell, I. C., 1902, Geology and groundwater resources of the Snake River Plains of Idaho: U.S. Geological Survey Bulletin 199, 192 p.

Smith, R. L., and Bailey, R. A., 1968, Resurgent cauldrons, *in* Coats, R. R., Hay, R. L., and Anderson, C. A., eds., Studies in volcanology, Geological Society of America Memoir 116, p. 613–662.

Smith, R. P., Hackett, W. R., and Rodgers, D. W., 1989, Surface deformation along the Arco rift zone, eastern Snake River Plain, Idaho: Geological Society of America Abstracts with Programs, v. 21, p. 146.

Spear, D. B., 1977, Big Southern, Middle, and East Buttes, *in* Greeley, R., and King, J. S., eds., Volcanism of the eastern Snake River Plain, Idaho: A comparative planetary geology guidebook: Washington, D.C., National Aeronautics and Space Administration, p. 113–120.

Spear, D. B., and King, J. S., 1982, The geology of Big Southern Butte, Idaho, *in* Bonnichsen, B., and Breckenridge, R. M., eds., Cenozoic geology of Idaho: Idaho Bureau of Mines and Geology Bulletin 26, p. 395–403.

Stanley, W. D., Boehl, J. E., Bostick, F. X., and Smith, H. W., 1977, Geothermal significance of magnetotelluric soundings in the eastern Snake River Plain–Yellowstone region: Journal of Geophysical Research, v. 82, p. 2501–2514.

Stearns, H. T., 1928, Craters of the Moon National Monument, Idaho: Idaho Bureau of Mines and Geology Bulletin 13, 57 p.

Stearns, H. T., Crandall, L., and Steward, W. G., 1938, Geology and groundwater resources of the Snake River Plain in southeastern Idaho: U.S. Geological Survey Water Supply Paper 774, 268 p.

Stickney, M. C., and Bartholomew, M. J., 1987, Seismicity and late Quaternary faulting of the northern Basin and Range province, Montana and Idaho: Bulletin of the Seismological Society of America, v. 77, p. 1602–1625.

Stone, G. T., 1967, Petrology of upper Cenozoic basalts of the Snake River Plain

[Ph.D. thesis]: Boulder, University of Colorado, 392 p.

—— , 1970, Highly evolved basaltic lavas in the western Snake River Plain, Idaho: Geological Society of America Abstracts with Programs, v. 2, p. 695–696.

Stout, M. Z., 1975, Mineralogy and petrology of Quaternary lavas, Snake River Plain, Idaho, and the cation distribution in natural titanomagnetites [M.S. thesis]: Calgary, Alberta, University of Calgary, 150 p.

Stout, M. Z., and Nicholls, J., 1977, Mineralogy and petrology of Quaternary lavas from the Snake River Plain, Idaho: Canadian Journal of Earth Sciences, v. 14, p. 2140–2156.

Stout, M. Z., Nicholls, J., and Kuntz, M. A., 1989, Fractionation and contamination processes, Craters of the Moon lava field, Idaho, 2000–2500 years B.P.; Continental magmatism abstracts: New Mexico Bureau of Mines and Mineral Resources Bulletin 131, p. 259.

Swanson, D. A., 1973, Pahoehoe flows from the 1969–1971 Mauna Ulu eruption of Kilauea Volcano, Hawaii: Geological Society of America Bulletin, v. 84, p. 615–626.

Swanson, D. A., Duffield, W. A., Jackson, D. B., and Peterson, D. W., 1979, Chronological narrative of the 1969–71 Mauna Ulu eruption of Kilauea Volcano, Hawaii: U.S. Geological Survey Professional Paper 1056, 55 p.

Takahashi, T. J., and Griggs, J. T., 1987, Hawaiian volcanic features; a photoglossary: U.S. Geological Survey Professional Paper 1350, p. 845–902.

Tanaka, K. L., Shoemaker, E. M., Ulrich, G. E., and Wolfe, E. W., 1986, Migration of volcanism in the San Francisco volcanic field, Arizona: Geological Society of America Bulletin, v. 97, p. 129–141.

Thompson, R. N., 1975, Primary basalts and magma genesis; II, Snake River Plain, Idaho, U.S.A.: Contributions to Mineralogy and Petrology, v. 52, p. 213–232.

Tilley, C. E., and Thompson, R. N., 1970, Melting and crystallization relations of the Snake River basalts of southern Idaho, USA: Earth and Planetary Science Letters, v. 8, p. 79–92.

Tilling, R. I., and seven others, 1987, The 1972–1974 Mauna Ulu eruption, Kilauea Volcano: An example of quasi-steady-state magma transfer: U.S. Geological Survey Professional Paper 1350, p. 405–469.

Walker, G.P.L., 1972, Compound and simple lava flows and flood basalts: Bulletin of Volcanology, v. 36, p. 579–590.

Wentworth, C. K., and Macdonald, G. A., 1953, Structures and forms of basaltic rocks in Hawaii: U.S. Geological Survey Bulletin 994, 98 p.

Wolfe, E. W., Garcia, M. O., Jackson, D. B., Koyanagi, R. Y., Neal, C. A., and Okamura, A. T., 1987, The Puu Oo eruption of Kilauea Volcano, episodes 1–20, January 3, 1983, to June 8, 1984: U.S. Geological Survey Professional Paper 1350, p. 471–508.

Womer, M. B., Greeley, R., and King, J. S., 1982, Phreatic eruptions of the eastern Snake River Plain, Idaho, *in* Bonnichsen, B., and Breckenridge, R. M., eds., Cenozoic geology of Idaho: Idaho Bureau of Mines and Geology Bulletin 26, p. 453–464.

Yoder, H. S., and Tilley, C. E., 1962, The origin of basalt magmas: An experimental study of natural and synthetic rock systems: Journal of Petrology, v. 3, p. 342–532.

Zoback, M. L., and Zoback, M. D., 1980, State of stress in the conterminous United States: Journal of Geophysical Research, v. 85, p. 6113–6156.

MANUSCRIPT ACCEPTED BY THE SOCIETY JULY 19, 1991

Printed in U.S.A.